UAB
Universitat Autònoma de Barcelona

Unravelling the dual role of senescent cells in breast cancer progression

Marta María Lalinde Gutiérrez

ADVERTIMENT. L'accés als continguts d'aquesta tesi doctoral i la seva utilització ha de respectar els drets de la persona autora. Pot ser utilitzada per a consulta o estudi personal, així com en activitats o materials d'investigació i docència en els termes establerts a l'art. 32 del Text Refós de la Llei de Propietat Intel·lectual (RDL 1/1996). Per altres utilitzacions es requereix l'autorització prèvia i expressa de la persona autora. En qualsevol cas, en la utilització dels seus continguts caldrà indicar de forma clara el nom i cognoms de la persona autora i el títol de la tesi doctoral. No s'autoritza la seva reproducció o altres formes d'explotació efectuades amb finalitats de lucre ni la seva comunicació pública des d'un lloc aliè al servei TDX. Tampoc s'autoritza la presentació del seu contingut en una finestra o marc aliè a TDX (framing). Aquesta reserva de drets afecta tant als continguts de la tesi com als seus resums i índexs.

ADVERTENCIA. El acceso a los contenidos de esta tesis doctoral y su utilización debe respetar los derechos de la persona autora. Puede ser utilizada para consulta o estudio personal, así como en actividades o materiales de investigación y docencia en los términos establecidos en el art. 32 del Texto Refundido de la Ley de Propiedad Intelectual (RDL 1/1996). Para otros usos se requiere la autorización previa y expresa de la persona autora. En cualquier caso, en la utilización de sus contenidos se deberá indicar de forma clara el nombre y apellidos de la persona autora y el título de la tesis doctoral. No se autoriza su reproducción u otras formas de explotación efectuadas con fines lucrativos ni su comunicación pública desde un sitio ajeno al servicio TDR. Tampoco se autoriza la presentación de su contenido en una ventana o marco ajeno a TDR (framing). Esta reserva de derechos afecta tanto al contenido de la tesis como a sus resúmenes e índices.

WARNING. The access to the contents of this doctoral thesis and its use must respect the rights of the author. It can be used for reference or private study, as well as research and learning activities or materials in the terms established by the 32nd article of the Spanish Consolidated Copyright Act (RDL 1/1996). Express and previous authorization of the author is required for any other uses. In any case, when using its content, full name of the author and title of the thesis must be clearly indicated. Reproduction or other forms of for profit use or public communication from outside TDX service is not allowed. Presentation of its content in a window or frame external to TDX (framing) is not authorized either. These rights affect both the content of the thesis and its abstracts and indexes.

Universitat Autònoma de Barcelona

Facultat de Medicina

Departament de Bioquímica i Biologia Molecular

Programa de Doctorat en Bioquímica, Biologia Molecular i Biomedicina

Unravelling the dual role of senescent cells in breast cancer progression

Thesis presented by Marta María Lalinde Gutiérrez for the degree of Doctor of Philosophy (PhD) in Biochemistry, Molecular Biology and Biomedicine by Universitat Autònoma de Barcelona

Barcelona, September 2024

Author:

Marta María Lalinde Gutiérrez

Co-directors:

Dr. Joaquín Arribas

Dra. Verónica Rodilla

Academic Tutor:

Dr. Joaquín Arribas

AKNOWLEDGEMENTS

“Recorre el camino solo y llegarás antes. Hazlo acompañado y llegarás más lejos”.

Desde siempre he sido una persona de equipo y hacer una tesis no iba suponer una excepción. Han sido 5 años de muchas (muchas) horas de trabajo, que sin el apoyo y el acompañamiento adecuado no hubieran tenido el gran resultado reflejado en esta tesis. Es mi momento de daros lar gracias:

En primer lugar, me gustaría agradecer a **Joaquín**, por haberme dado la oportunidad de formar parte de este equipo al que nos referimos como “lab”. Gracias por tu confianza desde el primer momento para liderar este proyecto, que ambos sabemos que no ha sido nada fácil. Sin tu apoyo y tu capacidad de resolución en los momentos clave, no habríamos sido capaces de montar una historia tan bonita como esta. Te estaré siempre agradecida por haberme dado la oportunidad de hacer este doctorado, que ha supuesto un entrenamiento de lo más completo, no solo a nivel científico, si no también personal.

Y si es por oportunidades, la siguiente persona a la que debo darle las gracias es a ti, **Vero**. Fuiste la primera en darle el sí a una chica que acababa de salir de la carrera y no sabía ni como coger una pipeta. Y aquí tengo que acordarme de **Cris** también, que junto contigo, fuisteis las primeras en confiar en mí. Gracias por tener la paciencia suficiente como para formarme e inculcarme tu pasión por la ciencia, sin la cual no habría sido capaz de llegar hasta aquí. Y gracias por confiar en mi para quedarme a cargo de este proyecto que, aunque demandante, no podría haber sido uno mejor.

Me gustaría dar también las gracias a **María Abad**, **Laura Soucek** y **Juan Ángel Recio**, por todos los consejos y sugerencias aportadas durante nuestras comisiones de seguimiento, que han sido claves para finalizar este trabajo. Y de la misma forma, me gustaría agradecer a los miembros del tribunal por haber accedido a formar parte de él y a dedicar su tiempo a revisar este trabajo.

Sandriña, las dos sabemos que con stickers me resultaría mucho más fácil agradecerte todo lo que tengo que agradecerte, pero vamos a tener que conformarnos con las palabras. Gracias por ser y por estar. Por ser la persona ideal para embarcarte en este proyecto desde el principio. Porque puedes quejarte (quejarnos) de las pocas ganas de trabajar que tienes (tenemos), pero el trabajo siempre sale perfecto contigo. Si se pudiera, esta tesis habría sido un "ft. Sandra" de manual, porque sin tus miles de PCRs, de inmunos y minutos compartidos con nuestros ratones, no tendría más que el título de esta tesis. Y precisamente porque son miles de minutos compartidos, dentro y fuera del lab, gracias por estar, siempre, cuando más te he necesitado. Con un tweet, un sticker o simplemente una sonrisa desde el pasillo de enfrente. Te lo digo poco, pero no por eso es menos cierto: Te quiero (siempre en mi equipo ;)).

Maca, ¡que hubiera sido de mi sin ti y sin esos momentos de poca productividad científica, pero muy productivos para no volvernos completamente locas! Gracias por estar desde el primer día, siempre al pie del cañón. Por estar siempre dispuesta a tirar de este carro, por ser referente y por estar siempre detrás (literal y metafóricamente) preparada para acudir al rescate. Doy gracias por todos estos años en los que, con nuestras innumerables charlas y debates, has conseguido hacerme mejor científica y, sobre todo, mejor persona. Esta unión marquesa-macarra ha resultado ser una simbiosis perfecta, que espero continue muchos años más (ahora sí, ambas como doctoras :)).

Y la tercera pata para este banco… **Santiaguito**, ¡el mejor compañero que alguien puede tener! (y el mejor amigo, el mejor científico, el mejor deportista... siempre el mejor jeje). Gracias por dejarte molestar, por todos los intentos de arreglar el mundo y las crónicas deportivas post-comidas. Por aportar calma y sensatez cuando más lo hemos necesitado y tener siempre una sonrisa preparada para levantar el ánimo. El mundo sería mejor con más

personas como tú, Danonino. Así que, permíteme dar las gracias por poder disfrutar de tu compañía en el lab y, sobre todo, de tu amistad. ¡Ahora te toca a ti! Te esperamos en el otro lado ;)

Pablito, gracias por estos últimos meses de acompañamiento mutuo. Da igual en el VHIO o en el IMIM, ten por seguro que ya no te vas a poder librar de mi :). **Jade**, thank you for your eternal smile and all the positive feedback. I am sure that you will have the best of the PhD experiences here.

Martita, gracias por tu actitud, siempre dispuesta a ayudar sin pedir nada a cambio. Ha sido un placer haber tenido la oportunidad de trabajar codo con codo contigo (aunque la distancia entre labs lo haya dificultado todo un poquito. **Ari**, **Judit**, el IMIM está en buenas manos con vosotras por allí. Gracias por vuestra paciencia infinita y por aportarme soluciones siempre que lo he necesitado. Y si hablamos de IMIM, I have to thank you, **Chris**, for the years we shared and for helping to take some of the workload off my shoulders when I needed it most.". Y por supuesto no me puedo olvidar de agradecer a las mejores vecinas que se puedan tener. **Albita, Anna** gracias por acogerme con los brazos abiertos en vuestros dominios y amenizar cada día que he pasado por allí.

Marta, **Susana**, mil gracias por vuestro trabajo invisible e invaluable. Sin vosotras, nuestro trabajo no existiría, así que gracias por ser parte fundamental de este equipo. Y hablando de trabajo invisible… **Helen**, mil gracias por todo el trabajo que haces. No podré nunca agradecerte suficiente el que me acogieras desde el minuto cero. Gracias por ser la mejor mami de lab que se pueda tener. Tengo intención de seguir acudiendo a nuestras meriendas de reinas, así que ya puedes ir avisando a Patri ;)

Mucha gracias, **Vanesa**, por estar siempre dispuesta a ayudarnos y por todo el trabajo que haces para facilitarnos un poco la vida en el lab. **Alex**, **Enriquito**, gracias por vuestro apoyo desde literalmente el principio de esta aventura. Quien nos iba a decir que los dos pipiolos que entraron hace 5 años en el lab iban a convertirse en doctores. Gracias por vuestro constante buen humor y todos los

momentos compartidos durante estos años. Y si echamos la vista atrás, hasta el comienzo, aparecen **Irene**, **Faiz**, **Mercedes**, **Bea**… Muchas gracias a todos por acogerme desde que pise el lab por primera vez y por hacerme sentirme siempre parte de él. **Fonsi**, siempre has sido un JAL adoptado y no puedo estar más agradecida por haber compartido tanto tiempo a tu lado, como compis de lab al principio y como amigos al final.

Tengo que dar las gracias a todos los estudiantitos que han ido pasando por el lab durante todos estos años, en especial a **Noelia**, **Júlia** y **Sveva**. Gracias por dejaros enseñar y por aportar vuestro granito de arena para completar este proyecto y mi formación profesional y personal. Mención especial a **Berta** que, aunque no he tenido yo el privilegio de tutorizarte, sí que me has amenizado estos últimos meses de escritura. Eres una persona 10 ;).

Y aunque no hayan participado directamente en este proyecto, estos cinco años se habrían hecho mucho más duros sin todas las personitas de VHIO con los que me he ido cruzando durante esta etapa (que no son pocas). Y no hablo solo de "**Souceks**", "**Tians**" o "**Serranos**", que por proximidad son con los que más he tenido la suerte de compartir espacio y tiempo. **Patri**, **Andrea**, **Alba**, **Judith**, **Anna**, gracias por acogerme como una más de la cuarta planta en esos momentos post-lab de los viernes, tan necesarios. **Sarita**, gracias por todos los momentos de desconexión y la paciencia de seguir ahí a pesar de los muchos momentos de desaparición. En general, gracias a VHIO por ser el mejor ambiente para vivir esta etapa.

La verdad es que mis gracias a VHIO van más allá de lo profesional. **Laia**, bendito el día que te acercaste y me invitaste a formar parte de este grupo maravilloso en que se ha convertido "mossos". Gracias por convertirte en mi pilar fundamental desde el principio y formar conmigo este peculiar matrimonio que, aunque ya no viva junto, sé que es para siempre (**Álex**, tú también vienes incluido en

este pack ;)). **Marina**, empezamos esta aventura llamada doctorado juntas, era de recibo acabarla a la vez. Gracias sobre todo por tu generosidad, no es fácil estar siempre para los demás y aun así sé que en ti siempre puedo encontrar apoyo y un consejo que me ayude a seguir. **Mercé**, gracias por tu eterno buen humor, tus inagotables anécdotas y por ser capaz de sacarme una sonrisa hasta en mis momentos más bajos. Gracias también por ser el nexo de este grupo, que me ha permitido conocer a tanta gente increíble que se ha convertido en imprescindible. **Ángela**, **María**, **Anabu**, doy gracias por el día en que decidisteis abandonar la terreta para venir a alegrarnos cada día con vuestra locura. No hay chupitos suficientes en el mundo con los que poder celebrar vuestra amistad (no hace falta que me lo demostréis ☺). **Pauliña**, gracias por decidir caer en este grupo. Teniendo en cuenta lo mucho que lo haces, podemos sentirnos afortunadas de que hayamos sido las elegidas para disfrutar de ti y de tus incontables anécdotas cada día. **Triana**, **Lily**, aunque a veces nuestras agendas no nos hayan permitido coincidir todo lo que querríamos, gracias por formar parte de todos los momentos inolvidables que hemos vivido a lo largo de estos años. **Clara**, **Belén**, **Alicia**, os tengo que dar las gracias, junto con **David**, **Antonio** y **Andrés**, por hacer crecer este grupo y por garantizar que las risas y los buenos momentos serán siempre una constante.

Y es que, a pesar de que a veces (más por la noche que por el día) me saquéis de quicio y no tenga más remedio que abandonaros a vuestra suerte, doy gracias cada día por teneros; por permitirme ser la pepito grillo de este grupo que me da la vida. Sois casa, y estando a 1000 Km de la mía, es algo que no dejaré nunca de agradeceros. Casi nunca os lo digo, pero lo pienso siempre: os quiero mucho.

Son muchos años en Barcelona y no he parado de conocer gente que hace que me quiera quedar. Desde mis compis de carrera a mis compis de máster, han sido siempre un motivo más para continuar en esta ciudad. Sandra, vuelvo a tener que darte las gracias por permitirme compartir momentos con tus compis de equipo (**Helena**,

Ari, **Marina**, **Ali**…) y muchas más en quienes he encontrado un espacio seguro y quienes han formado parte de mis findes y otros momentos de desconexión de estos años que han sido claves para conservar la cordura. Y si hablamos de cordura, que haya podido terminar esta tesis con la mía intacta ha sido en gran parte a ti, **Júlia**. Gracias por aportarme las herramientas necesarias para afrontar los momentos finales de esta tesis. **Chema**, gracias por la increíble portada de esta tesis y por acogerme, junto con **Uxía**, los últimos días de escritura de esta tesis. Seguro que nos esperan muy buenos momentos en este piso.

Pero por mucho que Barcelona sea el lugar donde vivo, Pontevedra siempre será hogar. Y eso es en gran parte gracias a vosotros, "Friends". **Sanmar**, **Mang**, **Lois**, **Marce**, **Gonzi**, **Adri, Laura**, **Ferri**, **Tilve**, si os doy las gracias de manera individual a cada uno, escribo otra tesis. Permitidme simplemente daros las gracias por acompañarme desde nuestros tiempos de instituto y por seguir siendo la razón de volver a casa tantos años después. Por mucho que pase el tiempo, sé que siempre estaréis, con un mensaje en la distancia o con un abrazo cuando vuelvo. Y ahí estará también mi familia gumera. **Alda**, **Mery**, **Noa**, **Alba**, **Ángela**, el concepto equipo nace con vosotras y me lo seguís demostrando año tras año desde hace 15 años ya. **Laura**, **Pili**, **Óscar**, es imposible echar la vista atrás y que no aparezcáis, gracias por seguir estando después de tantísimos años. Gracias, de corazón, a todas y todos por ser el mejor ejemplo de amistad y apoyo total.

Y de la familia que se elige, a la familia que te toca, que en mi caso no podría ser mejor. Gracias a mis **abuelos**, que ya no están, pero siempre han estado y estarán. Y a mis **abuelas**, por ser el ejemplo perfecto de lo que significa cuidar y amar de manera incondicional. A mis **tíos** y **primos** porque, aunque siempre habéis estado en la distancia, no os ha impedido estar y acompañarme todos estos años. **Padrino**, unas navidades preparando contigo un examen de biología de 3º de la E.S.O decidí que esto es a lo que me gustaría

dedicarme y no sabes lo que agradezco que, después de todo, puedas verme convertida en doctora.

Mami, **papi**, las gracias se quedan cortas. Gracias por darme todas las herramientas y recursos necesarios para que pudiera perseguir todo lo que me propusiera. Por ser siempre el balance perfecto entre prudencia y valentía. Con vosotros sé que puedo saltar tan alto como quiera y no importa si me caigo, porque seréis siempre mi red de seguridad. **Ramonito**, gracias por estar desde el principio de todo. Son 29 años (y nueve meses un poco apretados de más) de apoyo y amor incondicional. Sé que no sería quien soy, ni habría llegado tan lejos, de no haberte tenido siempre a mi lado. Los últimos agradecimientos son para vosotros, porque sé que serán siempre los primeros. Os quiero mucho.

INDEX

AKNOWLEDGEMENTS 2

LIST OF FIGURES 12

SUMMARY 15

RESUMEN 16

ABBREVATIONS 17

INTRODUCTION 21

1. CANCER 21
2. CELLULAR SENESCENCE 23
   - 2.1. Hallmarks of senescence 26
   - 2.2. Senescence in cancer 34
3. DUAL ROLES OF SENESCENCE IN CANCER 41
   - 3.1. Senescence, the first protection barrier against tumorigenesis 41
   - 3.2. Senescence: fuel for tumorigenesis 45
4. IN VIVO MODELS FOR MONITORING AND KILLING SENESCENCE 50

HYPOTHESIS 55

OBJECTIVES 55

MATERIALS & METHODS 56

RESULTS 70

1. SUSE SYSTEM: NEW MODEL TO STUDY SENESCENCE IN VIVO 70
   - 1.1 Characterization of the SuSe model as a new model for studying senescence in vivo 72
   - 1.2 PyMT/SuSe mice: a novel oncogenic in vivo model for studying the role of senescence in tumorigenesis 73
2. ELUCIDATING THE ROLE OF OIS IN TUMOR DEVELOPMENT 79
   - 2.1 Elimination of senescent cells at early stages promotes tumorigenesis 79
3. SENESCENT CELLS ARE NEEDED FOR MAINTAINING A PROTECTIVE TME IN EARLY DEVELOPMENT STAGES 83

3.1 Single-Cell RNA-sequencing analysis reveals that early senolysis reduces T cells and enhances macrophage infiltration 83
3.2 RNAseq of CD45+ populations reveals pro-tumorigenic macrophage profile following early senolysis 86
3.3 Elimination of the macrophage population induced by senolysis prevents its pro-tumorigenic effect. 89
4. SENESCENT CELLS MODULATE CYTOKINE RELEASE PATTERNS IN THE TME 92
4.1 Multiplex cytokine assay reveals differences in cytokine levels in 9-week tumors with and without senescent cells. 92
4.2 RNAseq analysis shows upregulation of CCL2, CCL3 and CCL7 in the immune population following early senolysis 95
4.3 scRNA-seq reveals macrophages as sources and responders to CCL2, CCL3 and CCL7 96
4.4 Pro-tumorigenic microenvironment derived from early senolysis favors metastatic tumor cell selection 100
4.5 CCL2 blockade mitigates pro-tumorigenic effects of early senolysis and exhibits anti-tumor activity when combined 103
5. UNDERSTANDING THE ROLE OF TIS IN CANCER TREATMENT EFFICACY 108
5.1 Utilizing the SuSe model to study TIS in syngeneic tumor systems 108
5.2 Targeting therapy-induced tumor senescent cells with the SuSe system demonstrates anti-tumor efficacy 110
5.3 PD-L2 blockade enhances anti-tumor efficacy by enabling CD8 T cell elimination of therapy-induced senescent cells 114
DISCUSSION 118
SENESCENT CELL IDENTIFICATION: THE CHALLENGE OF LACKING A UNIVERSAL MARKER 119
TO KILL OR NOT TO KILL SENESCENT CELLS? IN CANCER, TIMING HOLDS THE ANSWER 124
The immune system dictates the timing 127

FUTURE PERSPECTIVES OF SENOLYSIS AS CANCER TREATMENT .129
CONCLUSIONS 134
BIBLIOGRAPHY 136

LIST OF FIGURES

FIGURE 1. CANCER STATISTICS OF YEARS 2022 AND 2045. 21
FIGURE 2. NEW DIMENSIONS OF THE HALLMARKS OF CANCER. 23
FIGURE 3. DIVERSE FACTORS DRIVING SENESCENCE. 25
FIGURE 4. REGULATION OF THE CELL CYCLE: CHECKPOINTS AND INHIBITORY FACTORS.....27
FIGURE 5. MECHANISMS OF CELL CYCLE REGULATION AND SENESCENCE PATHWAYS. 29
FIGURE 6. P38α ACTIVITY INCREASES THE ACTIVITY OF A SASP 32
FIGURE 7. REGULATION OF SASP EXPRESSION BY P38MAPK, IL-1, IL-6 AND NFκB PATHWAYS. 33
FIGURE 8. RAS/RAF/MAPK AND PI3K/AKT/MTOR PATHWAYS ARE INVOLVED IN OIS. 37
FIGURE 9.DISTINCT CHEMOTHERAPY TREATMENTS CAN INDUCE TIS. 40
FIGURE 10. SENESCENT CELLS BEHAVE AS A BARRIER FOR TUMORIGENESIS. 44
FIGURE 11. PERSISTANCE OF SENESCENT CELLS IN THE TUMOR PROMOTES TUMORIGENESIS THROUGH THE SASP.....47
FIGURE 12. THE DUAL ROLE OF CELLULAR SENESCENCE IN CANCER..50
FIGURE 13. SCHEMATIC DESIGN OF INK-ATTAC ACTIVATION SYSTEM. 52
FIGURE 14. SCHEMATIC DESIGN OF P16-3MR ACTIVATION SYSTEM...53
FIGURE 15. GENERATION OF SUSE MICE. 71
FIGURE 16. MECHANISM OF THE SUSE SYSTEM.....72
FIGURE 17. VALIDATION OF P16/IL-6 CO-EXPRESSING CELLS APOPTOSIS IN VIVO FOLLOWING SENESCENCE INDUCTION IN VIVO. 73
FIGURE 18. GENERATION OF PYMT/SUSE MOUSE MODEL. 74
FIGURE 19. MONITORING CELLULAR SENESCENCE DURING TUMOR PROGRESSION. 75
FIGURE 20. VALIDATION OF THE MCHERRY/GFP REPORTER SYSTEM IN THE PYMT/SUSE MICE.....77
FIGURE 21. VALIDATION OF SUICIDE SYSTEM INDUCTION IN THE PYMT/SUSE MODEL. 78
FIGURE 22. ELIMINATION OF SENESCENT CELLS AT EARLY STAGES ACCELERATES TUMORIGENESIS.....80

FIGURE 23. ELIMINATION OF SENESCENT CELLS AT FIRST STAGES PROMOTES METASTASIS.....81
FIGURE 24. ELIMINATION OF SENESCENT CELLS AT LATE STAGES EXHIBITS A MODEST ANTI-TUMOR EFFECT. 82
FIGURE 25. SCHEMATIC VIEW OF SC-RNASEQ STRATEGY. 83
FIGURE 26. IMPACT OF EARLY AP21967-INDUCED SENESCENT CELL ELIMINATION ON TME COMPOSITION.....85
FIGURE 27. DIFFERENCES IN RNA EXPRESSION OF CD45+ POPULATION OF 9-WEEK SAMPLES TREATED WITH VEHICLE OR AP21967. 87
FIGURE 28. AP21967 TREATMENT AT 4 WEEKS PROMOTES MRC-1 MACROPHAGE POLARIZATION. 88
FIGURE 29. ELIMINATION OF THE MACROPHAGE POPULATION THAT APPEARS AFTER SENOLYSIS PREVENTS ITS PRO-TUMORIGENIC EFFECT. 90
FIGURE 30. ELIMINATING THE MACROPHAGE POPULATION THAT APPEARS AFTER SENOLYSIS PREVENTS THE INCREASE IN THE METASTASIS POTENTIAL. 91
FIGURE 31. ELIMINATION OF SENESCENT CELLS AT FIRST STAGES ALTERS CYTOKINE RELEASE PATTERN.....94
FIGURE 32. DIFFERENCES IN THE PATTERN OF EXPRESSION OF SOME CYTOKINES IN THE CD45+ OR CD45- POPULATION DEPENDING ON THE PRESENCE OF SENESCENT CELLS. 96
FIGURE 33. CCL2, CCL3 AND CCL7 ARE MAINLY EXPRESSED BY THE MACROPHAGE POPULATION. 98
FIGURE 34. SENESCENT CELLS REMOVAL CREATES A FEEDBACK POSITIVE LOOP OF CCL2, CCL3 AND CCL7 SECRETION THAT WILL RETAIN MACROPHAGES IN THE TUMOR. 99
FIGURE 35. EARLY SENOLYSIS PROMOTES A PRO-TUMORIGENIC MICROENVIRONMENT DRIVEN BY MACROPHAGES.....100
FIGURE 36. THE PRO-TUMORIGENIC MICROENVIRONMENT CREATED BY SENESCENT CELLS EARLY REMOVAL FAVOR SELECTION OF METASTASIS-PRONE TUMOR CELLS. 102
FIGURE 37. BLOCKING CCL2 PREVENTS THE PRO-TUMORIGENIC EFFECT OF EARLY SENOLYSIS.....105

FIGURE 38. BLOCKING CCL2 IN COMBINATION WITH EARLY SENOLYSIS REDUCES THE NUMBER OF LUNG METASTASIS. 106
FIGURE 39. EARLY SENOLYSIS HAS A PRO-TUMORIGENIC EFFECT DRIVEN BY MACROPHAGES. 107
FIGURE 40. SCHEME DESIGN OF TWO SYNGENEIC MOUSE MODEL USED FOR STUDYING TIS. 108
FIGURE 41. DOXORUBICIN TREATMENT INDUCES SENESCENCE IN PYMT/SUSE CELLS IN VITRO. 110
FIGURE 42. KILLING THERAPY-INDUCED SENESCENT TUMOR CELLS HAS AN ANTITUMORIGENIC EFFECT. 112
FIGURE 43. BLOCKING CD8 T CELLS PREVENTS THE ANTI-TUMOR EFFECT OF SENOLYSIS. 113
FIGURE 44. ELIMINATING SENESCENT CELLS FROM THE ENVIRONMENT DOESN'T HAVE AN EFFECT ON TUMOR GROWTH. 114
FIGURE 45. COMBINING TIS AND PD-L2 BLOCKADE HAS AN ANTI-TUMORAL EFFECT. 116

SUMMARY

Cellular senescence is multifaceted process characterized by a stable cell cycle arrest and the secretion of a variety of pro-inflammatory factors collectively known as the Senescence-Associated Secretory Phenotype (SASP). Previous studies have demonstrated the dual role of senescent cells in cancer: they can act as a crucial tumor-suppressive mechanism by preventing the proliferation of damaged cells, but their accumulation can also promote tumor progression through the SASP. Despite extensive research, the mechanisms underlying this duality remain incompletely understood. Therefore, gaining new insights into the role of senescent cells at different stages of tumor development is crucial for advancing anti-cancer and senolytic therapies.

In vivo models are invaluable for studying the dynamic processes and systemic effects of senescent cells. However, current models that detect and eliminate senescent cells typically rely on a single marker, such as p16. This approach is limited by the inherent heterogeneity of senescent cells, making it challenging to accurately identify them using only one marker, which complicates their therapeutic targeting in clinical settings

In this thesis, I describe a novel transgenic mouse model capable of tracking and eliminating cells expressing the senescence markers p16 and interleukin 6 (IL-6). By combining these two markers, we aimed to selectively target senescent cells *in vivo*, providing deeper insights into their contributions to breast cancer biology. Furthermore, this model has enabled us to unravel potential molecular pathways involving the immune system, thereby opening new avenues for the use of senolysis as an anti-cancer strategy.

RESUMEN

La senescencia celular es un proceso complejo caracterizado por una detención estable del ciclo celular y la secreción de diversos factores proinflamatorios conocidos como SASP. Estudios previos han demostrado el doble papel de las células senescentes en el cáncer: pueden actuar como un mecanismo supresor de tumores al impedir la proliferación de células dañadas, pero su acumulación también puede promover la progresión tumoral. A pesar de las numerosas investigaciones realizadas, los mecanismos subyacentes a esta dualidad siguen sin conocerse del todo.

Los modelos in vivo son muy valiosos para estudiar los procesos dinámicos y los efectos sistémicos de las células senescentes. Sin embargo, los modelos actuales que detectan y eliminan estas células suelen basarse en un único marcador, como p16. Este enfoque se ve limitado por la heterogeneidad inherente de las células senescentes, lo que dificulta su identificación precisa.

En esta tesis, se describe un nuevo modelo de ratón transgénico capaz de rastrear y eliminar células que expresan los marcadores de senescencia p16 e IL-6. Mediante la combinación de estos dos marcadores, hemos podido eliminar selectivamente las células senescentes in vivo, proporcionando una visión más profunda de su contribución a la biología del cáncer de mama. Así, este modelo nos ha permitido desentrañar posibles vías moleculares en las que interviene el sistema inmunitario, abriendo nuevas vías para el uso de la senolisis como estrategia anticancerígena.

ABBREVATIONS

ADCC	Antibody-dependent cell-mediated cytotoxicity
AUF1	AU-rich element RNA-binding protein 1
BAFF	B-cell Activating Factor
BTC	Betacelulina
BSA	Bovine serum albumine
CAF	Cancer-asscociated fibroblast
CCL2	C-C motif ligand 2 (
CCL3	C-C motif ligand 3
CCL5	C-C motif ligand 5
CCL7	C-C motif ligand 7
CCR1	C-C motif receptor 1
CCR2	C-C motif receptor 2
CCR5	C-C motif receptor 5
Casp8	Caspase 8
STING	Cgas–Stimulator of Interferon Genes
CXCL1	Chemokine (C–X–C motif) ligand 1
CXCL2	Chemokine (C–X–C motif) ligand 2
CAR	Chimeric antigen receptor
CXCL5	CXC motif ligand 5
cGAS	Cyclic GMP–AMP synthase
CDK	Cyclin-dependent kinase
CDKi	Cyclin-dependent kinase inhibitors
DC	Dendritic cells
DDR	DNA damage response
DMEM	Dulbecco's modified eagle's media
EGFP	Enhanced green fluorescent protein
FKBP	FK506-binding protein
FRB	FKBP12-rapamycin binding
GCV	Ganciclovir
GSEA	Gene set enrichment analysis
G-CSF	Granulocyte colony-stimulating factor
GM-CSF	Granulocyte monocyte Colony-Stimulating Factor
GFP	Green fluorescent protein

HRAS	Harvey rat sarcoma
HSP27	Heat shock protein 27
HCC	Hepatocellular carcinoma
HSV-TK	Herpes simplex virus 1 thymidine kinase
HLA-E	Hystocompatibility ligand antigen E
IL-1R1	IL-1 receptor
IRAK1	IL-1 receptor- associated kinase 1
IF	Immunofluorescence
IHQ	Immunohistoquemistry
ICAM	Intercellular Adhesion Molecule 1
IFN	Interferon
IL-1α	Interleukin 1 alpha
IL-1-ß	Interleukin 1 beta
IL-1-R	Interleukin 1 receptor
IL-10	Interleukin 10
IL-12	Interleukin 12
IL-13	Interleukin 13
IL-15	Interleukin 15
IL-17	Interleukin 17
IL-18	Interleukin 18
IL-19	Interleukin 19
IL-2	Interleukin 2
IL-2R	Interleukin 2 receptor
IL-21	Interleukin 21
IL-22	Interleukin 22
IL-23	Interleukin 23
IL-24	Interleukin 24
IL-25	Interleukin 25
IL-26	Interleukin 26
IL-27	Interleukin 27
IL-28	Interleukin 28
IL-29	Interleukin 29
IL-3	Interleukin 3
IL-30	Interleukin 30
IL-31	Interleukin 31
IL-32	Interleukin 32

IL-33	Interleukin 33
IL-33R	Interleukin 33 receptor
IL-4	Interleukin 4
IL-5	Interleukin 5
IL-6	Interleukin 6
IL-7	Interleukin 7
IL-8	Interleukin 8
LIF	Leukimia inhibitory factor
M-CSF	Macrophage colony-stimulating factor
Mrc-1	Manose receptor
MK2	MAPK-activated protein kinase 2
MMP	Metalloprotease
Mmp11	Metalloprotease 11
Mmp14	Metalloprotease 14
Mmp2	Metalloprotease 2
Mmp3	Metalloprotease 3
MMTV	Mouse mammary tumor virus
MDSC	Myeloid-derived suppressor cell
NK	Natural killer
NSCLC	Non-small cell lung cancer
OIS	Oncogene-induced senescence
Pan-K	Pan-keratin
Pten	PHOSPHATASE AND TENSIN HOMOLOG gene
PCR	Polymerase chain reaction
PyMT	Polyoma middle T
PD-1	Programmed Cell Death protein 1
PD-L2	Programmed cell death-ligand 2
ROS	Reactive oxygen species
RANKL	Receptor activator of nuclear factor kappa-B ligand
NKG2A	Receptor natural Killer group 2 member A
RBC	Red blood cell
RFP	Red fluorescent protein
RNAseq	RNA sequencing
SA-β-Gal	Senescence-associated ß-Galactosidase

SASP	Senescence-associated secretory phenotype
STAT3	Signal transducer and activator of transcription 3
scRNA-seq	Single-cell RNA-sequencing
SuSe	Suicidal senescence
TIS	Therapy-induced senescence
TME	Tumor microenvironment
TNFα	Tumor necrosis factor alpha
TGF-ß	Tumor necrosis factor beta
uPAR	Urokinase-type plasminogen activator receptor
VEGF	Vacular endothelial growth factor
WT	Wild-type
WHO	World health organization

INTRODUCTION

1. Cancer

According to the Global Cancer Observatory, part of the World Health Organization (WHO), there were an estimated 20 million cancer cases worldwide in 2022 **(Figure 1)** (1). Breast and lung cancers were the most common, contributing 12.5% and 12.2% of the total number of new cases diagnosed, respectively (2). Projections for 2045 indicate that both incidence and death rates are expected to increase, underscoring that cancer remains and will continue to be a leading cause of death globally **(Figure 1)** (3).

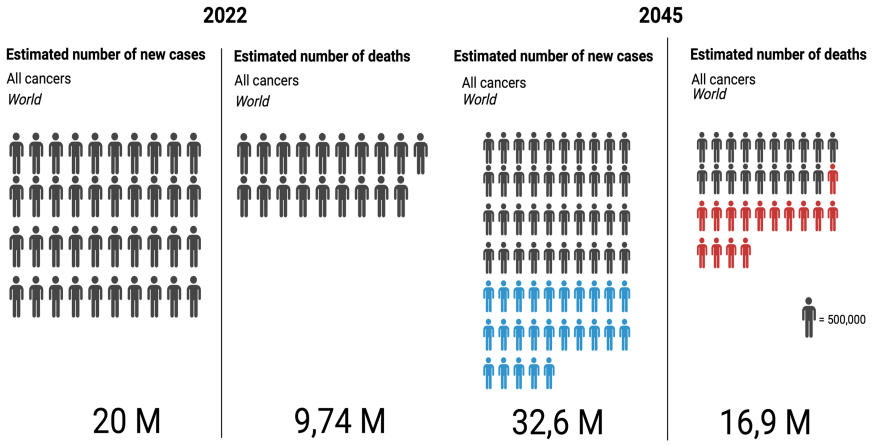


Figure 1. Cancer statistics of years 2022 and 2045.
Evolution of the estimated number of new cancer cases and deaths from the year 2022 (left) to the year 2045 (right). Data extracted from Cancer Tomorrow, IARC: https://gco.iarc.who.int

Cancer is a group of diseases characterized by the uncontrolled growth and spread of abnormal cells. It can arise in almost any part of the body, and often involves a combination of genetic factors and environmental exposure. In the year 2000, six hallmarks of cancer were initially proposed, providing a logical framework for

understanding the remarkable diversity of tumor pathogenesis (4). In the next elaboration of this concept, proposed 10 years later, the tumor microenvironment (TME) emerged as a fundamental aspect to be understood. Avoiding immune destruction by T and B lymphocytes, macrophages, and natural killer (NK) cells was identified as an “emerging hallmark” critical for supporting neoplastic proliferation (5). Additionally, genome instability and mutation, driving tumor progression and tumor-promoting inflammation, were incorporated as acquired enabling characteristics, culminating in a total of 10 hallmarks of cancer (6).

As knowledge of cancer mechanisms has progressed, other facets of the disease have emerged as potential refinements. Phenotypic plasticity and disrupted differentiation have been recognized as discrete hallmark capabilities, alongside non-mutational epigenetic reprogramming, and polymorphic microbiomes, which constitute distinctive enabling characteristics that facilitate the acquisition of hallmark capabilities (7).

Genome instability and mutation, sustained DNA damage can lead to deactivate tumor suppressor genes, disrupt essential cellular pathways and induce mutations that can activate proto-oncogenes, such as *Ras* or *MYC*. These activated proto-oncogenes can become oncogenes, driving the uncontrolled proliferation of cells and characteristic of tumorigenesis (8). Paradoxically, DNA damage can also trigger stable growth arrest as a protective mechanism against the propagation of damaged DNA, known as cellular senescence **(Figure 2)** (9).

Thus, senescence completes the new dimensions of cancer development and malignant progression (10).



Figure 2. New dimensions of the hallmarks of cancer.
Latest version of the hallmarks of cancer which include unlocking phenotypic plasticity, non-mutational epigenetic reprogramming, polymorphic microbiomes, and cellular senescence. Illustration adapted from "Hallmarks of Cancer: New dimensions" (10)

2. Cellular senescence

Cellular senescence can be defined as as the cellular ability to remain in permanent cell cycle arrest (11). The concept of senescence has evolved over time, transitioning from a static notion to being understood as a dynamic process. It was first observed in human fibroblasts in culture by Hayflick and Moorhead (11). As the number of cell divisions experienced by cultured cells accumulates and approaches a threshold, the cell population begins to divide more slowly and eventually stops growing, but this state does not entail cell death. Instead, the cells actively maintain active metabolism, although they do not respond to growth stimuli (12). This type of senescence is known as replicative senescence.

Years later, replicative senescence, was associated with other physiological mechanisms such as telomere shortening (13). Telomeres are repetitive DNA sequences located at the ends of linear chromosomes that serve to protect the DNA ends from degradation and recombination. However, due to the inherent limitations of the replication machinery, which cannot fully replicate the ends of linear DNA molecules, telomeres become progressively shorter with each round of cell division. When telomeres reach a critically short length, they are perceived as double-stranded DNA breaks, leading to telomere-initiated senescence or apoptosis. (14). Telomeres are elongated biologically by a ribonucleoprotein with DNA polymerase activity known as telomerase However, in most adult tissues, telomerase activity levels are insufficient to counterbalance the progressive telomere shortening that occurs with aging (15). Therefore, telomere shortening is a characteristic associated with aging, which has been extensively studied in the field of senescence.

In fact, the accumulation of senescent cells in aged tissues is believed to contribute to organ dysfunction through various mechanisms (16). Their accumulation interferes with tissue regeneration in a cell-autonomous manner, and it also limits the regenerative potential of stem cell pools in a cell-non-autonomous manner, contributing to various chronic age-related diseases (17). However, senescence is also responsible for maintaining tissue homeostasis, a fundamental aspect of various biological processes such as embryonic development, wound healing, and tissue remodeling (18). In fact, senescence essentially acts as a safeguard mechanism, preventing damaged or stressed cells from proliferating. This regulatory function is exemplified in various physiological contexts, including the development of different organs like the kidneys, the formation of specialized structures such as the

endolymphatic sac in the inner ear, and the establishment of vital support systems like the placenta (19).

Consequently, cellular senescence is now recognized as a multifaceted stress response that can be triggered by a myriad of factors, both intrinsic and extrinsic (20). These factors include a variety of cellular stresses, ranging from telomere shortening to the activation of oncogenes, oxidative and genotoxic stress induced by external factors like irradiation or chemotherapeutic agents, mitochondrial dysfunction, and dysregulation in epigenetic features **(Figure 3)** (21). The evolving understanding of senescence underscores the intricate interplay between cellular senescence and the various stressors encountered by cells, highlighting its significance in maintaining cellular integrity and overall tissue health.

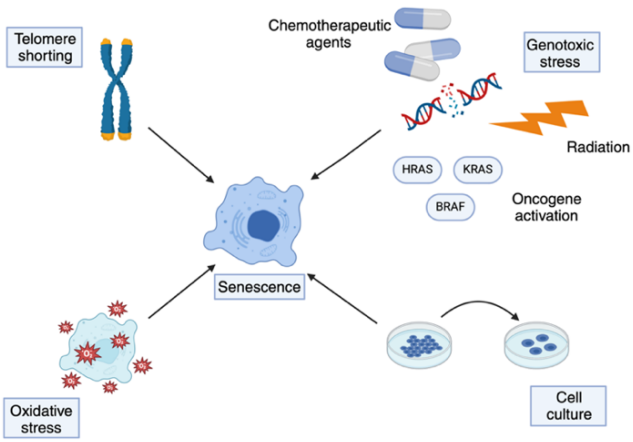


Figure 3. Diverse factors driving senescence.
Representation of different stimuli that create stressful conditions for the cell. Senescence functions as a self-defense mechanism to prevent the proliferation of potentially damaged cells. Illustration adapted from "The power and the promise of oncogene-induced senescence markers" (22).

2.1. Hallmarks of senescence

While the main and essential characteristic defining all types of senescence is the stable cell cycle arrest that limits the growth and proliferation of damaged or aged cells, other important characteristics have been studied as research in this field has gained interest. A thorough comprehension of the senescence phenotype is key to understanding the physiological functioning of senescent cells, their relationship with other cells and the microenvironment in which they are found.

The senescence phenotype is mainly characterized by the engagement of various cyclin-dependent kinase inhibitors (CDKi), an increased lysosomal content, and enhanced secretion of proinflammatory and tissue-remodeling factors (22).

2.1.1. Cell cycle inhibitors associated with senescence.

The cell cycle, a series of events that lead to a cell growth, replication, and division into two daughter cells, is a tightly regulated process. It encompasses a series of intricate processes, starting by duplication of genetic material during S phase and culminating in the precise segregation of two identical daughter cells during M phase**.** Preceding S phase, the cell enters a critical preparatory gap phase known as G1, during which the cell's progression through the cycle is determined. Driving this progression are the regulatory cyclin-dependent kinases (CDKs). At the beginning of G1, cyclin D-Cdk4/6 monophosphorylates pRB, which is bound to E2F transcription factors. Once the cell passes the restriction point, cyclin E-Cdk2 hyperphosphorylates pRB. This causes it to dissociate from the E2F factors, which then translocate to the nucleus and activate transcription of S phase genes (23) **(Figure 4)**. The two main pathways controlling these CDKs to prevent continuous division are the p16/pRB and the p53/p21 axis.

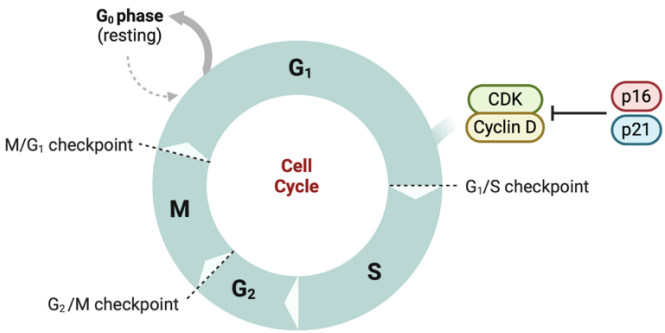


Figure 4. Regulation of the Cell Cycle: Checkpoints and Inhibitory Factors.
This diagram illustrates the regulation of the cell cycle, highlighting the key checkpoints and inhibitory factors involved in maintaining cellular homeostasis. CDKs and their associated cyclins drive cell cycle progression, while CDKIs like p16 or p21 impose regulatory control.

p16, encoded by the human gene *Cdkn2a*, plays a crucial role in regulating cell cycle progression and senescence (23). It is a specific inhibitor of the cyclin-dependent kinases CDK4 and CDK6 (24). Its main function is to prevent cell transition from G1 to S phase, leading to subsequent proliferation arrest by rendering the retinoblastoma protein (pRB) in a hypophosphorylated state **(Figure 5)** (25). After its first description, it was observed that p16 levels accumulated progressively with the proliferative history of cells in culture, despite having long telomeres and high levels of telomerase (26). This telomere-independent clock was abrogated in cells genetically deficient in the *Cdkn2a* locus, proving that cells in culture possess at least two independent clocks: one is telomere dependent and mostly registers the accumulated number of cell divisions; the other clock is p16 dependent and mainly records the exposure of cells to mitogenic stimulation (27).

The p53/p21 pathway also plays a crucial role in regulating cell cycle progression and senescence. *ARF*, a splicing variant of *Cdkn2a* (24), acts as a tumor suppressor by interacting with p53, a

homotetrameric transcription factor that is induced by DNA damage or inappropriate mitogenic signaling (28). The p53-responsive gene products include *Cdkn1a*, which encodes for the potent inhibitor of CDKs named p21, and Mdm2, which is a negative feedback regulator that helps terminate the p53 response (29). By inhibiting Mdm2, ARF stabilizes and activates p53 and activation and accumulation of p53, through protein stabilization, can lead to cell-cycle arrest or apoptosis **(Figure 5)** (30).

In cases of oncogene activation, inappropriately increased E2F or Myc signals trigger ARF expression and activate p53 to induce either cell-cycle arrest or apoptosis, depending on the biological context (29). Like what p16 does, the p21 protein exerts its inhibitory effect on cyclin-CDK complexes, including CDK1, CDK2, CDK3, CDK4, and CDK6, crucially impeding hyperphosphorylation of RB, thereby regulating cell cycle progression **(Figure 5)** (31). Although p21 is consistently upregulated in response to different senescence-inducing stimuli, its expression is part of a more generic DNA damage response (DDR), which makes it difficult to use it as a unique senescence marker (21).

In summary, both pathways are complex, having several upstream regulators activators and downstream effectors as well as modifying side branches, including "cross talk" between the pathways. Whereas p16 is an inhibitor of the cyclin-dependent kinases CDK4 and CDK6 and acts by imposing a G1 cell cycle arrest, ARF regulates p53 stability through inactivation of the p53-degrading ubiquitin ligase MDM2 **(Figure 5)**. Importantly, one difference between these pathways is that the p16/pRB pathway imposes an essentially irreversible arrest of cell proliferation, whereas p53/p21 does not necessarily result in an irreversible growth arrest (32). To illustrate, although the expression of p21 may be important for cellular senescence initiation, its expression is transient after senescence initiation and does not persist during the maintenance

phase(24). Additionally, not all cells that express p21 are senescence and p21 upregulation occurs in the implementation of cellular quiescence, and thus may lead to false-positive detection of senescent cells.

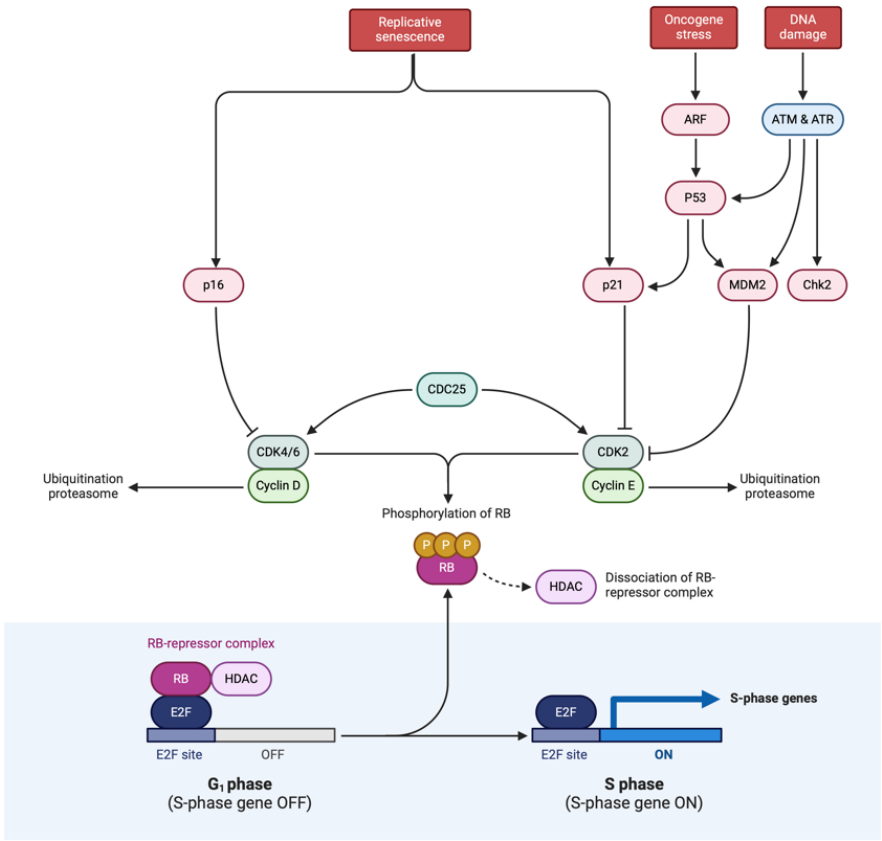


Figure 5. Mechanisms of Cell Cycle Regulation and Senescence Pathways. *Summary of key mechanisms in cell cycle regulation and pathways leading to cellular senescence. CDK4/6-Cyclin D and CDK2-Cyclin E complexes drive the cell cycle by phosphorylating RB, releasing E2F to activate S-phase genes. Checkpoints like G1/S monitor DNA integrity, with p16 and p21 inhibiting CDKs to halt progression. DNA damage and oncogene stress activate ATM/ATR, stabilizing p53, which induces p21 to inhibit CDKs and maintain RB in a hypophosphorylated state, blocking the cell cycle. The roles of MDM2 in p53 regulation, CDC25 in CDK activation, and ubiquitination in protein degradation highlight the dynamic regulation ensuring cellular homeostasis and preventing uncontrolled proliferation.*

2.1.2. Senescence-associated ß-Galactosidase activity

In addition to the overexpression of p16, p21 or p53, senescent cells exhibit additional characteristics that need to be considered when defining a senescent cell. The first and most widely used assay for senescence is the cytochemical detection of β-galactosidase activity at pH 6. This enzyme activity is normally assayed in cultured cells or tissue sections using the chromogenic substrate 5-bromo-4-chloro-3-indolyl β-d-galactopyranoside (X-Gal), or the fluorescent analogue fluorescein-di-β-dgalactopyranoside (FDG) (33). While the optimal pH to detect lysosomal β-galactosidase would be 4.0, it was observed that an abnormal lysosomal activity associated with senescent cells enables the detection of β-galactosidase at a suboptimal pH of 6.0 (34). At first it was not clear whether the so-called "senescence-associated ß-Galactosidase" (SA-β-Gal) was a distinct enzyme that was induced during senescence or whether it was a consequence of increased expression and/or altered activity of the lysosomal β-galactosidase. Finally, it was demonstrated that the increased SA-ß-Gal activity was derived from the increased lysosomal content of senescent cells (35). Indeed, an increased number of lysosomes and elevated lysosomal activity had been associated with replicative senescence for many years (36).

Although SA-ß-Gal activity is generally accepted as a marker of senescence, both *in vitro* and *in vivo*, there is evidence for a positive SA-β-Gal reaction during cellular stress that is unrelated to senescence. A positive result for SA-ß-Gal reaction upon serum withdrawal or high confluency in cell culture are just some examples (34). Thus, we cannot consider SA-ß-Gal as a universal marker of senescence.

2.1.3. Senescence-Associated Secretory Phenotype

The genotoxic stress, whether caused by oncogene expression or any other agent that results in DNA damage, leads to the activation of numerous downstream effectors that are normally transient. However, the persistent activation of the p53 and Rb pathways in senescent cells results in the secretion of a diverse array of pro-inflammatory cytokines, chemokines, growth modulators, angiogenic factors, and matrix metalloproteinases, referred to as the Senescence-Associated Secretory Phenotype (SASP).

SASP expression is controlled by several signaling pathways in at least two distinct waves. After a senescence stimulus, the p38MAPK pathway gets activated by an increase in NFκB transcriptional activity, resulting in a transitory increase of numerous SASP factors (37). This initial activation first declines and subsequently increases once more. This second increase occurs at a post-transcriptional level, p38α activity increases the activity of MAPK-activated protein kinase 2 (MK2), a SASP effector kinase that modulates heat shock protein 27 (HSP27) and AU-rich element RNA-binding protein 1 (AUF1) that elevates SASP mRNAs stability **(Figure 6)** (38).

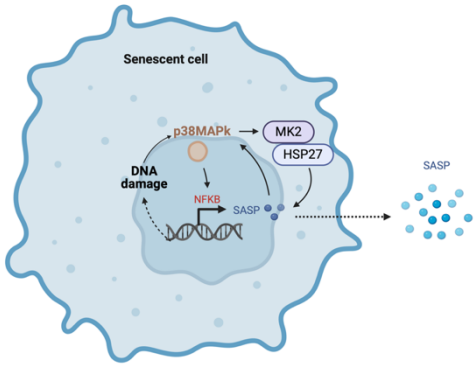


Figure 6. p38α activity increases the activity of a SASP
A senescence insult results in the activation of the p38MAPK pathway, mediated by an increase in NFκB transcriptional activity. This initial activation first declines and subsequently increases once more in a second post-transcriptional wave. p38α activity rises the activity of MK2, which modulates HSP27 that increases SASP mRNAs stability.

Another controller of SASP factors expression is mTOR signaling. It has been described that activated mTOR signaling can promote translation of some SASP factors, like interleukin 1 alpha (IL-1α), in senescent human fibroblasts induced by oncogenic *RAS* expression or radiation **(Figure 7)** (37,39). Moreover, IL-1α by binding to IL-1 receptor 1 (IL-1R1), which promotes the recruitment of IL-1 receptor-associated kinase 1 (IRAK1) can also activate NFκB pathway **(Figure 7)** (40). IL-6 is another factor that can also maintain senescence in a paracrine manner through the activation of signal transducer and activator of transcription 3 (STAT3) **(Figure 7)** (22). Chemokine (C–X–C motif) ligand 1 (CXCL1) and Chemokine (C–X–C motif) ligand 2 (CXCL2) are just other examples of some factors that can mantain cell cycle arrest and senescence (40).

It has also been described that Cyclic GMP–AMP synthase (cGAS) pathway can contribute to the SASP. This pathway typically detects cytosolic DNA to activate immune responses to viral infections. However, in senescent cells, cytoplasmic chromatin fragments activate the cGAS–Stimulator of Interferon Genes (STING) pathway, leading to SASP production **(Figure 7)**(41).

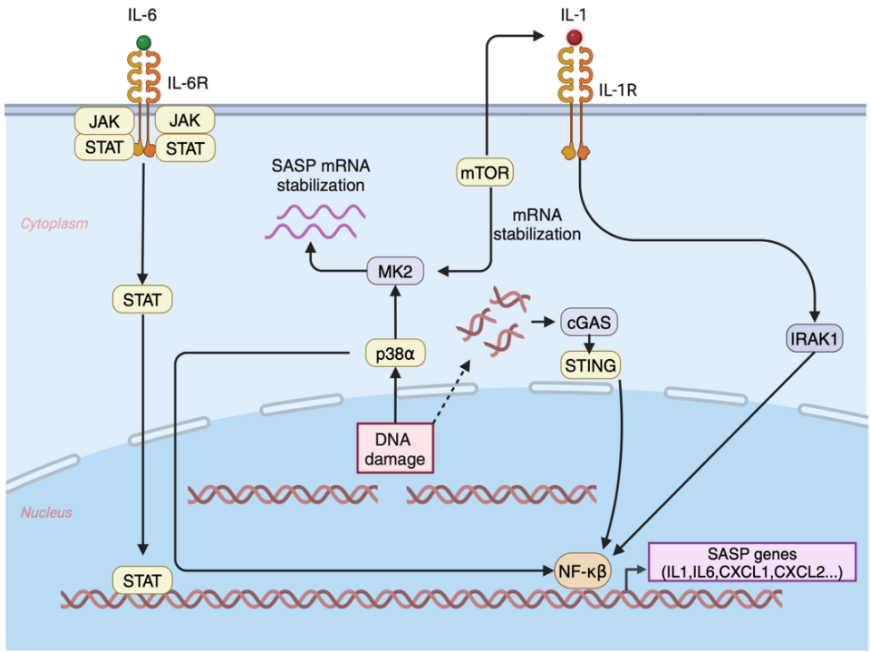


Figure 7. Regulation of SASP Expression by p38MAPK, IL-1, IL-6 and NFκB Pathways.

Upon DNA damage, the p38MAPK pathway is activated, leading to an increase in MK2 activity, which stabilizes SASP mRNA. This process involves the transient activation of NFκB, which increases SASP genes expression, such as IL-1, IL-6, CXCL1 or CXCL2. IL-6 can activate NFκB via STAT pathway and IL-1 via mTOR pathway. Moreover, cGAS also contributes to the SASP via STING pathway.

This secretory phenotype is, in fact, a key feature of senescent cells and is responsible for many of the pathophysiological effects associated with senescence. Interestingly, it mediates the reinforcement and spread of senescence through autocrine and paracrine signaling. Notably, the composition and concentration of the SASP can vary significantly depending on factors such as the duration of senescence, the origin of the pro-senescent stimulus (that is oncogene versus DNA damage, etc), and the specific cell type involved. In this regard, several studies have examined the effects of inducing senescence by different means, on the same cell type. For instance, a study using mesenchymal stromal cells treated

with oxidative stress, X-ray radiation and chemotherapy revealed that although at transcriptional level numerous pathways were commonly regulated, only a reduced number of proteins were shared (39).

It is important to notice that the SASP factors and many of the changes associated with senescent cells are not exclusive to senescence. Non-senescent cells can also express these characteristics, such as cancer-associated fibroblasts (CAFs) that closely mimic almost every characteristic of senescent fibroblasts, like the secretion of factors typically associated with senescence. The key difference, however, is that CAFs retain the ability to proliferate. (37). Therefore, relying on a single marker of senescence can lead to misleading results when identifying a senescent cell. To avoid this, most of the researchers in the field use a combination of at least two to four markers such as the expression of SA-β-Gal along with p16 or p21 and the expression of main SASP factors, like IL-6 or IL-1α, to identify senescent cells (42).

Having explained the phenomenon of cellular senescence and the distinct hallmarks, we now delve into the intricate relationship between senescence and cancer. Next section will explore how senescent cells influence both tumor progression and suppression, as well as the mechanisms through which they interact with surrounding cells and tissues. Understanding these interactions is crucial for developing or improving therapeutic strategies that can effectively inhibit cancer growth.

2.2. Senescence in cancer

Two main mechanisms exist by which a tumor cell may enter senescence: Oncogene-Induced Senescence (OIS) and Therapy-Induced Senescence (TIS).

2.2.1. Oncogene Induced Senescence (OIS)

The main signaling pathways involved in OIS are the p53/p21 and p16/Rb pathways, crucial for tumor suppression. Paradoxically, oncogenic activation can also lead to the expression of senescence-related genes, contributing to the senescence phenotype. In fact, the first evidence of OIS was documented during transduction of primary diploid fibroblasts with an activated Harvey rat sarcoma (HRAS)G12V allele, which resulted in an enlarged, flattened morphology and stalled mitotic activity (42). These findings were later corroborated *in vivo* in 2005 (43), confirming that some oncogenic driving pathways, such as RAS/RAF/MAPK, are involved in driving senescence. Another example is the PI3K/AKT/mTOR pathway, typically associated with cell growth and survival, which can also contribute to senescence when dysregulated, linking metabolic stress with senescence induction **(Figure 8)** (9).

Given that this type of senescence induction relies on the overexpression of activated oncogenes, the balance between the level of expression required to induce cell cycle arrest or neoplastic transformation is crucial (44). This is logical, given that, as previously stated, oncogenic signaling is transmitted through complex cascades of mediators that exert some negative-feedback regulation that can prevent the full activation of its downstream effectors. The first study demonstrating this phenomenon *in vivo* showed mice carrying endogenous activated oncogene *KRAS* that were able to develop premalignant lung lesions after months of latency, but few lesions progressed to be fully malignant tumors (45). In this case, the RAS/RAF pathway induces a negative feedback loop that attenuates activated protein MAPK and PI3K signaling, leading to senescence and opposing oncogenic Ras activity **(Figure 8)**. Another example is human naevi harboring the oncogenic V600E

mutation in BRAF, which showed cell cycle arrest and SA-βGal activity, with mosaic expression of p16 and no p53 upregulation or telomere attrition, suggesting that other mechanisms contribute to senescence induction in this context (46).

While most studies of OIS have centered on this chronic RAS/RAF/MAPK signaling, there is a growing interest in understanding the senescence phenotype due to hyperactivation of the PI3K/AKT pathway. It has been demonstrated that deletion of phosphatase and tensin homolog gene (*PTEN)* in the murine prostate epithelium resulted in benign neoplastic lesions and increased SA-βGal staining. Conversely, hyperactivation of the PI3K/AKT pathway triggers senescence in human cells by promoting enhanced p53 protein synthesis via mTORC1 **(Figure 8)**, despite not displaying a DDR or DNA-damage foci, and they maintain low levels of p16 and phosphorylated p53 (47). In any case, it is important to note that for any type of OIS to happen, the p53/p21 or p16I/Rb pathways must be functional.

Mouse models expressing activated oncogenes laid the foundation for the study of OIS *in vivo*, highlighting its role in tumorigenesis and its potential as a therapeutic target. Moreover, the development of much more sophisticated models, expressing the oncogene in an inducible manner, allowed to play with the timing of senescence induction. In the same way, genetic engineering has made it possible to combine this strategy with the induced depletion of the main agents in the regulation of senescence, such as p16, p21, or p53. One example is an innovative model in which liver cancer cells can be selectively driven into a senescent state through the genetic activation of endogenous p53 that offers a powerful approach for investigating senescence surveillance mechanisms (48).

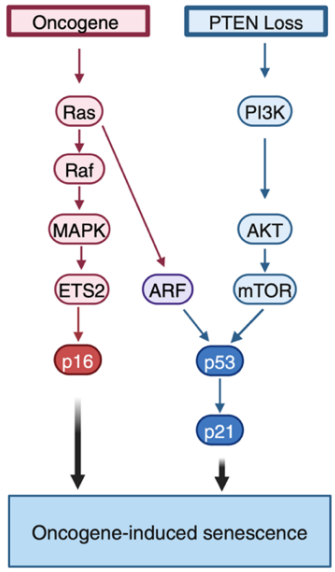


Figure 8. RAS/RAF/MAPK and PI3K/AKT/mTOR pathways are involved in OIS. *Ras activation ends in activation of p16 through the cooperation of MAPK signaling cascade. Ras activation can also stabilize p53 expression through ARF pathway. Loss of tumor suppressor gene PTEN induce activation of P13K pathway that will activate mTOR pathway, ending in the expression of p21.*

In conclusion, OIS serves as a critical mechanism by which tumor cells initially respond to and manage the cellular stress induced by oncogene expression or the loss of tumor suppressor mechanisms. Thereby, OIS can influence tumor progression and potentially contribute to cancer development if bypassed.

2.2.2. Therapy Induced Senescence (TIS)

Cancer therapy has traditionally relied on cytotoxic treatment strategies to eradicate tumors. In the early 2000s, landmark studies demonstrated that certain cancer therapies could trigger a senescent-like state in tumor cells, effectively halting their proliferation (49,50). This concept was designated as Therapy-Induced Senescence (TIS).

Unlike cell death, which was assumed the ultimate outcome of traditional anticancer treatments, TIS relies on inducing a stable state of non-division, effectively "locking" the cancer cells in a state where they no longer proliferate. The cellular decision between apoptosis and senescence is dependent, in part, on the magnitude of stress to which cancer cells are exposed. Lower levels of damage may trigger senescence-associated antiproliferative responses without activating the cascades of caspase activity that commit the cell to apoptosis (50). This approach has gained significant interest as an alternative or complementary strategy to traditional cytotoxic therapies. In fact, a variety of drugs have been shown to induce TIS, with some of the most common including DNA-damaging agents, such as doxorubicin and cisplatin, as well as other chemotherapeutic compounds like etoposide, paclitaxel, or CDK4/6 inhibitors, such as Palbociclib (51).

Doxorubicin is a DNA intercalating agent that prevents replication by blocking topoisomerase enzymes from re-ligating DNA strands after supercoil unwinding. It also promotes histone eviction from chromatin, evoking a DNA-damage response and promoting changes in the epigenome and transcriptome (52). This agent is used to treat a variety of cancers, including breast cancer, and can induce senescence by activating the p53 pathway. Importantly, doxorubicin can induce senescence both in tumoral and in nonmalignant cells, like vascular smooth muscle cells, other stromal cells, and human and mouse dermal cells **(Figure 9)** (53). Similarly, cisplatin, a platinum-based drug, induces extensive DNA cross-linking, leading to accumulation of oxidative stress that will induce cell cycle arrest and subsequent senescence via p16 pathway (**Figure 9)**. Cisplatin has been reported to induce cellular senescent-like growth arrest in nasopharyngeal carcinoma cell lines and in head and neck squamous cell carcinoma cells (52).

Another well-known chemotherapy drug is paclitaxel, which belongs to a family of microtubule inhibitors and is used to treat different types of solid tumors, such as breast or non-small cell lung cancer (NSCLC) (54). This drug impedes normal microtubule spindle dynamics, compromising the metaphase-anaphase transition, thus arresting the cell at mitosis **(Figure 9)**. It is known that paclitaxel treatment induces senescence *in vitro* in both cancer and non-cancer cells (53). Moreover, a study that shows the increasing in bioluminescence in p16 reporter mice, proved paclitaxel can induce senescence in noncancerous tissues *in vivo* (55).

Beyond traditional chemotherapy, certain targeted therapies can also induce senescence. CDK4/6 inhibitors, such as palbociclib, are alternative drugs used to treat several types of cancer, including ER+ breast cancer (56). Palbociclib targets CDK4 and CDK6, producing a cell-cycle arrest in the G1 phase, mimicking the mechanism of action of p16 **(Figure 9)**. In fact, there are studies showing palbociclib to induce cellular senescence in different types of cancer, like breast, gastric or hepatocellular carcinoma (57,58). However, it is important to notice that SA-β-galactosidase positivity was the method used to identify senescent cells, while the establishment of an irreversible proliferative arrest was not entirely measured. Moreover, given that palbociclib functions as a CDKi rather than a genotoxic agent, its induction of cellular senescence is expected to exhibit a degree of reversibility, as it does not induce irreversible damage to the genetic material of the cells (59). Moreover, inhibitors of the BRAF pathway, used in treating melanoma, and agents targeting the PI3K/AKT/mTOR pathway can also induce senescence in specific cancer types (60).

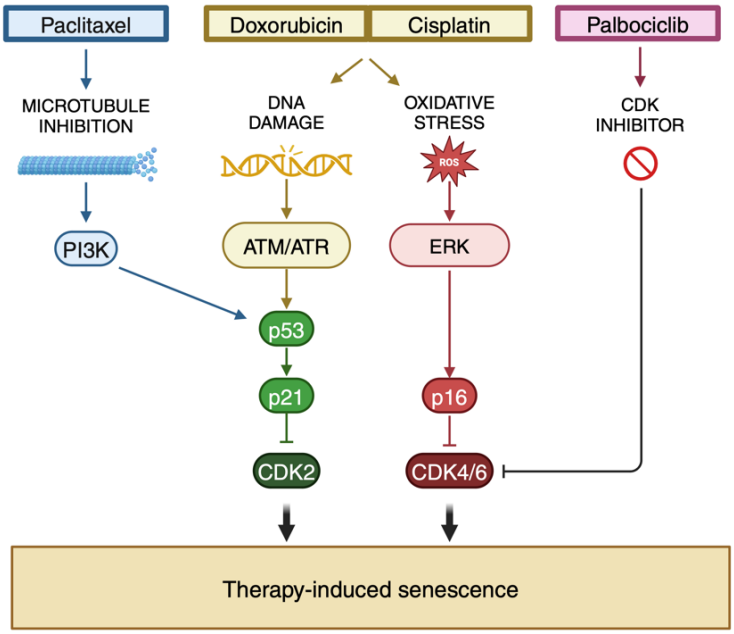


Figure 9.Distinct chemotherapy treatments can induce TIS.
Doxorubicin is a DNA intercalating agent that promotes DNA damage and can induce senescence by activating the p53 pathway. Cisplatin induces extensive DNA cross-linking, leading to accumulation of oxidative stress that will induce cell cycle arrest and subsequent senescence via p16 pahtway. Paclitaxel is a microtubule inhibitor drug that will induce senescence throughout the PI3K pathway. Palbociclib is CDKi that will mimic the action of p16, promoting senescence through blocking of CDK4/6.

Additionally, radiotherapy involves the use of high-energy electrically charged ions to cause permanent DNA damage on cancer cells, ultimately leading to cell death. Given its broad applicability, radiotherapy is employed in the treatment of various types of cancer (61). Interestingly, research has shown that ionizing radiation can induce the expression of SA-β-galactosidase in some cell lines, indicating that radiotherapy can be also an inductor of senescence (62,63).

In summary, conventional cancer treatments, including chemotherapy and radiotherapy, have been proved to induce senescence rather than causing apoptosis of cancer cells. This shift towards TIS as a mechanism of action highlights the importance of

exploring how senescence influences cancer progression and treatment responses. Understanding the role of TIS in cancer can be crucial for developing strategies to potentially improve therapeutic outcomes and address the limitations of current treatments.

3. Dual roles of senescence in cancer

As outlined in previous sections, the impact of senescence varies and can sometimes have opposing effects, depending on the cell of origin and the specific tissue involved. When discussing tumorigenesis, it is also essential to consider the mechanism by which the tumor cell entered senescence and the moment in which senescence is induced. Thus, senescence can have both a protective role and a pro-tumorigenic role, depending on a variety of factors.

3.1. Senescence, the first protection barrier against tumorigenesis

Cancer cells progress through an evolutionary process in which somatic cells undergo mutations and escape the usual controls that prevent excessive growth. To avoid uncontrolled cell division, multiple mechanisms have evolved (64). Some of these mechanisms are internal to the cell, like those that limit cell-cycle progression, while others involve signals from the cell's surrounding environment, which encourage the cell to stay in its designated role.

Several reports have demonstrated that OIS occurs during the early stages of tumor development, in both mouse models and humans (43,65). Thus, oncogenic stress progressively intensifies during tumor development, with senescence being triggered at a stage when tumorigenesis has begun but has not yet advanced to full malignancy. This process helps to keep the tumor in a non-aggressive, pre-malignant state (66). This fact suggests that OIS

may function as a potential tumor suppressor mechanism **(Figure 10).**

On the contrary, the absence of OIS allows the path to oncogene-driven malignant progression to remain free of impediment. In some cases, tumor cells may acquire downstream mutations that prevent the onset of senescence, even with elevated expression levels of p16, ARF, or p53 (67). In fact, in mice whose cells do not respond to senescence signals or whose genes encoding p53 or p16 proteins are inactivated, cells fail to senesce in response to multiple stimuli; meanwhile, all the mice develop cancer at an early age (68). Additionally, in humans, certain tumors may overexpress p16, but this overexpression becomes irrelevant if the tumor lacks RB function (69). And the same will happen if p53 is mutated, something that happens in about half of all human cancer cases (70).

Once the tumor is fully developed, TIS can also facilitate the reduction of tumor growth, as those senescent tumor cells that do not undergo apoptosis following the action of the chemotherapy compound will cease their proliferation. However, due to the stress associated with the aberrant intracellular and extracellular characteristics inherent to tumors, chemotherapy agents may not exert a uniform effect on all cells. Therefore, many cells will undergo apoptosis or senescence while another fraction within the tumor will be able to proliferate successfully (22).

3.1.1. Senescence and the immune system

More and more evidence suggest that several SASP factors are pivotal players in immunosurveillance within the TME. These factors induce or enhance senescent-associated growth arrest in both autocrine and paracrine manners, playing a key role in propagating senescence and recruiting immune cells, thereby inhibiting cancer progression **(Figure 10)** (37).

Thus, in addition to the fact that cell cycle arrest itself acts as a brake on tumor growth, certain changes undergone by senescent cells facilitate the surveillance exerted by the immune system on the tumor. There is a study showing that pre-malignant senescent hepatocytes secrete chemokines and cytokines that allow them to be targeted for clearance by the immune system, a process termed 'senescence surveillance' (71). Specifically, Ras-specific Th1 lymphocytes are detected in mice where OIS is triggered, demonstrating that this surveillance mechanism relies on CD4+ T-cell-mediated adaptive immune response. In fact, in the same study they demonstrate how failure of immune surveillance leads to the development of hepatocellular carcinomas (HCCs), highlighting the importance of senescence surveillance as an extrinsic component of the senescence anti-tumor barrier **(Figure 10)** (71).

Another article demonstrates the participation of NK cells in the clearance of senescent tumor cells triggered *in vivo* by inducible p53 expression. Iannello *et al.* correlate p53 expression with the secretion of various cytokines with the potential to recruit NK cells towards the tumor **(Figure 10)** (72). Also, a more recent study shows that senescent cells combine several features that render them highly efficient in activating dendritic cells (DC) and antigen specific CD8 T cells. This includes the release of alarmins, activation of IFN signaling, enhanced MHC class I machinery, and presentation of senescence-associated self-peptides that can activate CD8 T cells **(Figure 10)** (73). Notably, Chemokine (C–X–C motif) ligand 2 (CCL2), when secreted by senescent cells, serves as a beacon for myeloid cells, which subsequently engage cytotoxic NK cells, ultimately thwarting tumor immune surveillance (74). Conversely, Tumor necropsy factor alpha (TNFα) and Intercellular adhesion molecule 1 (ICAM1) stimulate NK cell-mediated

immunosurveillance, thereby contributing to tumor regression **(Figure 10)** (75).

Additionally, SASP factors not only reinforce immunosurveillance, but also remodel tissues in a paracrine manner through cytokines such as IL-1, IL-6, and interleukin 8 (IL-8), which alter the proliferation and migration capabilities of adjacent cells, including stromal, immune, and cancer cells **(Figure 10)** (76).

It is also important to note that not only the constituents of the SASP are context-dependent but that even a single SASP factor can be pro- or anti-tumorigenic depending on the biological context (52).

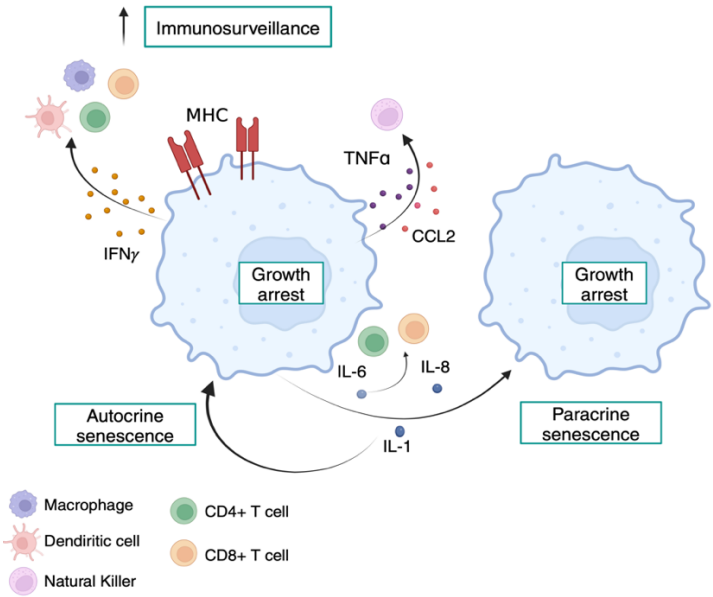


Figure 10. Senescent cells behave as a barrier for tumorigenesis.
Schema of the different ways senescent cells play an anti-tumoral role. Growth arrest prevents the proliferation of malignant cells. MHC expression is increased in senescent cells, favoring the infiltration of CD8+ T cells. *Moreover, senescent cells modify the microenvironment through the SASP, increasing immunosurveillance in the tumor:* IFNγ attract dendritic cells. natural killer cells and activate T cells. TNFα and CCL2 can ultimately activate natural killer cells, while IL-6 can attract T cells and also induce paracrine senescence in neighbor cells. IL-8 and IL-1 also contribute to maintaining senescence in the tumor, in an autocrine and paracrine way.

In summary, oncogene-induced senescent cells serve as an initial barrier against tumorigenesis, halting the proliferation of potentially cancerous cells. Moreover, the secretion of SASP factors by these senescent cells can stimulate immune surveillance mechanisms, further inhibiting tumor growth. Given these roles in impeding tumorigenesis and enhancing immunosurveillance, inducing senescence emerges as a promising anti-cancer strategy.

3.2. Senescence: fuel for tumorigenesis

While OIS may act as a barrier to tumorigenesis initially and chemotherapy treatments may contribute to tumor growth arrest, the persistence of senescent cells can paradoxically fuel tumor growth and progression, mainly through the SASP. In fact, SASP factors can be instrumental in tumorigenesis and metastasis, shaping the intricate dynamics of the TME **(Figure 11)**.

Key SASP factors implicated in tumor progression include the previously mentioned IL-6 and IL-8 or CCL5, which promotes cancer cell proliferation through c-MYC and cyclin D1 (77). Additionally, it has been described that when senescence is originated, senescent cells can stimulate mitogenic signaling cascades in cancer cells, working synergistically with metalloproteases (MMPs) to hasten cancer progression and metastasis. In fact, MMPs are also described to be part of the SASP **(Figure 11)**. They act as master regulators of cancer invasiveness by degrading extracellular matrix components, facilitating tumor dissemination. Importantly, other factors secreted by senescent cells, such as CXCL5 and VEGF can contribute to increased blood vessel density in tumors, also promoting metastasis **(Figure 11)**. (78). Other factors, such as TNFα that induces ROS in cancer cell lines or TGF-β that promotes extracellular matrix deposition, cell migration, and metastasis, are also part of the SASP factors described to promote tumorigenesis

(Figure 11) (60). Furthermore, it has been demonstrated that CCL2 recruits myeloid cells with dual roles—either eliminating senescent cells by enhancing NK cells (75) or promoting cancer progression, depending on the context, as the recruitment of immune-suppressive myeloid cells to tumors by this cytokine can block the action of T cells, fostering tumorigenesis **(Figure 11)** (40). In conclusion, these SASP factors collectively contribute to the complex interplay within the tumor microenvironment, exerting profound influences on tumorigenesis and metastasis.

In addition to the SASP, senescent cells have other mechanisms to protect themselves from immunosurveillance following tumor progression. Different studies in aging have described how senescent cells evade immune clearance through mechanisms involving HLA-E expression. Specifically, senescent cells upregulate HLA-E, a non-classical MHC-class Ib molecule, which inhibits interaction with the inhibitory receptor NKG2A expressed on NK and CD8+ T cells **(Figure 11)** (79). Moreover, senescent cells can bypass CD8+ T cell-mediated surveillance by expressing immune checkpoints such as PD-L1, which suppresses the cytotoxic action of these T cells (80). In addition, Dr. Manuel Serrano and colleagues have recently described the role of PD-L2, the other ligand that interacts with the PD-1 receptor, in contributing to the inhibition of T cell activation in a senescence context. Our group collaborated in this study that reveals that chemotherapy triggers the expression of PD-L2 in senescent cancer cells, leading to the accumulation of tumor senescent cells **(Figure 11)**. These senescent cells create an immunosuppressive environment, by attracting myeloid-derived suppressor cells (MDSCs) through CXCL1 expression, which hinders the anti-tumor immune response, thereby reducing the effectiveness of chemotherapy. The findings highlight the significance of senescent cells in tumor immune evasion and

suggest that targeting senescent cells by blocking PD-L2 expression may enhance the therapeutic efficacy of chemotherapy (81).

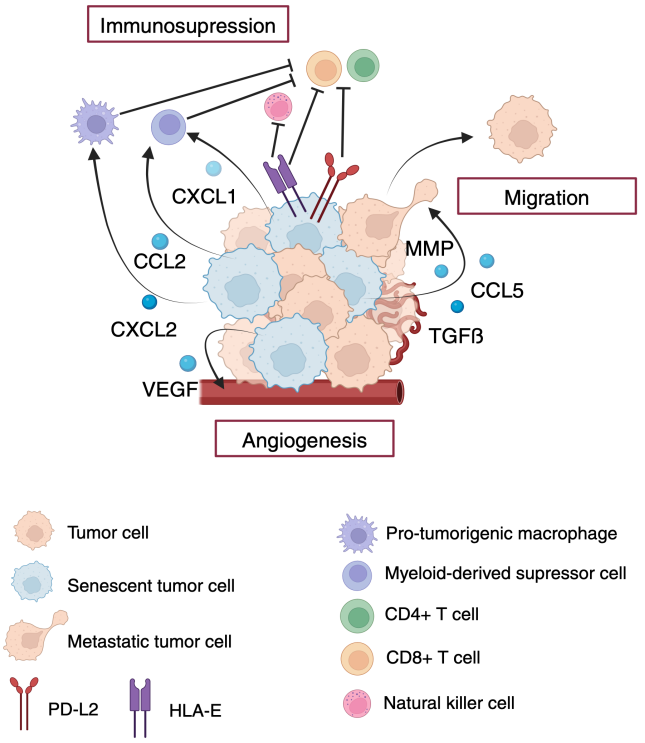


Figure 11. Persistance of senescent cells in the tumor promotes tumorigenesis through the SASP.

Schematic view of a tumor with senescent tumor cells secreting different SASP factors that ultimately contribute to tumorigenesis and metastasis. CXCL1 and CCL2 attracts myeloid derived suppressor cells while CXCL2 attracts pro-tumorigenic macrophages. Both populations block the action of T cells, contributing to an immunosuppressed microenvironment. Moreover, senescent cells can increase the expression of molecules that block the action of T cells, such as PD-L2 and HLA-E, protecting themselves from being eliminated. Senescent cells secrete VEGF and TGFß that contribute to angiogenesis and secretion of MMPs or CCL5 contribute to increase the migration capacity of tumor cells.

Given these facts, anti-cancer strategies that combine senescence induction and killing of those senescent cells, which is known as senolysis, emerge as a promising new approach. This approach follows a "one-two punch" sequential therapy rationale. First, the use

of pro-senescence therapies to induce senescence in cancer cells stop the tumor growth, and then is followed up with agents that selectively kill the senescent cancer cells that can be promoting the growth of the remaining proliferative cells (82).

3.2.1. Senolysis as an anti-tumor strategy

A key point in the one-two punch approach is the development of drugs that specifically kill senescent cells, so-called senolytics.

Senolytics research has gained interest in the recent years, both in the development of anti-age related or and anti-cancer treatments. Typically, the targets of these drugs are senescent cell-associated components, such as the anti-apoptotic protein BCL-2. Thus, flavonoids, like quercetin and other drugs that inhibit BCL-2 have already been proven to selectively kill some types of senescent cells, both *in vitro* and *in vivo* (51). With regard to flavonoids, a number of clinical trials, like NCT04063124 or NCT04685590, are already being conducted with the objective of evaluating the combination of dasatinib, a tyrosine kinase inhibitor, and quercetin in patients. However, the impact of senescence and senolysis on the therapeutic efficacy of the treatment will not be assessed in these trials.

On the other hand, secondary effects of BCL-2 inhibitors, such as Navitoclax, derived of its lack of specificity in killing just senescent cells, limited its clinical use (51). Therefore, some approaches have been investigated for using Navitoclax in a safer way. (51). Some studies have explored targeting drugs specifically toward senescent cells by leveraging their higher SA-ß-Gal activity. For example, nanoparticles like a galactose derivative prodrug of navitoclax (Nav-Gal) have demonstrated increased specificity for cisplatin-induced senescent A549 cancer cells in vitro. Furthermore, this combination has shown to be effective in eliminating senescent cancer cells, showing anti-tumorigenic effect in vivo while minimizing secondary effects. In addition to finding new drugs to kill senescent cells,

retrospective analysis is another way to test the potential of drugs repurposed as senolytics. For example, we had the opportunity to collaborate with Dr. Collado's group in a study published in 2019, demonstrating that cardiac glycoside compounds can also be used to selectively kill senescent cells (83).

Besides small molecules, senolytics can encompass cell therapies. Senescent cells can be targeted by exploiting their immunogenic profile, making the development of antibodies against senescent-specific antigens an increasingly promising approach in the field. These antibodies can work by enhancing antibody-dependent cell-mediated cytotoxicity (ADCC) or conjugated with senolytics (51). Furthermore, a recent study has demonstrated the design of chimeric antigen receptor (CAR) T cells targeting the urokinase-type plasminogen activator receptor (uPAR) that have been shown to successfully eliminate senescent cells both in vitro and in vivo following TIS, leading to extended survival. (84).

In summary, senolytics show promise in the treatment of not only cancer but for other age-related diseases. However, despite the many advances that have been made recently, there are still too many hurdles that limit the potential use of senolysis as an anti-cancer therapy. The first and most important limitation is the lack of a universal marker for the precise identification of senescent cells. Therefore, the search for a biomarker or biomarkers that can track senescence as well as serve as a target for directing therapies is one of the main goals of the field. Secondly, the timing of the "one-two punch" strategy is an additional issue that needs to be carefully addressed, as there is a delicate balance between shifting senescent cells from an anti-tumorigenic to a pro-tumorigenic state **(Figure 12)**.

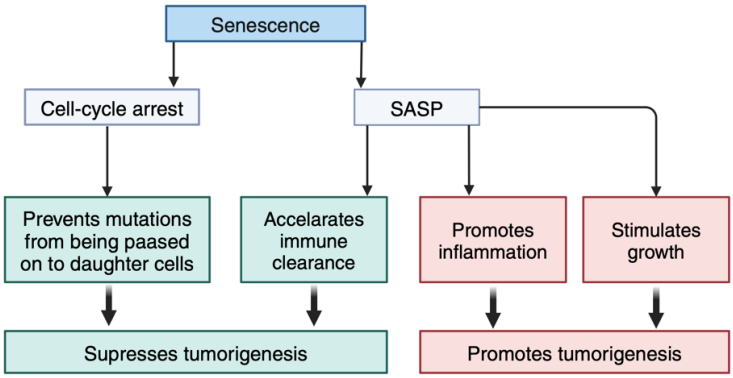


Figure 12. The dual role of cellular senescence in cancer.
Senescence-induced cell-cycle arrest can prevent mutations from being passed on to the next generation of cells and accelerate immune clearance through the SASP, resulting in suppression of tumorigenesis. However, the SASP can also contribute to a pro-inflammatory and growth-stimulatory microenvironment that can promote tumor development.

4. *In vivo* models for monitoring and killing senescence.

While significant progress has been made in modeling and understanding cellular senescence, there are still important challenges in fully recapitulating and validating senescence induction. *In vivo* models play a crucial role in elucidating this intricate biology of senescence, offering invaluable insights into its physiological relevance and potential therapeutic applications.

To investigate the mechanisms by which cellular and tissue states are reprogrammed in response to senescence, various mouse models have been developed to induce this process. In the context of cancer research, Scott Lowe's group recently created a senescence-inducible model in which through the genetic modulation of endogenous p53 liver cancer cells can be selectively driven into a senescent state. Using this model, researchers have shown that, beyond the SASP, senescence induces significant changes in the cell-surface proteome and signaling pathways, altering how cells respond to the stimuli of the environment. This

rewiring, in conjunction with the SASP, ends in the enhancing of their immunogenic potential (48).

Besides being able to recapitulate the senescence phenotype in living organisms, there is also a need for targeting senescent cells *in vivo*. Therefore, much effort has been devoted to obtaining mouse models modified so senescent cells can be traceable and killed. To date, the majority of these models are based on the expression of only one of the canonical senescent cell markers, p21 or p16.

The first inducible p21-Cre mouse model was generated by researchers from the Mayo Clinic to monitor and manipulate p21-highly-expressing senescent cells *in vivo* (85). However, the role of p21 in senescence remains controversial, as it has been demonstrated that p21 expression is needed for senescence initiation but tends to decrease over time (24). Therefore, its reliability as a unique senescence biomarker is debatable. In this regard, most of the research has been focused on developing p16-based mouse models.

Researchers from the University of Texas Southwestern Medical Center developed a p16-luciferase knocking mouse model (p16-LUC). This model expresses the fusion protein of human p16 and firefly luciferase, allowing for faithful reporting of p16 expression in a noninvasive way. Allowing a lifelong assessment of luminescence, it revealed an exponential increase of p16/Luc positive cells with aging, providing insights into the dynamics of p16 gene expression and its role in aging and cancer progression (86). And among the models based on the expression of p16 for targeting senescent cells *in vivo*, we can highlight those developed by the laboratories of Prof. Van Deursen and Prof. Campisi.

The Van Deursen group has developed a mouse model called INK-ATTAC that allows for the inducible elimination of p16-positive

senescent cells. In this model, *Cdkn2a/p16* promoter (INK) controls the expression of the transgene that encodes a FK506-binding protein (FKBP), fused to a Caspase 8 (Casp8) moiety and an Enhanced Green Fluorescent Protein (EGFP) domain (ATTAC) **(Figure 13)**. The unique aspect of this model is that the Casp8 moiety remains inactive until a specific drug, often a small-molecule compound like AP20187 or similar, is administered. The drug binds specifically to the FKBP domain, causing Casp8 activation through dimerization and leading to apoptosis of exclusively p16-expressing cells. The effective clearance of these cells can be tracked thanks to the expression of EGFP **(Figure 13)**. Thus, this mouse model allows for the inducible removal of p16-positive senescent cells, demonstrating a delay in age-related pathologies dependent on p16 induction. This model has been used to show the delay in cataracts, sarcopenia, and pancreatic β-cell dysfunction (87,88).

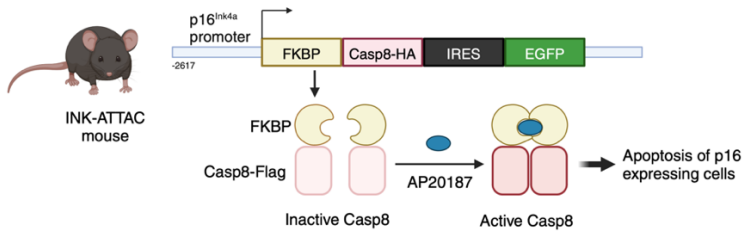


Figure 13. Schematic design of INK-ATTAC activation system.
P16 promoter controls the expression of FKBP, Casp8 protein and EGFP. AP20187 administration induce Casp8 activation through dimerization, ending in the apoptosis of p16 expressing cells. Figure adapted from "Clearance of p16 Ink4a-positive senescent cells delays ageing-associated disorders" (88).

Similarly, Campisi's lab has developed another genetically engineered mouse strain that enables researchers to visualize and eliminate senescent cells within the animal. Commonly referred to as the p16-3MR model, it contains a trimodal (3MR) reporter fusion protein containing luciferase for detection by luminescence, red fluorescent protein (mRFP) for sorting, and a truncated herpes

simplex virus 1 thymidine kinase (HSV-TK). Ganciclovir (GCV), a nucleoside analog with ahigh affinity for HSV-TK, converts it into a toxic DNA chain terminator, causing fragmentation of genomic and mitochondrial DNA and apoptosis selectively in HSV-TK expressing cells **(Figure 14)**. The *Cdkn2a/p16* promoter drives the 3MR construct expression, allowing researchers to track p16-expressing senescent cells over time with the mRFP and observe their distribution within tissues. Also, the inclusion of the *TK* gene enables targeted cell ablation using GCV treatment, allowing the study of the consequences of senescence clearance (89,90). Researchers have utilized this model to investigate the role of senescence in conditions such as cigarette smoke exposure-related lung pathologies, cancer, atherosclerosis, and age-related disorders. (89–91).

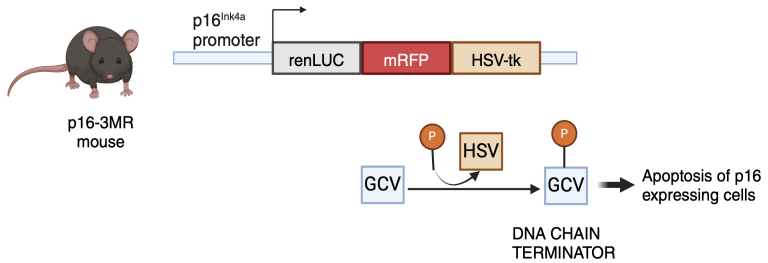


Figure 14. Schematic design of p16-3MR activation system.
Cdkn2a/p16 promoter controls the expression of LUC protein, mRFP and HSV-tk. Upon ganciclovir (GCV) administration, HSV-tk converts it into DNA chain terminator that promotes the apoptosis of p16-expressing cells, Figure adapted from "Systemic cleareance of p16^{INK4a}-positive senescent cells mitigates age-associated intervertebral disc degeneration" (92).

In summary, both the Van Deursen and the Campisi transgenic mouse models provide a valuable tool for studying cellular senescence in living organisms and for understanding the role of senescence in health and disease. Nevertheless, these, and other transgenic models that have been developed to date, present a significant drawback: the reliance on a single senescence marker.

Thus, INK-ATTAC and p16-3MR are models designed exclusively to eliminate cells overexpressing p16. However, as previously stated, the expression of this gene cannot be taken as a singular marker of senescence, as certain cells expressing p16 are not senescent (24). In fact, these models are hardly useful to study the role of senescence in cancer because it is well described that p16 is frequently overexpressed in highly proliferative tumors, including breast cancer (93). In consequence, in currently available models, transformed non-senescent p16-expressing cells would be also targeted in addition to senescent cells, making them unsuitable to functionally characterize the role of senescence in tumors.

In conclusion, despite the numerous efforts on defining senescent cells, the heterogeneity of their phenotype highlights the need for more refined and specific tools to target senescent cells accurately and effectively. In this sense, designing a mouse model based on the combination of two markers of senescent cells constitute a rational approach. Targeting cells expressing p16, which is consistently expressed in senescent cells, and IL-6, one of the most commonSASP effectors, may ensure more reliable outcomes in elucidating the role of senescent cells in cancer development.

HYPOTHESIS

Senescent cells play a dual role in cancer progression, functioning both as tumor suppressors and promoters. The use of a novel transgenic mouse model, based on the expression of p16 and IL-6, has the potential to uncover new insights into the mechanisms underlying this duality, thereby offering new possibilities for employing senolysis as a cancer treatment.

OBJECTIVES

The main objective of this thesis is to elucidate the role of senescent cells in tumor development and to identify the key players involved in this process.

The specific aims of my research are:

1. To generate and characterize a novel *in vivo* model for monitoring and eliminating senescent cells, referred to as the SuSe model.
2. To assess the presence of OIS at different stages of tumor progression
3. To investigate the role of OIS in tumor progression by selectively eliminating p16/IL6-positive cells
4. To determine the impact of TIS on the efficacy of cancer treatment.

MATERIALS & METHODS

1. Mice models

P16pro-FRB-Casp8/HA-Cherry mouse model

The P16pro-FRB-Casp8/HA-Cherry (p16-mCherry) transgenic construct was made as follows. A 1200-bp segment of the murine p16 promoter was extracted from mCdkn2apro-Luc construct kindly gifted by Dr Serrano's group and cloned into the pC4-RHE vector (containing FRB-CAS8), kindly gifted by Dr. Doug Green and followed by an IRES-mCherry sequence from the pMCSV-IRES-Cherry plasmid (#52114, Addgene). Transgenic founders were obtained by pronuclear injection of the p16-mCherry construct into FVB oocytes in the Mouse Mutant Core Facility of IRB (Institute of Research in Biomedicine) in Barcelona. Mice were genotyped for the p16-mCherry construct by Polymerase Chain Reaction (PCR) using the following primers: forward primer, CGATCCTTTAGCGCTGTTTC and reverse primer CTTGGAGGAGGTCCTTGACA, on the mice third week of life.

IL6pro-FKBP-Casp8/HA-GFP mouse model

The IL6pro-FKBP-Casp8/HA-GFP (IL6-GFP) transgenic construct was made as follows. A 1400-bp segment of the murine *Il6* promoter was first amplified by PCR amplified from murine DNA The resulting DNA was purified and integrated in a pC4-Fv1E, that is the FKBP-CAS8-containing vector kindly gifted by Dr. Doug Green. The IL6pro-FKBP-Casp8 segment was then inserted into pBlueScriptII plasmid conteining GFP (Addgene). Transgenic founders were obtained by pronuclear injection of the IL6-GFP construct into FVB oocytes in the Mouse Mutant Core Facility of IRB in Barcelona. Mice were genotyped for the IL6-GFP construct by PCR using the following primers: forward primer GAGCCCACCAAGAACGATAG, and

reverse primer CAGTGGCACCATAGGCATAA, on the mice third week of life.

SuSe mouse model

SuSe mice were the result of the crossing of p16-mCherry mouse model and IL6 -GFP mouse model. Mice were genotyped for both constructs by PCR using the respective primers for each construct on the mice third week of life.

MMTV-PyMT model

MMTV-PyMT (PyMT) mice were acquired from The Jackson Laboratory (Bar Harbor, ME). Male PyMT mice were mated with FVB-Wild type (WT) females. Mice were genotyped for the *PyMT* allele by PCR using the forward primer, CGCACATACTGCTGGAAGAA and reverse primer, TGCCGGGAACGTTTTATTAG on the mice third week of life.

PyMT/SuSe model

PyMT/SuSe mice were obtained crossing male MMTV-PyMT mice and female SuSe mice. Mice were genotyped for the PyMT allele and the constructs p16-mCherry and IL-6-GFP by PCR on the mice third week of life.

Syngeneic mouse models

PyMT/Suse cells were implanted in FVB mice of 5 weeks of life and PyMT cells were implanted in SuSe mice of the same age. In both cases 500.000 cells were implanted in two flanks of the mice.

All mice were on a FVB background. All studies were performed in accordance with the ARRIVE guidelines and the 3 Rs rule of Replacement, Reduction and Refinement principles. Mice were housed in a specific pathogen–free environment. and treated

following the protocols approved by the Ethical Committee for the Use of Experimental Animals (CEEA) at VHIO, Barcelona, Spain.

2. Tumor derived cells lines

PyMT-SuSe primary cell line was obtained from tumors of a PyMT/SuSe mouse. Two tumors were excised and immediately preserved in PBS at 4ºC. Mechanical disaggregation was performed using blades to cut the tumors into small pieces followed by enzymatic digestion in 300 U/ml collagenase IA (#C2674, Sigma-Aldrich) and 100 U/ml hyaluronidase IS (#H3506, Sigma-Aldrich) DMEM F-12 medium. The tube was incubated on a shaker (200rmp at 37ºC) for 1h. After washes with PBS, cells were resuspended in DMEM media supplemented with fetal bovine serum (FBS) 5% (#10270-106), L-Glutamine 2mM (#X0550-100, Invitrogen), 1M HEPES (#H0887, Sigma), 0'5 μg/ml hydrocortisone, 20 ng/ml EGF (AF-100-15, Bionova Cientifica), Cholera toxin 100 ng/ml (#C8052, Merck Life Science) and insulin 10μg/ml (#41400045, Sigma) to facility the growth and selection of epithelial cells in p100 plates. Once PyMT-Suse cells were stablished in culture, they were maintained in DMEM-12 (1:1) medium supplemented with 10% FBS, 1% glutamine and 1% Penicillin/streptomycin and incubated at 37ºC in a humidified atmosphere containing 5% carbon dioxide. The cells were passaged when they reached 80% to 90% confluence.

PyMT cell line was obtained from tumors of a PyMT mouse, following the same procedure as the PyMT/SuSe cells and maintained under the same conditions.

3. Treatments in vivo and monitoring tumor growth

In every *in vivo* experiment tumor growth was monitored using calipers using the formula (length x width2) x (π/6) twice a week. Body weight of the mice was also measured twice a week.

AP21967 treatment

For AP21967 (#635055, Takara) treatments, PyMT/SuSe animals were injected intraperitoneally (i.p.) every 3 days with 0.2 μg g−1body weight of the heterodimer-inducing drug from the fourth or the ninth week of the mice life until the thirteenth week of the mice life.

Treatment in the syngeneic model started 10 days after cell implantation and was administered twice a week during 28 days.

Blocking and depleting strategies

For elimination of macrophage population in PyMT/Suse mice, mice were treated twice a week, starting at week 9 after birth, with liposomes containing 5 mg/ml of clodronate or PBS as control (#C-005, Liposoma BV).

For selective blocking of PD-L2 in 9-week-old PyMT mice, mice were treated every three days with 100 µg of anti-PD-L2 (TY25, #BE0112, BioXCell) until the week 13 of the mice life. For selective elimination of T cell populations same regimen of treatment was followed with anti-CD4 (GK1.5, #BP0003-1, BioXCell), anti-CD8α (2.43, #BE0061, BioXCell) or IgG2b (LTF-2, #BP0090, BioXCell) as an isotype control.

For selective elimination of T cell populations in FVB mice with PyMT/Suse orthotopic tumors, mice were treated twice a week (i.p.), starting 10 days after surgery, with 100 µg each of anti-CD8α (2.43, #BE0061, BioXCell) or IgG2b (LTF-2, #BP0090, BioXCell) as an isotype control.

Chemotherapeutic agents

For doxorubicin treatment in the syngeneic models, the drug was administered via i.p once a week and treatment started 10 days after cell implantation. For the treatment in the PyMT mice, the drug was

also administered via i.p once a week, but treatment started at the ninth week of the mice life and ended at the thirteenth week. Drug was administered at a 4mg/Kg dose.

4. DNA extracting protocol

A small piece of ear tissue was excised from the mice and placed into an Eppendorf tube. To this, 75 μL of Buffer A (25 mM NaOH + 0.2 mM EDTA) was added. The sample was then incubated in a thermocycler at 98°C for 1 hour to facilitate lysis, followed by cooling to 15°C until the next step. Subsequently, 75 μL of Buffer B (40 mM Tris-HCl, pH 5.5) was added to neutralize the reaction. The mixture was centrifuged at 4000 rpm for 3 minutes to pellet debris, and the supernatant containing the extracted DNA was then used for PCR.

5. Senescence induction in vitro

PyMT-SuSe cells were seeded in a six-well plate at a density of 200.000 cells/well, and at 100.000 cells/well as control. After 24h, cells were treated with different concentrations of doxorubicin over a period of five days to find the best concentration to induce senescence. The different concentrations of doxorubicin used were: 50ng/ml, 75ng/ml, 100ng/ml, 125ng/ml and 150ng/ml. For the following experiments the doxorubicin dose used to induce senescence *in vitro* was 92 nM.

6. SA-ß-Gal staining

Mammary tumor samples

Mammary gland samples were whole mounted using a fixative solution of 2% of Glutaraldehyde (10%) (#G6257, Sigma) 50% of Paraformaldehyde (4%) (#2529311315, Panreac) diluted in PBS. Overnight staining with Senescence β-galactosidase staining kit (#9860, Cell signaling) was performed directly in the fixed samples, previous to their inclusion in paraffin. Using the Leica microtome

system, 3 µm thick sections were obtained and counterstained with Liquid-Stable Nuclear Fast Red (#1B1369-500ML, VWR Life Science AMRESCO).

Cell cultured samples

PyMT/Suse cells seeded in a 6-well plate at a density of 200.000 cells/well and treated with doxorubicin at a 92 nM concentration were fixed at RT for 15 min in fixative solution (#11674, Cell signaling) Overnight staining with Senescence β-galactosidase staining kit (#9860, Cell signaling) was performed directly in the fixed cells.

7. Immunofluorescence staining

GFP and mCherry staining in mammary tumor samples

Mammary glands were formalin-fixed and paraffin-embedded. Using the Leica microtome system, 4 µm thick sections were obtained in Superfrost Plus Microscope Slides (#631-0108, VWR).

Paraffin sections were overheated overnight at 60ºC. Before immunostaining, deparaffinization and hydration in xylene and graded ethanol was performed. The standard antigen retrieval method was done using citrate buffer (ph6). Slides were incubated with 3% BSA + 0,3% Triton in PBS for 1h at RT. They were then incubated with the primary antibodies GFP at 1:1000 (#Ab13970, Abcam) and mCherry at 1:200 (#AB0081, SicGen) at 4 °C overnight. The following day, slides were washed 3 times using PBS and incubated with the secondary antibodies FITC anti-chicken (#Ab63507, Abcam) and Alexa Fluor 568 anti-goat (#A11057, Life Technologies) both diluted 1:500 in Envision FLEX antibody diluent (#K8006, Dako) for 1h in darkness at RT. After washing 3 times with PBS, slides were mounted using Mounting Medium with DAPI – Aqueous Fluoroshield (#ab104139, Abcam). Images were captured using an inverted fluorescence microscope with 20X objective.

CD68 and CCL2, Mrc1 staining in mammary tumor samples

Paraffin sections were overheated overnight at 60ºC. Before immunostaining, deparaffinization and hydration in xylene and graded ethanol was performed. The standard antigen retrieval method was done using citrate buffer (ph6). Slides were incubated with 3% BSA + 0,3% Triton in PBS for 1h at RT. The slides were then incubated with the primary antibodies CD68 at 1:100 (#Ab53444, Abcam) and CCL2 at 1:200 (#Ab25124, Abcam) or Mrc1 at 1:100 (#Ab64693, Abcam) at 4 °C overnight. After incubation, slides were washed 3 times using PBS and secondary antibodies Alexa Fluor 647 anti-rat (#A21247, Invitrogen) and Alexa Fluor 488 anti-rabbit (#A11008, Invitrogen) respectively were added, both at 1:500 for 1h at RT. Samples were washed again 3 times with PBS and mounted using Mounting Medium with DAPI – Aqueous Fluoroshield (#ab104139, Abcam)

Images were captured using an inverted fluorescence microscope with 20X objective and analyzed using Fiji.

GFP and mCherry staining in cell cultured samples

PyMT-SuSe cells were seeded in p12 well plates with glass cover slips at a density of 100.000 cells/well. After 24h, cells were treated with Doxorubicin 92 nM to induce senescence or PBS as control. After 5 days, cells were rinsed three times in 1X PBS. Cells were fixed at RT for 15 min in PFA 4%. Following, we used 3% BSA-PBS for blocking the cells. After 1 hour at RT, cells were incubated overnight at 4ºC with 100μl of primary antibody anti-GFP (#Ab13970, Abcam) diluted 1:1000 in 3% BSA-PBS and 100μl of primary antibody anti-mCherry (#AB0081, SicGen) diluted 1:200 in 3% BSA-PBS. 1X PBS was used to wash the cells three times for 5 min, before the cells were incubated with 100μl of secondary antibody FITC anti-chicken (#Ab63507, Abcam) and Alexa Fluor 568 anti-goat (#A11057, Life Technologies) both diluted 1:500 in Envision FLEX

antibody dilouent (#K8006, Dako) for 1h in darkness at RT. Mounting Medium with DAPI – Aqueous Fluoroshield (#ab104139, Abcam) was used to mount coverslips (ECN 631-1575, VWR) into superfrost slides. Pictures from these samples were taken using a Nikon Ti-E Eclipse Inverted Fluorescence Microscope DIC. The obtained images were analyzed with Fiji software.

8. Immunohistoquemistry staining

Mammary tumor samples

Mammary glands were either formalin-fixed or whole mounted, as previous described, and paraffin-embedded. Using the Leica microtome system, 3 µm thick sections were obtained and IHC experiments were performed using the Dako EnVision+ System-HRP kit.

Paraffin sections were overheated overnight at 60ºC. Before immunostaining, deparaffinization and hydration in xylene and graded ethanol was performed. Antigen retrieval was performed using buffer (pH-9) by boiling followed by washing in PBS and blocking for endogenous peroxidase for 15 min at RT. The slides were washed with PBS and, after 1 hour of incubation with 3% BSA blocking solution or 10%FBS + 1%BSA in TBS + 0,025% Triton for CD4/CD8 samples, each of them was incubated with primary antibody PD-L2 (1:100, #49189, Cell Signaling), CD3 (1:100, #ab16669, Abcam), CD4 (1:1000, #ab183685, Abcam) or CD8 (1:2000, #ab217344, Abcam) at 4 °C overnight. Followed by washing, they were incubated with System- HRP Labelled Polymer Anti-Rabbit (#K4003, Dako) secondary antibody for 1 hour at RT. The tissues were counterstained with hematoxylin (#H-3404, Vector laboratories) after the substrate DAB, (#K3468, Dako) reaction step.

Samples were dehydrated by the ethanol-xylene gradient and mounted using DPX mountant for histology (#06522, Sigma Aldrich).

Lung samples

Full lungs were formalin-fixed and paraffin-embedded. Using the Leica microtome system, 4 µm thick sections were obtained in superfrost slides and IHC experiments were performed using the Dako EnVision+ System-HRP kit.

Paraffin sections were overheated overnight at 60ºC. Before immunostaining, deparaffinization and hydration in xylene and graded ethanol was performed. Antigen retrieval was performed using citrate buffer (pH-6) by boiling followed by washing in PBS and blocking for endogenous peroxidase for 15 min at RT. Samples were washed three times with PBS, blocked using 10%FBS + 1%BSA in TBS + 0,025% Triton for 2h at RT and washed again. Slides were incubated with primary antibody PAN-K (1:40, #ab8068, Abcam) overnight at 4ºC. Samples were then washed 3 times using PBS and incubated with System- HRP Labelled Polymer Anti-Mouse (#K4001, Dako) for 1h at RT. The tissues were counterstained with hematoxylin H-3404, Vector laboratories after the substrate DAB (#K3468, Dako) reaction step. Lung sections were dehydrated by the ethanol-xylene gradient and mounted using DPX mountant for histology (#06522, Sigma Aldrich).

9. Single-cell RNAseq

Tissue from the mammary glands of PyMT/SuSe mice of 4 and 9 weeks of life, treated with either vehicle or AP21967 from the fourth week, were harvested and immediately placed in cold 1XPBS. Mechanical disaggregation was performed using blades to cut the tumors and tissues into small pieces, followed by enzymatic digestion in 300 U/ml collagenase IA (#C2674, Sigma-Aldrich) and 100 U/ml hyaluronidase IS (#H3506, Sigma-Aldrich) DMEM F-12

medium. After 45 minutes of incubation at 37ºC with shaking at 10g, the tissue mixture was filtered through 100 µm strainers (#732-2759, VWR). After washing with 1XPBS to ensure maximum cell recovery, strainers were discarded and cell suspension spined at 400g. Cell pellet was further subjected to RBC lysis once and washed with 1XPBS. After lysis, cells were counted, and viability was assessed to ensure that more than 85% of cells were viable. Single cells were then captured using a microfluidic platform and processed for library preparation. Libraries were sequenced on an Illumina NovaSeq, aiming for a depth of 50,000 to 100,000 reads per cell. Data was processed using the Cell Ranger pipeline, followed by downstream analysis using Seurat. Seurat objects were generated from counts matrices and using the arguments “min.cells = 3” and “min.features = 200”, which include only those features (genes) detected in at least 3 cells and cells that have at least 200 features detected respectively. Due to their different behavior in terms of i) number of unique genes expressed by each cell (nFeatureRNA), and ii) the percentage of mitochondrial genes (percent.mt), different subsets were applied to each sample before the integration. Analyses were conducted under R version 4.1.2 (R Core Team 2021).

10. CD45+ cell sorting

Tissue from the mammary glands of PyMT/SuSe mice that were 4 weeks-olds and 9 or 13 weeks of life, treated with either vehicle or AP21967 from the week 4, was harvested and immediately placed in cold 1XPBS. Mechanical disaggregation was performed using blades to cut the tumors and tissues into small pieces, followed by enzymatic digestion in 300 U/ml collagenase IA (#C2674, Sigma-Aldrich) and 100 U/ml hyaluronidase IS (#H3506, Sigma-Aldrich) DMEM F-12 medium. After 45 minutes of incubation at 37ºC with shaking at 10g, the tissue mixture was filtered through 100 µm

strainers (#732-2759, VWR), and further disaggregated by pressing it against the strainer using the rough surface of a syringe plunger base to ensure complete dissociation. After washing with 1XPBS to ensure maximum cell recovery, strainers were discarded and cell suspension spined at 400g. Cell pellet was further subjected to RBC lysis once and washed with 1XPBS. After lysis, cells were stained with 1/300 anti-mCD45-AF488 (#103122) antibody. Cells were then washed with 1× PBS and resuspended in Zombie Aqua viability marker and acquired on Spectral Aurora Sorting equipment (Cytek).

11. Bulk RNAseq of CD45-sorted cells

RNA was extracted from CD45-sorted cells using the RNeasy Mini Kit (QIAGEN). Libraries for RNA-seq were prepared at the Institute for Research in Biomedicine (IRB) Barcelona Functional Genomics Core Facility using standard operating procedures. Briefly, mRNA was isolated from 1.5 µg of total RNA using the NEBNext Poly(A) mRNA Magnetic Isolation Module (New England Biolabs). Next-generation sequencing libraries were prepared from the purified mRNA using the NEBNext Ultra II RNA Library Prep Kit for Illumina (New England Biolabs). An equimolar pool was prepared and sequenced on a NextSeq 550 (Illumina) at the IRB. A minimum of 32.2 million reads were obtained for all samples. Raw sequencing reads in the fastq files were processed through the nf-core/rnaseq pipeline (Ewels et al. 2020) version 3.10.1. The differential gene expression analysis was assessed with voom+limma in the limma package version 3.55.4 (ME.Ritchie and GK.Smyth 2015) using R version 4.3.0. Genes with low expression were detected using “filterByExpr” function (Chen, Lun, and Smyth 2016) implemented in edgeR(MD.Robinson, DJ.McCarthy, and GK.Smyth 2010), and excluded from the analysis. Raw library size differences between samples were treated with the weighted “trimmed mean method” TMM (MD.Robinson and A.Oshlack 2010) implemented in the

edgeR package (MD.Robinson, DJ.McCarthy, and GK.Smyth 2010). The normalized counts were used in the unsupervised analysis, PCA and clusters. For the differential expression analysis, raw counts were modelled using voom approach in limma package. Correction for multiple comparisons was performed using false discovery rate (FDR) (Y.Benjamini and Y.Hochberg 1995), obtaining the adjusted p-values. Genes were considered to be differentially expressed between studied conditions if the adjusted p-value was < 0.05 and the $|logFC| > 1$.

Pre-Ranked Gene Set Enrichment Analysis (GSEA) (A.Subramanian 2005) implemented in clusterProfiler (Yu et al. 2012) package version 4.8.1 was used in order to retrieve enriched functional pathways. The ranked list of genes was generated using the -log(p-value)*signFC for each gene from the statistics obtained in the DE analysis with limma (ME.Ritchie and GK.Smyth 2015). Functional annotation was obtained based on the enrichment of gene sets belonging to gene set collections in Molecular Signatures Database (MSigDB) version 2023.

12. Procartaplex cytokine assay

ProcartaPlex™ Mouse Immune Monitoring 48-Plex (EPX480-20834-901, lot 323053-005, ThermoFisher Scientific) kit was employed, using protein extracts from mammary glands of PyMT/SuSe mice that were 4 weeks-old and 9 or 13 weeks-old, treated with either vehicle or AP21967 from the week 4. Protein extracts were isolated by lysing the cells in homemade lysis buffer (130 mM NaCl, 0.01% NP-40, 1% glycerol, 2 mM EDTA pH 8 and 20mM Tris-HCl pH 7.4), supplemented with phosphatase the inhibitors 5 µM b- Glycerolphosphate, 5 mM sodium fluoride, 1 mM sodium orthovanadate and cOmplete TM EDTA-free Protease

Inhibitor Cocktail (#COEDTAF-RO, Sigma- Aldrich, 1 tablet per 10 ml lysis buffer).

The manufacturer's instructions were followed during the assay, all samples, standards, and blanks were assayed in duplicate and the plate was read using a Luminex xMAP INTELLIFLEX. Results of the next cytokines were obtained using the ProcartaPlex analysis app (https://apps.thermofisher.com/apps/procartaplex):

BAFF, G-CSF, GM-CSF, IFN-α, IFN-γ, IL-1 alfa, IL-1-ß, IL-2, IL-3, IL-4, IL-5, IL-6, IL-7, IL-9, IL-10, IL-12p70, IL-13, IL-15/IL-15R, IL-17A, IL-18, IL-19, IL-22, IL-23, IL-25, IL-27, IL-28, IL-31, IL-33, LIF, M-CSF, RANKL, TNF-α, CXCL5, CCL11, CXCL1, CXCL10, CCL2, CCL7, CCL3, CCL4 CCL5, BTC, leptina, VEGF-A, IL-2R, IL-7R alfa and IL-33R.

CCL2 and IL-31 levels were certified by ELISA (#BMS6005 and #BMS6030, ThermoFisher) using the same protein extracts and following the manufacturer's instructions.

13. Flow Cytometry assay

Livers from SuSe mice treated with either PBS, doxorubicin (10 mg/Kg) or doxorubicin and AP21967 (0.2 μg g−1body weight) for two weeks were collected and immediately placed in cold 1XPBS. Mechanical disaggregation was performed using blades to cut the tissues into small pieces, followed by enzymatic digestion in 300 U/ml collagenase IA (#C2674, Sigma-Aldrich) and 100 U/ml hyaluronidase IS (#H3506, Sigma-Aldrich) DMEM F-12 medium. After 45 minutes of incubation at 37ºC with shaking at 10g, the tissue mixture was filtered through 100 µm strainers (#732-2759, VWR). After washing with 1XPBS to ensure maximum cell recovery, strainers were discarded and cell suspension spined at 400g. Cell pellet was further subjected to RBC lysis once and washed with 1XPBS. After lysis, cells were blocked for 20 minutes at 4ºC in home-

made FACS (fluorescence activate cell sorting) buffer, composed by 1XPBS, 2.5 mM EDTA, 1% BSA, and 5% horse serum (#26050088, Life Technologies). Zombie Aqua (#423101, Biolegend) was used as a viability marker at 1/1000 dilution. Stained samples were measured in the LSR Fortessa cytometer (BD Biosciences) and analyzed using FlowJo software.

14. Statistics

Data are represented as average ± standard deviation (SD) and were analyzed using the two-sided Student's t-test using Excel or two-way ANOVA using Prism. For *in vivo* experiments, syngeneic mice were allocated randomly in treatment groups and growth curves were compared using two-way ANOVA. Data was considered statistically significant when p value < 0.05. Statistical details can be found in the figure legends. Efforts were made to reduce the number of animals used in the experiments.

RESULTS

1. SuSe system: new model to study senescence *in vivo*

There is no universal marker for senescent cells, and models based on single markers (REFs), such as p16, can fail to fully and unequivocally identify these cells *in vivo* in mouse models. Therefore, a need exists for a more accurate model that allows for the tracking of senescent cells and their controlled elimination. To address this, our laboratory developed two new transgenic mice, each based on a different genetic construct.

The first construct expresses an FK506 binding protein fused to caspase 8 protein (FKBP–CASP8), followed by a green fluorescent protein (GFP) driven by the murine *IL6* promoter **(Figure 15)**. The second construct involves an FKBP12-rapamycin binding (FRB) fused to the apoptotic protein caspase 8 (FRB–CASP8) and is followed by a red fluorescent protein (mCherry), all under the control of a minimal *Cdkn2a*/p16 promoter fragment **(Figure 15).** In both constructs, the fluorescent reporter is cloned downstream of the fusion protein coding sequence, separated by an internal ribosome entry site (IRES). Crossing these two mice resulted in a new transgenic mouse model that can express both constructs P16pro-FRB-Casp8/HA-Cherry and IL6pro-FKBP-Casp8/HA-GFP in every cell of the mouse. This murine line was named SuSe (Suicidal Senescence) model **(Figure 15)**.

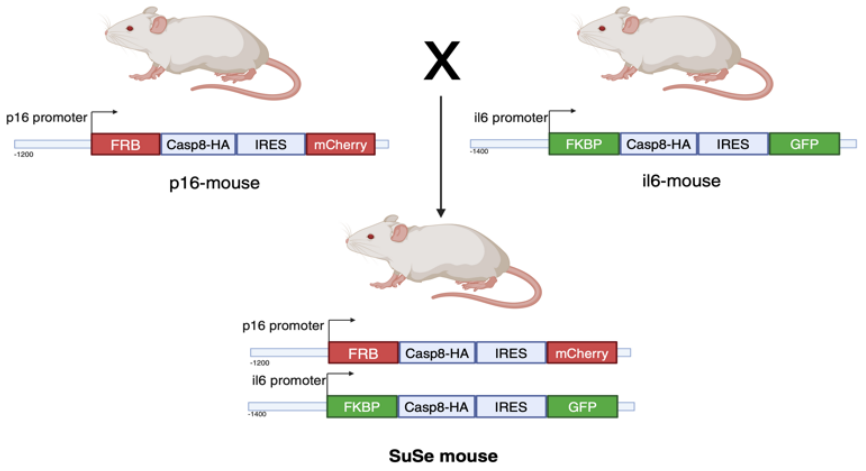


Figure 15. Generation of SuSe Mice.

This figure illustrates the constructs used to generate two transgenic mouse models: the p16 and the IL-6, and the breeding strategy to generate SuSe mice containing both construcst. The p16-mouse, which carries a construct with Cdkn2a/p16 promoter driving the expression of FRB, Casp8-HA, and mCherry, is crossed with the il6-mouse, which has a construct with il6 promoter driving the expression of FKBP, Casp8-HA, and GFP. The resulting SuSe mouse inherits both transgenes, allowing for the specific identification and manipulation of senescent cells in vivo.

This model is designed to track and ablate p16/IL-6-positive senescent cells, thanks to the expression of the fluorescent reporters, GFP and mCherry, surrogate markers of p16 and IL-6 expression respectively, since their expression is controlled under the same promoter. The elimination of these double positive cells is achieved through administration of a compound named AP21967. This compound binds to the FKBP domain and FRB domain, causing the FKBP-FRB fusion and the consequent CASP8 homodimerization, thereby inducing apoptosis in cells co-expressing *Cdkn2a*/p16 and IL-6. Importantly, the CASP8 remain inactive unless dimerization is induced by AP21967 **(Figure 16)**.

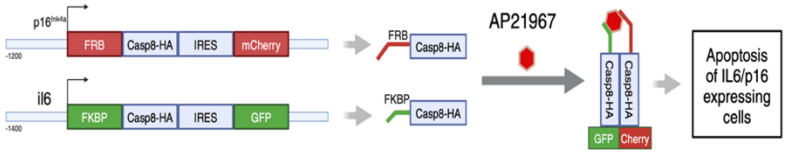


Figure 16. Mechanism of the SuSe system.

The p16 construct drives the expression of FRB, Casp8-HA, and mCherry, while the il6 construct drives the expression of FKBP, Casp8-HA, and GFP. Upon administration of the dimerizer AP21967, FRB and FKBP bring together Casp8-HA, resulting in the activation of Caspase-8 and subsequent apoptosis of cells expressing both p16 and il6.

1.1 Characterization of the SuSe model as a new model for studying senescence *in vivo*

To validate the SuSe system *in vivo*, young mice were treated with the DNA-damaging agent doxorubicin, which is known to induce senescence at high doses mainly in the liver. After treating the SuSe mice once a week for 2 weeks with 10 mg/Kg, mice were sacrificed and livers were obtained **(Figure 17, A)**. Analyses using flow cytometry demonstrated an increase in GFP and mCherry double positive cells after doxorubicin treatment. Subsequent treatment with AP21967, the dimerizer activating FKBP-FRB fused Casp8, resulted in the reduction of cells expressing GFP and mCherry-expressing cells to basal levels, confirming the ability of the SuSe system to eliminate cells that are transcriptionally active for *cdkn2a*/p16 and *Il6* genes **(Figure 17, B)**.

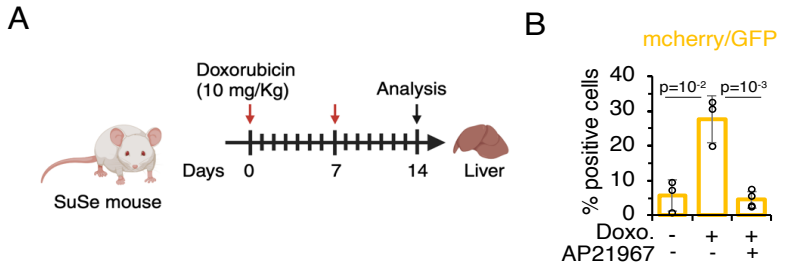


Figure 17. Validation of p16/IL-6 co-expressing cells apoptosis in vivo following senescence induction in vivo.

A. Schematic of the treatment schedule of SuSe mice, which were treated once a week for 2 weeks with PBS, doxorubicin (Doxo), or a combination of Doxo and AP21967. B. Flow cytometry analysis quantifying the percentage of mCherry and GFP-positive cells in liver samples. Results are presented as means ± standard deviations for three mice. Statistical comparisons were performed using Student's t-test, with a p-value of <0.05 considered statistically significant.

In summary, these results validate our new transgenic model, the SuSe mouse, for identifying cells co-expressing *Cdk2a*/p16 and *IL6 in vivo* and for eliminating these cells upon administration of AP21967.

1.2 PyMT/SuSe mice: a novel oncogenic *in vivo* model for studying the role of senescence in tumorigenesis

After successfully generating and validating our SuSe model, we proceeded with the primary objective of this thesis, which was to elucidate the role of senescent cells in tumor progression. To achieve this goal, we crossed our SuSe mice with a well-characterized breast cancer experimental model, the MMTV-PyMT mice (PyMT). This model consists of the Mouse Mammary Tumor Virus (MMTV) promoter to drive the expression of the Polyoma Middle T Antigen (PyMT). The MMTV promoter ensures that the *PyMT* oncogene is specifically expressed in mammary tissues, leading to tumor formation. The utilization of this mouse model offered a distinct advantage due to its well-defined tumor stages. At

four weeks, mice initiate tumor development, progressing into palpable tumors by nine weeks and evolving into fully developed carcinomas by thirteen weeks (94). This model is also widely used to study metastasis, as 90% of the mice will develop lung metastasis after their 13th week of life (94). Therefore, we developed a unique transgenic mouse model, named PyMT/SuSe, which spontaneously develops breast tumors and lung metastasis at later stages, and can be used to track and kill those cells co-expressing p16 and IL-6, representing senescent cells, at any stage of the tumorigenesis **(Figure 17)**.

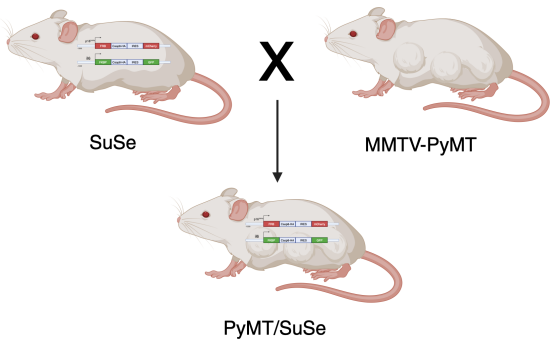


Figure 18. Generation of PyMT/SuSe mouse model.
The breading strategy involved crossing a female mouse carrying the SuSe transgenes with a male mouse carrying the PyMT mutation. The resulting PyMT/SuSe mice inherit the three transgenes, allowing for the specific identification and manipulation of senescent cells in a model that develops breast tumors.

Our first goal was to study the relevance of senescence in the process of tumorigenesis. For that, we assessed the percentage of senescent cells present in each of the stages of tumor progression. To monitor cellular senescence throughout tumor development, we collected mammary gland samples of the PyMT/SuSe mice at key time points, specifically from four to nine weeks, and thirteen weeks. We initially used SA-ß-Gal staining as a surrogate marker for identifying the senescent cells. Although SA-ß-Gal cannot serve as the unique marker for senescence, it is highly valuable for an initial assessment **(Figure 19, A)**.

Results show that the percentage of SA-ß-Gal-positive cells, the blue ones, was notably higher in the early stage of tumor development (4 and 5 weeks), reaching more than 50% of the total tumor epithelial population. This percentage gradually decreased throughout tumor progression, dropping to 15% in the intermediate stage (9 weeks) and further decreasing to 5% at the 13-week stage **(Figure 19, B)**. This observation indicates that cellular senescence activity is more frequent at in the initial stages of tumor development.

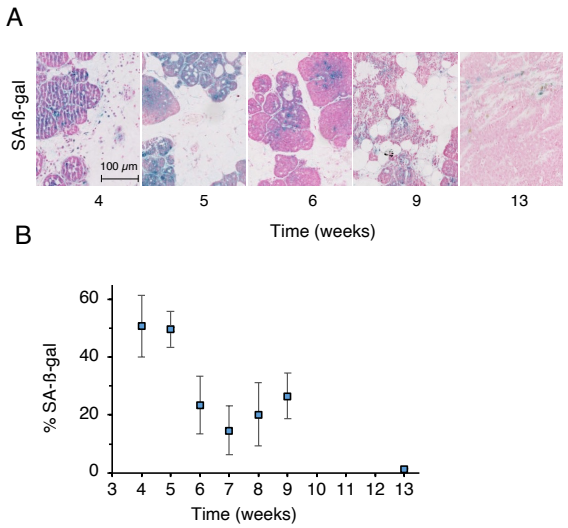


Figure 19. Monitoring cellular senescence during tumor progression.
A. *SA-ß-Gal staining performed in mammary gland samples from mice aged 4, 5, 6, 9 or 13 weeks.* ***B.*** *Quantification of the percentage of SA-ß-Gal positive cells among all epithelial cells in the samples, based on the ratio of blue (positive) cells to pink (negative) cells. Results are expressed as means ± standard deviations for two mice.*

Subsequently, to validate the results obtained with the SA-ß-Gal staining and also to prove that we can identify senescent cells with our SuSe system, we tracked senescence in the principal stages of tumorigenesis, 4 weeks, 9 weeks and 13 weeks. We compared the numbers of cells double positive for mCherry and GFP by immunofluorescence (IF) stanning with the percentage of cells

exhibiting SA-ß-Gal **(Figure 20, A)**. As expected, the correlation analysis between SA-ß-Gal and IF staining revealed a stronger association with the percentage of double positive cells than with cells expressing either mCherry (*Cdkn2a*/p16) or GFP (*IL6*) alone **(Figure 20, B)**. Noteworthy is the presence of a 20% of cells expressing p16 without concurrent IL6 expression at four weeks and, conversely at thirteen weeks, a significant percentage of IL6 positive cells were identified without simultaneous p16 expression **(Figure 20, B)**. These findings suggest the existence of potentially non-senescent cells that express either p16 or IL-6 alone highlighting the advantage of our SuSe model, which offers enhanced specificity through the dual-marking of senescent cells.

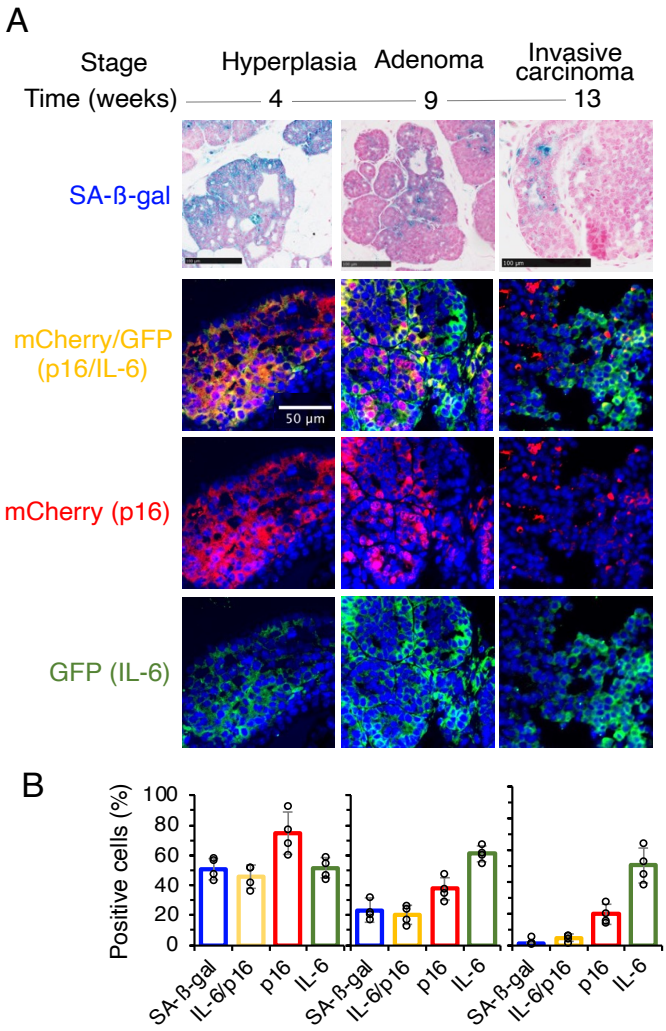


Figure 20. Validation of the mCherry/GFP reporter system in the PyMT/SuSe mice.

A. *Mice were euthanized at different time points corresponding to the indicated tumor stages: hyperplasia (4 weeks), adenoma (9 weeks) and invasive carcinoma (13 weeks). Mammary glands were processed and stained for SA-ß-gal or analyzed by IF to visualize the expression of the mCherry (red) and GFP (green) reporters under the control of p16 and/or IL-6 promoters.* ***B.*** *Quantification of positive cells in the samples. For SA-ß-gal-stained samples, the ratio of blue (positive) cells to pink (negative) cells was calculated. For IF, the ratio of red (p16-positive) or green (IL6-positive) cells to blue (negative) cells was calculated. The ratio of yellow (double-positives) cells was calculated by overlapping the green and red stainings. Results are expressed as means ± standard deviations for at least three mice.*

Having established the suitability of the model to follow senescent cells through tumorigenesis, we next sought to analyze the potential of our system to eliminate senescent cells on demand. For that purpose, we explored the capacity of senescent cell elimination upon AP21967 treatment in tumors. We started treating the mice when they were 4 weeks old, as it is the stage with higher senescent activity. After two weeks of treatment, AP21967 efficiently cleared double p16/IL-6 positive cells, while the percentage of cells expressing either p16 or IL-6 remained constant **(Figure 21)**. These results underscore the value of SuSe mice in specifically monitoring and targeting senescent cells during tumor progression.

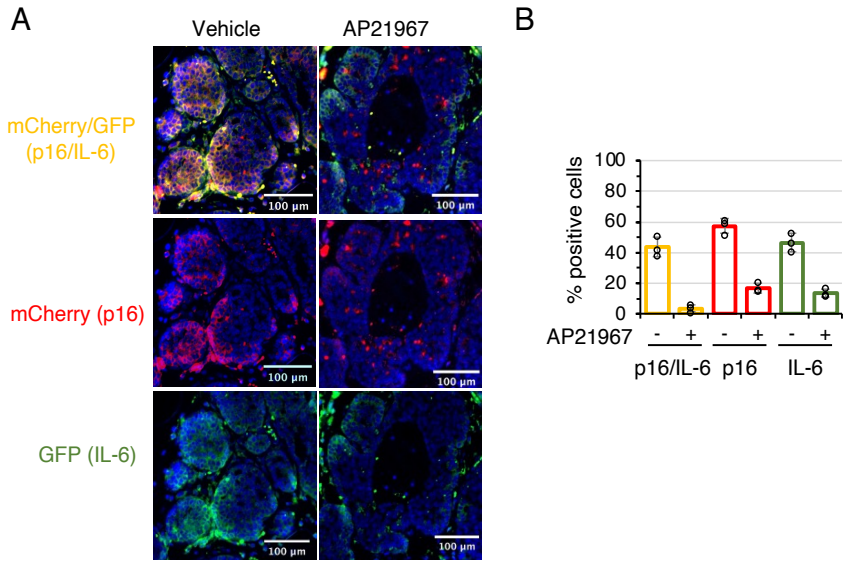


Figure 21. Validation of suicide system induction in the PyMT/SuSe model.
A. *Mice were euthanized after treatment with either AP21967 or vehicle twice a week for two weeks i.p. IF staining was performed on mammary gland samples to visualize mCherry (red) and GFP (green) positive cells, and double positives (yellow) by overlapping both images.* ***B.*** *Quantification of positive cells in the samples. The ratio of p16-mCherry/IL-6-GFP (yellow), p16-mCherry (red), or IL-6-GFP (green) expressing cells to total cells (blue) was calculated. Results are expressed as means ± standard deviations for at least three mice.*

Overall, we have validated the use of the spontaneous tumor model with the suicide cassette, PyMT/SuSe, demonstrating that the double-positive cells correspond with SA-ß-Gal expression and can be specifically eliminated. We also observed that, under baseline conditions, the proportion of senescent cells in this model decreases as the tumor progresses. Therefore, our next objective was to explore how the targeted senolysis at various stages may impact tumor growth and metastasis, thereby elucidating the role of senescent cells in tumorigenesis.

2. Elucidating the role of OIS in tumor development

2.1 Elimination of senescent cells at early stages promotes tumorigenesis

Given that senescence activity is higher at first stages, we first explore the effect of start eliminating senescent cells at 4 weeks of age. We compared the progression of primary mammary tumors in PyMT/SuSe mice treated with AP21967 or vehicle alone, continuing treatment until week 13 **(Figure 22, A)**. Interestingly, elimination of senescent cells at these early stages led to accelerated tumor progression **(Figure 22, B)**. To confirm that this effect was specifically due to the elimination of senescent cells and not a side effect of the AP21967 compound, we performed the same treatment strategy in PyMT mice, which lack the SuSe constructs. In these mice, tumor progression was not affected by AP21967 treatment **(Figure 22, C)**

These results confirmed that the observed increase in tumor volume after treatment from the hyperplasia stage was attributable to the SuSe system and the subsequent elimination of senescent cells, suggesting a protective role of senescent cells in the early stages of tumor development.

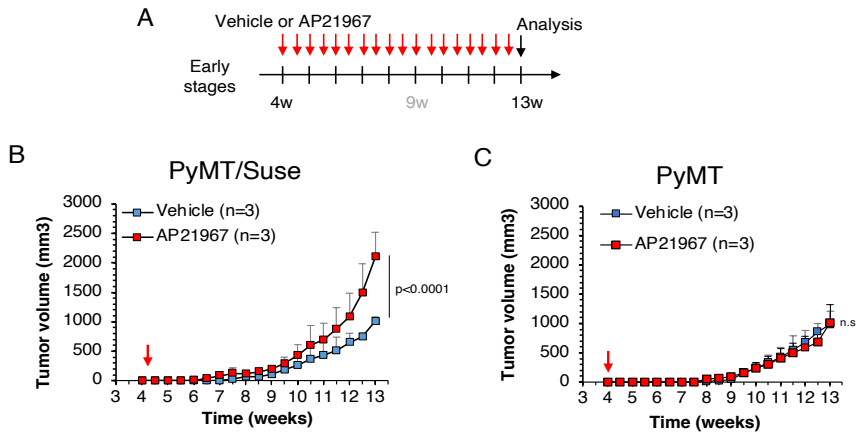


Figure 22. Elimination of senescent cells at early stages accelerates tumorigenesis.
A. *Treatment scheme showing the initiation of treatment with AP21967 or vehicle at 4 weeks of age and analysis at 13 weeks.* ***B.*** *Tumor growth in PyMT/SuSe mice was monitored twice a week. Mean tumor volumes of 4 mice are represented, with corresponding standard deviations.* ***C.*** *Tumor growth in PyMT mice, monitored in the same way as* ***B.*** *Statistical comparisons were performed using two-way ANOVA. A p-value <0.05 was considered statistically significant and ≥0.05 non-significant (n.s).*

Next, we sought to determine whether this increased primary tumor development following early senolysis was also accompanied by an increase in metastatic capacity. We analyzed the lungs of the mice treated with either vehicle or AP21967, which were necropsied at 13 weeks. Pan-keratin (Pan-K) staining by IHC was performed on five different cut sections of each lung **(Figure 23**, **A)**, and the number of metastases was quantified **(Figure 23**, **B)**. The results demonstrated that the elimination of senescent cells in the early stages of tumor development also significantly increased the number of metastases of PyMT/SuSe mice. Furthermore, the average size of the metastases was also increased by 4-fold **(Figure 23**, **B)**. In contrast, PyMT mice showed no differences in metastasis between vehicle and AP21967 treatments **(Figure 23**, **C,D)**, indicating that the observed effects were due to the elimination of p16/IL6-expressing cells, reinforcing the hypothesis that senescent cells play a protective role in early stages of tumor development.

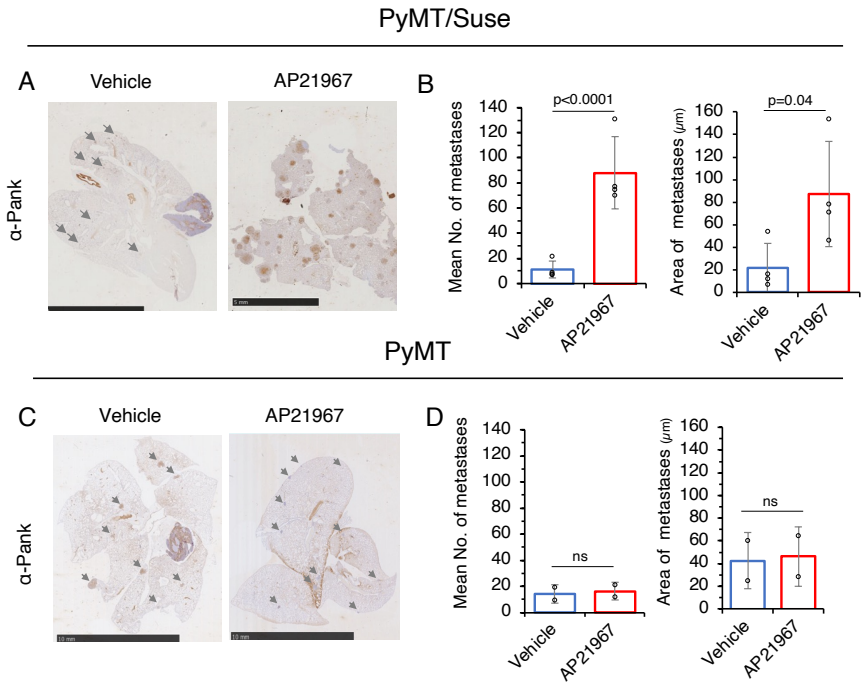


***Figure 23. Elimination of senescent cells at first stages promotes metastasis**. **A.** Pan-K IHC staining in lungs from 13-weeks old mice treated with vehicle or AP21967 from the 4th week of life. **B.** Quantification of the number of metastasis (left) and the area of the metastasis (right) of lungs from PyMT/SuSe mice. Results are expressed as means ± standard deviations of 4 mice. **C.** Quantification of the number of metastasis (left) and the area of the metastasis (right) of lungs from PyMT Results are expressed as means ± standard deviations of 2 mice. Statistical comparisons were performed using Student's t-test. A p-value <0.05 was considered statistically significant and ≥0.05 non-significant (n.s).*

Once we had determined the effect of eliminating senescent cells at early stages, we proceeded to study the impact of eliminating this population at later stages of tumor progression. We started treating PyMT/SuSe mice when they were 9 weeks old, when the tumors were at an intermediate adenoma stage. We followed the same twice-a-wee treatment strategy with either AP21967 or vehicle and sacrificed the mice when they were 13 weeks old **(Figure 24, A)**. Interestingly, the elimination of senescent cells at this later stage does not lead to the acceleration of tumorigenesis. In fact, if there

was any effect, it appeared to be antitumorigenic, as evidenced by a slightly lower tumor volume at 13 weeks in mice treated with AP21967 **(Figure 24, B)**. When analyzing metastasis in the lungs of these mice we observed a slight reduction in the number of metastases from a mean of 10 in vehicle-treated mice to a mean of 6 in AP21967-treated mice **(Figure 24, C)**.

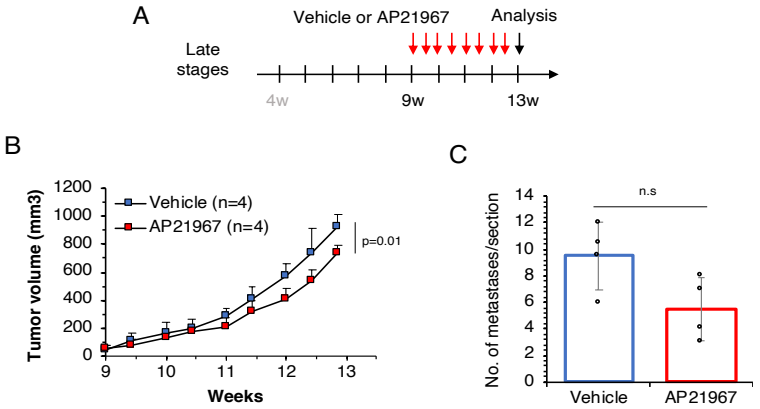


Figure 24. Elimination of senescent cells at late stages exhibits a modest anti-tumor effect.

A. *Treatment scheme showing the initiation of treatment with AP21967 or vehicle at 9 weeks of age and analysis at 13 weeks.* ***B.*** *Tumor growth in PyMT/SuSe mice was monitored twice a week from 9 to 13 weeks of age. Mean tumor volumes of 4 vehicle-treated mice are shown in blue, and of 4 AP21967-treated mice in red, with corresponding standard deviations.* ***C.*** *Quantification of the number of metastasis of PyMT/SuSe mice, represented as means ± standard deviations of 4 mice treated with vehicle or AP21967. Statistical comparisons were performed using two-way ANOVA for* ***B*** *and Student's t-test for* ***C****. A p-value <0.05 was considered statistically significant and ≥0.05 non-significant (n.s).*

Collectively, these findings suggest that senescent cells play a role in tumoral development, exerting distinct influences depending on whether the tumor is in its initiation phase or has progressed to a more advanced stage.

3. Senescent cells are needed for maintaining a protective TME in early development stages

3.1 Single-Cell RNA-sequencing analysis reveals that early senolysis reduces T cells and enhances macrophage infiltration

To gain insights into the mechanism behind this dual role of senescent cells in tumor progression, we performed single-cell RNA-sequencing (scRNA-seq) to have a complete view of the TME at the different stages of tumor progression. Thus, we took mammary glands samples of untreated PyMT/SuSe mice at four, nine and thirteen weeks. In addition, we treated some mice at four weeks with the AP21967 to have tumor samples at nine weeks that grew without senescent cells.

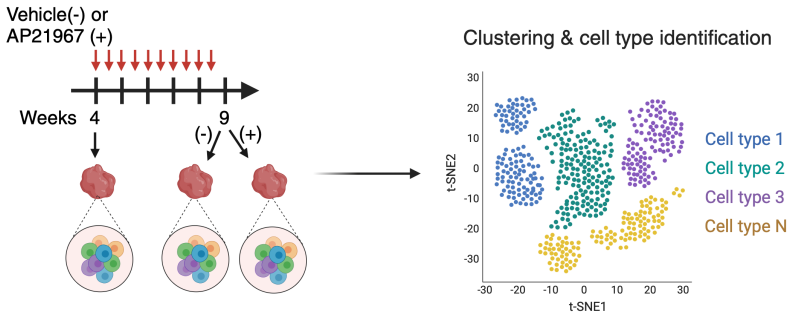


Figure 25. Schematic view of sc-RNAseq strategy.
PyMT/SuSe mice were treated either with vehicle or AP21967, starting at week 4 of the mice life, until the week 9. Tumors were taken from a 4-weeks old mouse and treated 9-weeks old mice for its digestion and consequent single cell analysis by RNA sequencing.

The scRNA-seq analysis revealed significant insights regarding the TME at the adenoma stage (9-week-old). Specifically, treatment with AP21967 resulted in profound changes in the immune cell compartment compared to untreated samples **(Figure 26, A)**. Precisely, tumors that developed in the absence of senescent cells exhibited a marked decrease in T cell populations, including both

CD4+ and CD8+ T cells, alongside an increase in macrophage number. Additionally, epithelial and endothelial cells were significantly increased in the 9-week sample treated with AP21967 **(Figure 26, A, B)**. Unfortunately, for unknown reasons, senescent cells could not be recovered in any of the samples, a challenge also noted by other researchers (ref).

To validate these transcriptomic results, we performed IHC staining, on sections of the same samples used for the scRNA-seq experiment, which were previously fixed in paraffin. We also included additional samples from 9-week-old mice treated with either vehicle or AP21967. IHC results confirmed a decrease in the CD4+ and CD8+ T cell population and an increase in the CD31-positive population, which is a marker of endothelial cells, in the samples treated with the AP21967 **(Figure 26, C)**.

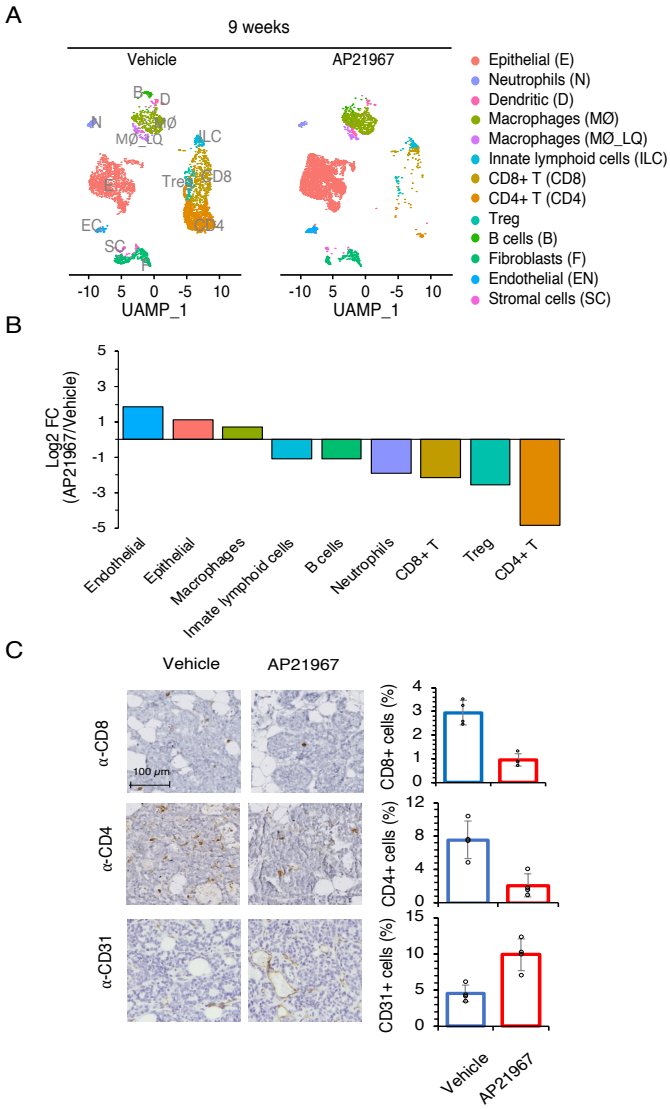


Figure 26. Impact of early AP21967-induced senescent cell elimination on TME composition.

A. *UMAP plot showing cell type population from single-RNA sequencing data of mammary gland samples from 9-week-old mice treated either with vehicle (left) or AP21967 (right). Each point represents an individual cell, and different colors indicate distinct cell type clusters.* ***B.*** *Logarithmic fold change representation of the number of cells in different populations as shown in the UMAP plot, comparing samples from 9-week-old mice treated with vehicle or AP21967.* ***C.*** *IHC staining of CD8, CD4 and CD31, with corresponding quantification. Quantitative results are shown as means ± standard deviations of 3 mice.*

These findings align with the phenotype observed when senescent cells were removed at the beginning of tumorigenesis. The increase in epithelial cells is in line with the accelerated tumor progression previously observed **(Figure 22)** while the increase in endothelial cells suggest enhanced malignant vascularization. Additionally, the reduction of the T cell population suggests a loss of immunosurveillance, which, in combination with the increase in macrophages, contributes to a more pro-tumorigenic microenvironment.

3.2 RNAseq of CD45+ populations reveals pro-tumorigenic macrophage profile following early senolysis

Regarding the macrophage population, we wanted to exert a more in-deep analysis trying to elucidate if, beyond increasing the number of macrophages, the population changed its expression pattern to a more pro-tumorigenic profile. However, we recognized that scRNA-seq analysis alone did not provide sufficient resolution to extract quantitative information regarding the expression of specific genes. Therefore, to gain a deeper understanding of the tumor landscape after senescent cell removal, we performed a bulk RNAseq analysis of the immune compartment.

We first sorted cell populations based on CD45 expression, a general marker of immune cells to focus on gene expression within the immune compartment (CD45+ population). To complement this approach, we also analyzed the non-immune (CD45-) compartment of the tumors.

We followed the same strategy as with the scRNAseq, comparing 9-week-old samples treated and untreated with AP21967 from the fourth week onward. Among the top 50 genes upregulated after senolysis were *Cd5l, Mrc1*, *Cd209*, and *Cd163*, all of which are associated with a pro-tumorigenic phenotype of macrophages **(Figure 27, A)**. Conversely, *il17, il21* and *il22* appear among the top

50 genes downregulated genes **(Figure 27, A)**, which are mainly expressed by the T cell population and codify for cytokines described for enhancing anti-tumor immune response. Quantitative analysis showed differences above of two-fold in all of them **(Figure 27, B)**. Collectively, these results indicate an increase in pro-tumorigenic macrophage-associated genes and downregulation of T cell-related genes after early senolysis, consistent with the increase in macrophages and a decrease in T cells seen in the scRNA-seq analysis **(Figure 26)**.

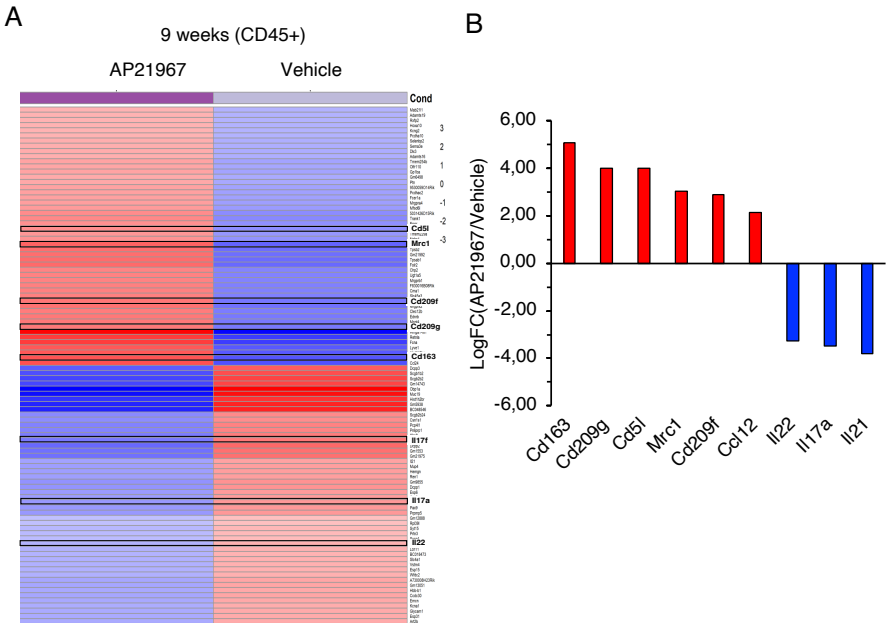


Figure 27. Differences in RNA expression of CD45+ population of 9-week samples treated with vehicle or AP21967.

A. *Heatmap showing genes upregulated (red) and downregulated (blue) in the CD45+ population of 9-week-old samples, comparing AP21967-treated mice to vehicle-treated mice.* ***B.*** *Logarithmic fold change of RNA count expression in CD45+ cells, comparing samples from 9-week-old mice treated with vehicle or AP21967.*

We further confirmed that the macrophage population emerging after early senolysis indeed expressed genes associated with a more pro-tumorigenic phenotype. IF staining against CD68, a general

macrophage marker, combined with an anti-MRC1 antibody **(Figure 28, A)** revealed that both the percentage of cells expressing CD68 and those expressing Mrc1 were increased in AP21967-treated samples, validating the RNAseq data **(Figure 28, B)**.

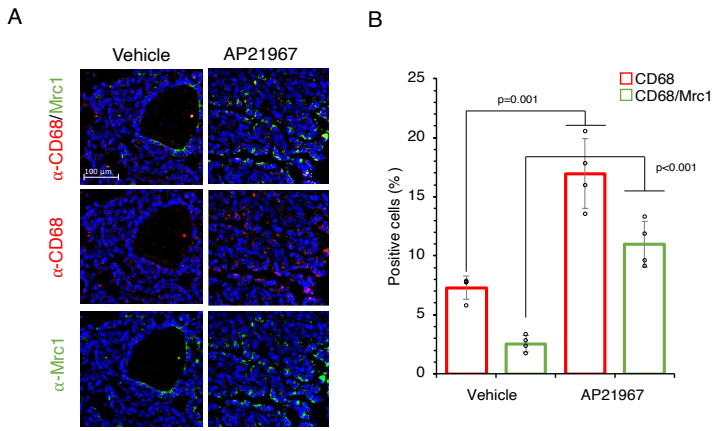


Figure 28. AP21967 treatment at 4 weeks promotes MRC-1 macrophage polarization.

A. *IF staining of CD68 (red) and Mrc1 (green) in mammary gland samples from 9-weeks old mice treated with vehicle or AP21967.* ***B*** *Quantification of the number of cells positive for CD68 (red) or Mrc1 (green) relative to total cells (blue). Results are shown in percentage means ± standard deviations of 3 mice. Statistical comparisons were performed using Student's t-test. A p-value <0.05 was considered statistically significant.*

These findings, combined with the ScRNA-seq analysis, demonstrate that the removal of senescent cells at 4 weeks not only increases the number of macrophages within the tumor but also promotes a more pro-tumorigenic phenotype in this population. Additionally, reduced T cell infiltration indicates an immunosuppressive environment. This pro-tumorigenic shift in the TME correlates with the accelerated tumor progression observed upon early-stage senolysis, confirming the protective role of senescent cells in controlling tumor progression through their interaction with the immune system. These intriguing results warrant further investigation into the exact mechanisms behind the interaction between senescent cells, macrophages, and T cells.

3.3 Elimination of the macrophage population induced by senolysis prevents its pro-tumorigenic effect.

To correlate the increased presence of macrophages with the immunosuppressive effect we observed following senolysis, we attempted to reverse this effect by depleting the macrophage population. To do so, we employed a drug called clodronate, which can be administered in liposomes and it is used to kill macrophages (95).

We initiated senolysis from the fourth week of age until the ninth week, at which point AP21967 treatment was discontinued and clodronate treatment began **(Figure 29, A)**. As controls, we included AP21967 and vehicle treated mice without clodronate. This approach aimed to test whether eliminating the macrophage population that emerges after senolysis could reverse the observed increase in tumor growth. Our results revealed that sequential treatment with AP21967 and clodronate prevented the pro-tumorigenic effect of senolysis, whereas the combination of vehicle and clodronate exhibited no significant effect **(Figure 29, B)**.

Moreover, IF staining for CD68 confirmed the effectiveness of clodronate, showing total elimination of the macrophage population, either in the presence or absence of senolysis **(Figure 29, C)**. However, in the absence of senolysis, no impact on tumor growth was observed, indicating that the upregulation of pro-tumorigenic macrophages is a direct consequence of senolysis.

To provide further clarification regarding the anti-tumor effect and the potential involvement of T cells, IHC staining for CD3 and CD8 was conducted in order to observe the lymphocyte infiltration of the tumors. It is noteworthy that the CD3+ and CD8+ percentages, which were nearly absent following AP21967 treatment, increased after macrophage depletion, regardless of previous senolysis **(Figure 29,**

D). However, the increase was more pronounced when senescent cells were previously eliminated, indicating that macrophage depletion can restore a beneficial outcome following senolysis.

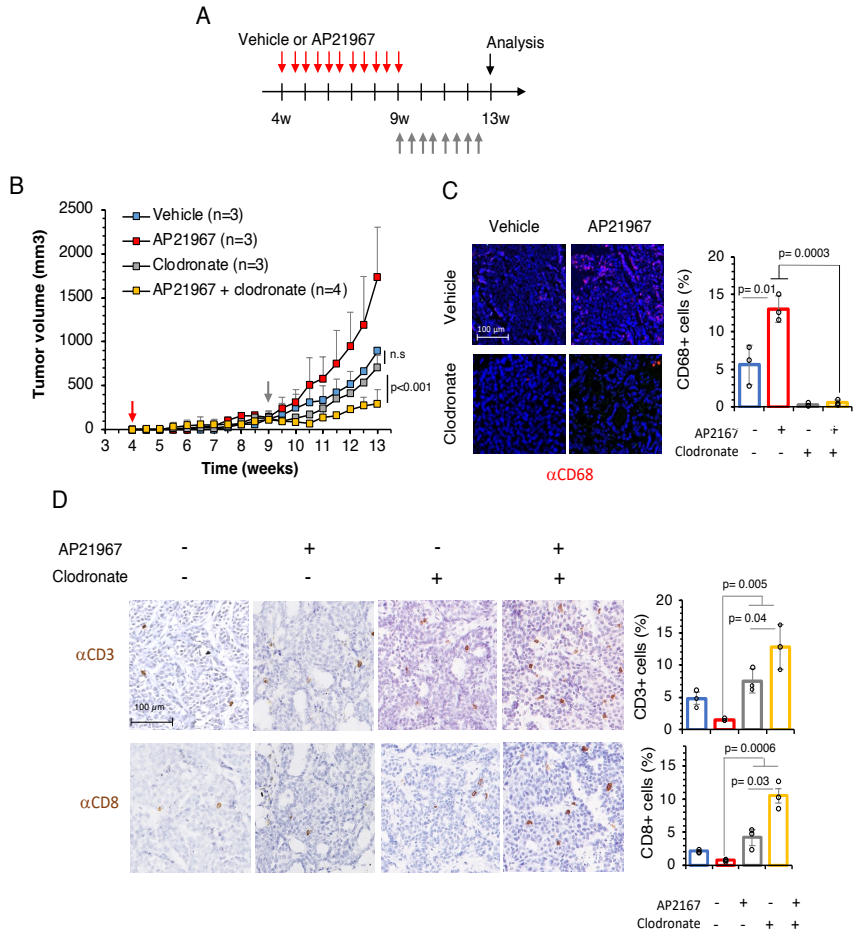


Figure 29. Elimination of the macrophage population that appears after senolysis prevents its pro-tumorigenic effect.

A. *Scheme of the treatment schedule. Vehicle or AP21967 is treated i.p from week 4 to week 9, twice a week. Clodronate treatment starts at 9 week and is treated i.p twice a week,* ***B.*** *Tumor growth from 4 to 13 weeks of age, is represented as mean tumor volumes with its standard deviations.* ***C*** *IF staining of CD68 (red) in 13-weeks samples and quantification of the percentage of cells expressing CD68. Results are represented as mean of number of positive cells (red) respective the total cells (blue) of 3 mice, alongside its standard deviation. P-values are reported directly in the Fig.s. Statistical comparisons were performed using two-way ANOVA for* ***B*** *(p-values of last points are represented in the graphs) and Student's t-test for* ***D****. A p-value <0.05 was considered statistically significant and ≥0.05 non-significant (n.s).*

Next, we analyzed the effect of macrophage depletion on lung metastases using pan-k IHC staining **(Figure 30**, **A)**. The results indicated that eliminating the macrophage population mitigates the increase in metastasis observed with AP21967 treatment, as the average number of metastases was reduced to levels comparable to the vehicle-treated samples. However, this depletion did not mitigate the size of the metastases in two of the three mice analyzed **(Figure 30**, **B)**. Samples treated with clodronate in combination with the vehicle exhibited similar numbers and size of metastases as those treated with vehicle alone, suggesting that clodronate did not exert an effect on its own. These results demonstrated that eliminating the macrophage population that appears after senolysis prevents the derived increase in the metastasis potential of tumor cells, although it cannot prevent the increase in the metastasis size.

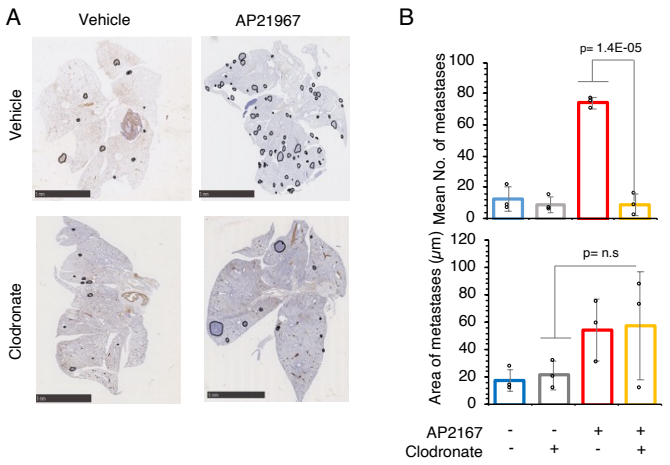


Figure 30. Eliminating the macrophage population that appears after senolysis prevents the increase in the metastasis potential.

A. *IHC of pan-K in lungs from 13-week mice treated with vehicle, AP21967 treated alone or in combination with clodronate.* ***B.*** *Quantification of number of metastasis (up) and mean of their areas (bottom), represented as means ± standard deviations of 3 mice. P-values are reported directly in the figures. Statistical comparisons were performed using Student's t-test. A p-value <0.05 was considered statistically significant and >0.05 non-significant (n.s)*

Based on our results, we hypothesized that early senolysis leads to an increase in anti-inflammatory and pro-tumorigenic macrophages. These macrophages, in turn, inhibit effector T cells, contributing to tumor progression by creating an immunosuppressive TME. This suggests that the timing of senolysis is critical, as it influences the balance between immune activation and suppression, potentially affecting tumor outcomes.

4. Senescent cells modulate cytokine release patterns in the TME

Having identified the key cellular players involved in the interplay between senescent cells and tumor cells, we next sought to investigate the molecular basis of this crosstalk. Understanding these mechanisms could uncover novel pathways and potentially actionable therapeutic targets for exploiting senolysis as a cancer treatment.

4.1 Multiplex cytokine assay reveals differences in cytokine levels in 9-week tumors with and without senescent cells.

We investigated the variations in cytokine levels across different stages of tumor development using a multiplex cytokine assay to analyze a panel of 48 cytokines in samples obtained from mice at 4, 9, and 13 weeks of age. These samples included those treated with AP21967 and untreated controls for a comprehensive analysis.

Our primary focus was to examine the 9-week samples, where we observed notable differences in cytokine expression depending on the presence of senescent cells. Particularly, C-C motif ligand 7 (CCL7), C-C motif ligand 3 (CCL3), and CCL2 were the cytokines that presented a higher increase when senescent cells are removed, whereas interleukin 17a (IL-17a), IL-6, and interleukin 31 (IL-31) levels were reduced in AP21967-treated samples **(Figure 31, A)**. Furthermore, we analyzed the levels of these cytokines between the

early and intermediate stages of tumor development to confirm that the elimination of senescent cells was in fact changing the pattern of expression. Results shown in **(Figure 31, B)** corroborated that senolysis exacerbated the differences between these stages. Importantly, while efficient, multiplex cytokine assay is a high-throughput approach, it needs further validation by traditional ELISA. Results analyzing CCL2 and IL-31 confirmed the consistent patterns of increase and decrease, respectly **(Figure 31, C)**, thereby validating the array results.

The cytokines showing the most significant differences, CCL7, CCL3, and CCL2, are chemokines involved in immune cell recruitment, particularly macrophages (96), which are associated with poor prognosis as they promote tumor growth, angiogenesis, and metastasis (97). Their increase correlates with the increase in the number of macrophages seen in the scRNA-seq **(Figure 26)**. Conversely, the reduction in IL-6 is in line with the elimination of p16/IL-6 expressing cells, while the decrease in IL-17a, also noted in the RNAseq analysis **(Figure 27)**, correlates with the dissapearance of the CD4+ T cell population (98). IL-31, a cytokine mainly released by T cells that contributes to anti-tumor immunity in breast cancer (99), also showed a decrease, which is consistent with the reduced T cell infiltration following early senolysis **(Figure 26)**.

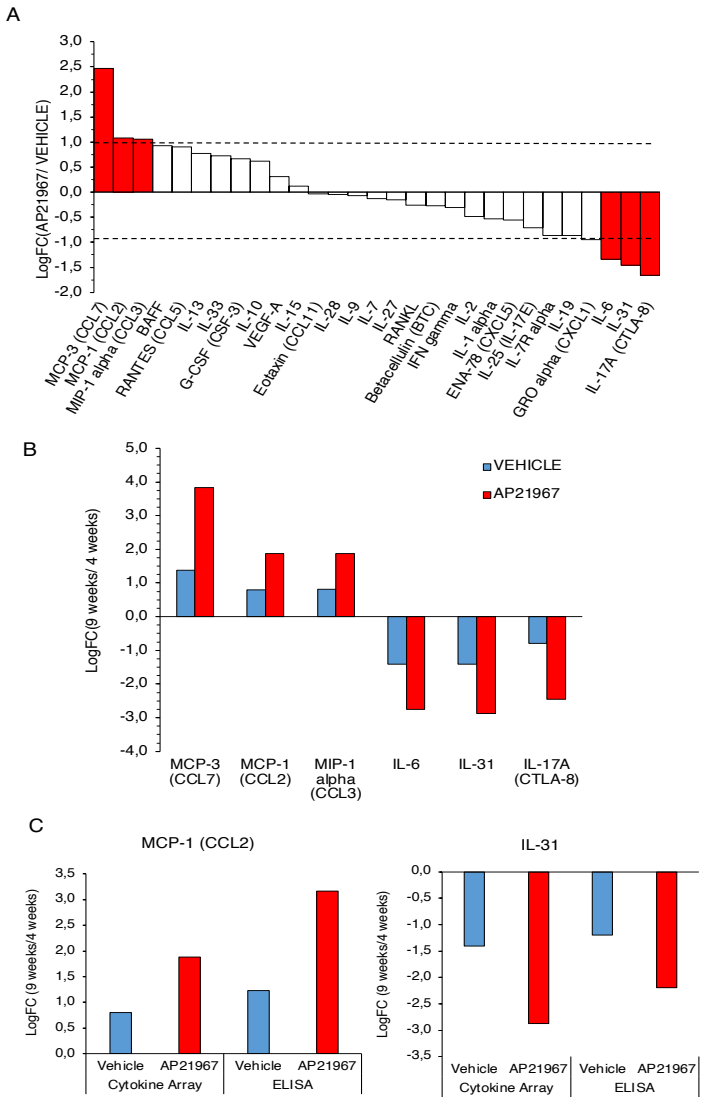


Figure 31. Elimination of senescent cells at first stages alters cytokine release pattern.

__A.__ Logarithmic fold change in the concentration of different cytokines. Cytokines with a logarithmic fold change greater than one are highlighted in red. __B.__ Logarithmic fold change in the concentration of the cytokines highlighted in red in panel A, comparing samples from 9-week-old and 4-week-old mice. __C.__ Comparison of the logarithmic fold change in the concentration of CCL2 and IL-31 between 4-week and 9-week samples, obtained from the multiplex cytokine assay assay (left) and by ELISA (right).

4.2 RNAseq analysis shows upregulation of CCL2, CCL3 and CCL7 in the immune population following early senolysis

We then investigated the source of these cytokine expression changes. Therefore, we looked for differences in the RNA expression of CCL7, CCL2, CCL3, IL-6, IL-31 and IL-17 in the RNAseq data in CD45+ or CD45- population. We were able to perform the analysis for all cytokines except IL-31, which was not found in the sequencing data.

When comparing 9-week samples treated or not treated with AP21967, we found similar results to those obtained with the multiplex cytokine assay. Of interest, CCL7 shows an increase of expression in the CD45+ population and a decrease in the CD45- population **(Figure 32)**. This observation can be explained as this cytokine by the fact that CCL7 is secreted by macrophages (100), a population that is increased after senolysis, as well as by senescent cells (37), which are eliminated by AP21967 treatment. Similarly, the increase in CCL2 and CCL3 were predominantly seen in the immune population **(Figure 32)**. Conversely, cytokines that decreased after senolysis, such as IL-6, showed a higher reduction in the CD45- population than in the CD45+ population **(Figure 32)**. This result is consistent with the elimination of the p16/IL-6 population, which showed to be predominant in the first stages of the tumor development **(Figure 20)**. IL-17, known to be expressed exclusively by CD45+ cells, also decreased in this population**.**

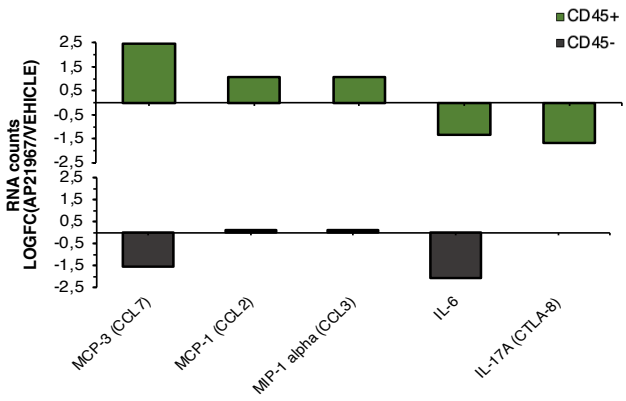


Figure 32. Differences in the pattern of expression of some cytokines in the CD45+ or CD45- population depending on the presence of senescent cells. *Logarithmic fold change in the CD45+ sorted population (green) and in the CD45- sorted population (black, compairing 9-weeks samples treated with vehicle or AP21967, of CCL7, CCL2, CCL3, IL-6 and IL-17.*

4.3 scRNA-seq reveals macrophages as sources and responders to CCL2, CCL3 and CCL7

To prove that the increse of CCL2, CCL3 and CCL7 correlates with the increase in the macrophage population after senolysis, we analyzed our scRNA-seq data to identify the cell population expressing these cytokines. The analysis confirmed that the predominant population secreting these cytokines at 9 weeks was indeed the macrophages. Their expression slighlty increased after senolysis, though these cytokines were also expressed by macrophages in vehicle-treated samples **(Figure 33)**. Notably, CCL2 was also expressed by the epithelial and fibroblast populations after AP21967 treatment **(Figure 33**, **A)**, consistent with RNA-seq data. The expression of this cytokine in this population is usually related with a more pro-tumorigenic profile (101), suggesting that elimination of senescent cells also afects directly to the selection of more aggressive tumor cells.

It is noteworthy that distinct subpopulations of macrophages secrete CCL2 and CCL3, while the same subpopulation exhibited secretion of CCL2 and CCL7 **(Figure 33)**. These two last cytokines are

described as chemoatractant for macrophages and can induce the secretion of certains cytokines in other macrophages, such as CCL3 (100). These results suggest an interaction between macrophages that depends on the cytokines released by this population .

To further investigate these macrophage interactions, we analyzed the expression of cytokines receptors. The presence of CCR2, the receptor for CCL2, as well as CCR1 and CCR5, which have been previously described as capable of binding both CCL3 and CCL7, was investigated. The analysis of the sample treated with AP21967 reveals that all receptors are also predominantly expressed by macrophages, with subpopulations exhibiting varying levels of expression, being CCR1 and CCR5 expression more homogeneous **(Figure 34, B)** compared to CCR2 **(Figure 34, A)**. These findings confirm that macrophages are both the source and the receptors of the cytokines upregulated after senolysis.

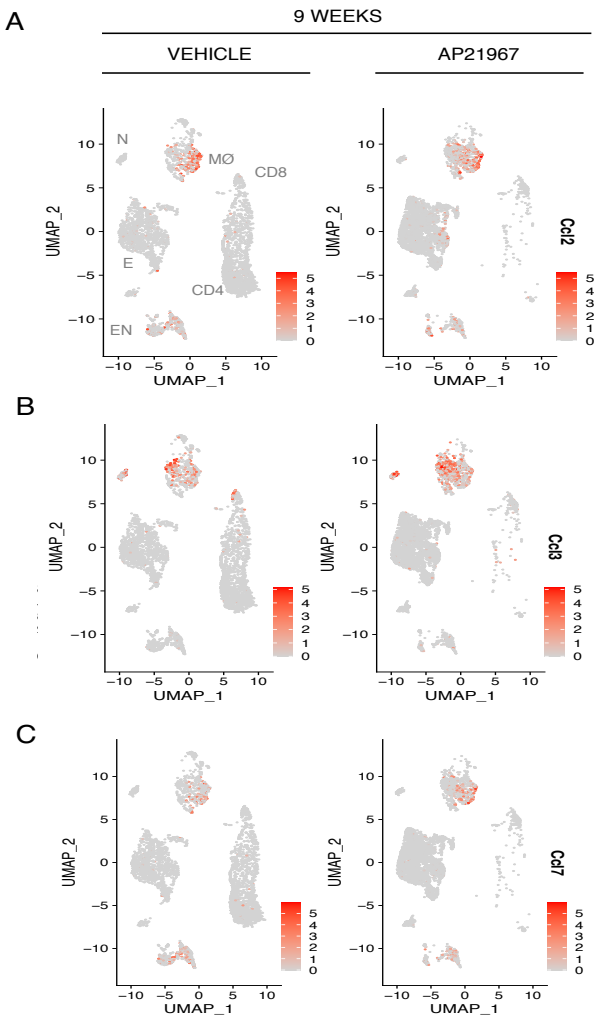


Figure 33. CCL2, CCL3 and CCL7 are mainly expressed by the macrophage population.

UMAP plots of single-cell RNA sequencing data showing the expression of CCL2 ***(A),*** *CCL3 (**B**) and CCL7 (**C**) in the TMEof 9-week-old mice treated with vehicle (left column) or AP21967 (right column). Each plot represents individual cells, with red indicating higher expression levels of the respective cytokines. Cell type populations are labeled as N (Neutrophils), E (Epithelial cells), MØ (Macrophages), CD4 (T cell CD4+) CD8 (T cell CD8), and EN (Endothelial cells)*

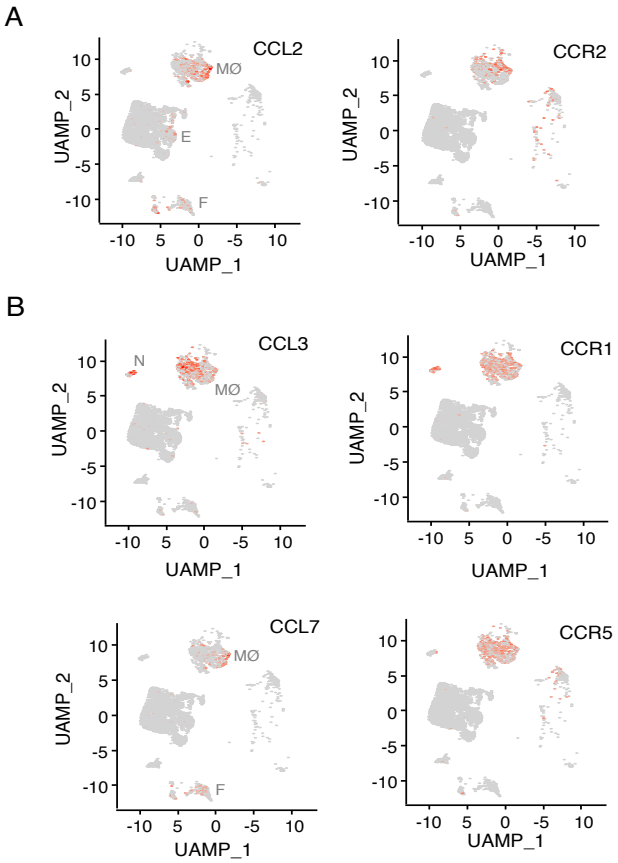


Figure 34. Senescent cells removal creates a feedback positive loop of CCL2, CCL3 and CCL7 secretion that will retain macrophages in the tumor.

A. *UMAP plots of single-cell RNA sequencing data showing in red the expression of CCL2 (left) and CCR2 (right) in the TME of 9-week-old mice treated with AP21967.* ***B.*** *UMAP plots of single-cell RNA sequencing data showing in red the expression of CCL3 (up left), CCR1(up right), CCL7 (down left) and CCR5 (down right) in the TME of 9-week-old mice treated with AP21967. Cell type populations are labeled as E (Epithelial cells), MØ (Macrophages), F (Fibroblasts) and N (neutrophils).*

In summary, these findings show that CCL7, CCL2 and CCL3 are secreted by the macrophages, and suggests the existence of a feedback loop that ultimately results in the expansion of pro-tumorigenic macrophages **(Figure 35)**.

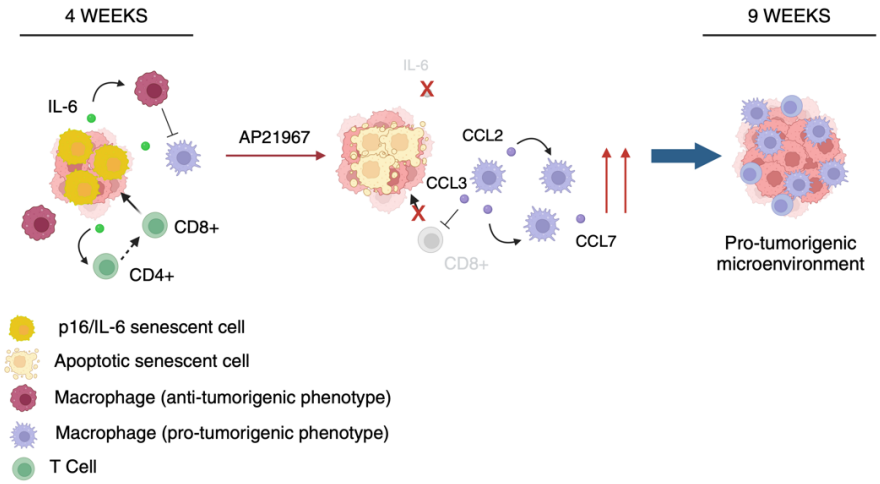


Figure 35. Early senolysis promotes a pro-tumorigenic microenvironment driven by macrophages.

Working model where p16/IL-6 senescent cells maintain a balanced immune environment necessary in early stages for tumor surveillance. Elimination of these cells promotes a more pro-tumorigenic microenvironment through the differentiation and survival of pro-tumorigenic macrophages, which release CCL2, CCL3, and CCL7, and the disappearance of the T cell population.

4.4 Pro-tumorigenic microenvironment derived from early senolysis favors metastatic tumor cell selection

We further sought to determine whether the change in the cytokine pattern release could also affect metastasis. To this end, we analyzed the cytokine data from the 13-week timepoint and we could observe that CCL2 and CCL7 remained upregulated in the AP21967-treated samples at this stage. In addition, the following cytokines exhibited a logarithmic fold change above one: LIF (Leukimia Inhibitory Factor), G-CSF (Granulocyte Colony-Stimulating Factor), BAFF (B-cell Activating Factor), CXCL1, CXCL10, M-CSF (Macrophage Colony-Stimulating Factor) and IL-6 **(Figure 36, A)**. LIF, CXCL1 and CXCL10 are often associated with promoting tumor progression, by supporting cancer cell survival, when secreted by tumor cells (100). G-CSF and M-CSF promotes the differentiation and survival of macrophages, contributing to

immune evasion(102). Moreover, all of these cytokines are known to facilitate metastasis by aiding tumor cell migration and invasion (103).

To elucidate which type of population was secreting these cytokines within the TME, we looked at their expression in our RNAseq data of sorted populations. We confirmed their upregulation in the CD45- population **(Figure 36, B)** and we saw a change in the pattern of expression of these cytokines depending on the presence of senescent cells in the tumor development. Thus, in vehicle samples these cytokines are mainly expressed by the CD45+ sorted population, while in the case of AP21967 treated samples, is the CD45- sorted population the one expressing these cytokines **(Figure 36, C)**.

To complete the analysis on the epithelial and stromal population, we also performed a Gene Set Enrichment Analysis (GSEA) on the RNAseq 13-week CD45-. The analysis revealed that the top five upregulated gene hallmarks in samples treated with AP21967 were TNFα signaling via NFκB, epithelial mesenchymal transition (EMT), coagulation, apoptosis, and IL-6/JAK/STAT3 signaling **(Figure 36, B)**. Among these hallmarks, TNFα signaling via NFκB, EMT, and IL-6/JAK/STAT3 signaling shared multiple upregulated genes related to metastasis. Specifically, beyond IL-6, these hallmarks include multiple MMPs, including Mmp2, Mmp3, Mmp11, and Mmp14, among other genes that further confirm the higher metastatic profile of tumor cells that grew without senescent cells.

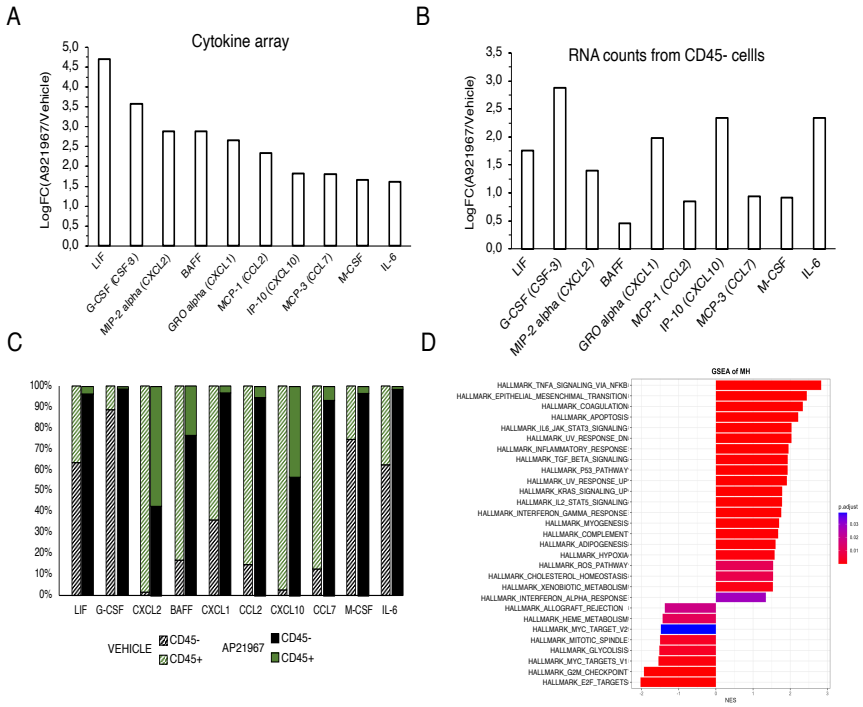


Figure 36. The pro-tumorigenic microenvironment created by senescent cells early removal favor selection of metastasis-prone tumor cells.

A. *Logarithmic fold change in cytokine concentration of 13-weeks samples treated with vehicle or AP21967 greater than 1.5.* ***B.*** *Percentage representation of cytokine expression in CD45+ (green) and CD45- (black) sorted populations. Discontinuous lines represent vehicle-treated samples, and full-color bars represent AP21967-treated samples.* ***C.*** *Logarithmic fold change greater than 1.5 in RNA counts from the CD45- population of 13-week-old samples treated with AP21967 in comparison with vehicle.* ***D****. GSEA plot showing the hallmarks of genes upregulated and downregulated of 13-week-old samples, comparing AP21967-treated samples to vehicle-treated samples.*

In summary, these findings suggest that the protumorigenic microenvironment promoted by macrophages at 9 weeks after early senolysis, favors the selection of primary tumor cells more prone to metastasize, which continue to secrete pro-tumorigenic cytokines at later stages.

4.5 CCL2 blockade mitigates pro-tumorigenic effects of early senolysis and exhibits anti-tumor activity when combined

To validate the hypothesis of macrophages being retained in the TME by the increased releasing of the aforementioned cytokines by this population, we performed functional analyses. Of the three cytokines, we chose to block CCL2 using a monoclonal antibody against it, as it has also been described to play a role in metastasis (104).

We started treating the mice with the anti-CCL2 antibody, alone or in combination with the AP21967, at 4 weeks **(Figure 37, A)**. The outcome showed that combining senolysis with CCL2 blockage not only prevented the pro-tumorigenic effect seen after the AP21967 treatment, but also had an anti-tumor effect compared to vehicle-treated mice **(Figure 37, B)**. Additionally, treatment with the anti-CCL2 antibody alone showed a small anti-tumor effect compared to the vehicle arm, but not as pronounced as when combined with senolysis. This could be due to the elimination of pre-existing protumorigenic macrophages, that are further increases when senescent cells are eliminated.

To confirm that anti-CCL2 treatment was in fact reducing the number of macrophages within the tumor, we performed IF staining for CD68 and CCL2 in the end-point samples. As expected, As expected, CCL2 blockade reduced the number of macrophages that had increased after senolysis **(Figure 37, C)**. Regarding CCL2 expression, we observed no significant differences in the percentage of cells expressing this cytokine between samples treated with vehicle and the anti-CCL2 antibody alone. However, the number of tumor cells stained for CCL2, which increased in AP21967-treated samples, was reduced when combined with anti-CCL2 **(Figure 37, C)**.

To correlate the reduction in the macrophage population with the anti-tumor effect seen, we also performed IHC staining for CD3 and CD8 in the same samples. The results revealed that the infiltration of CD3+ and CD8+ T cells was higher in samples treated with the combination of AP21967 and the anti-CCL2 antibody than in those treated with the anti-CCL2 antibody alone **(Figure 37, D)**.

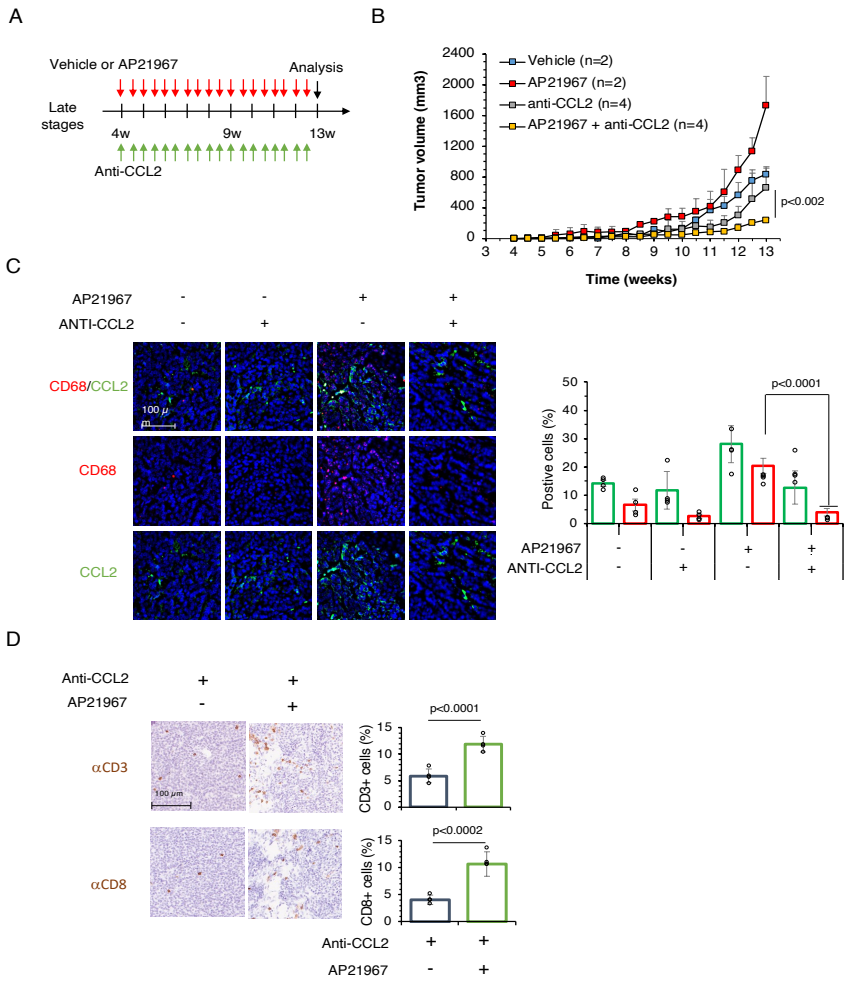


Figure 37. Blocking CCL2 prevents the pro-tumorigenic effect of early senolysis.

A. *Treatment strategy. Vehicle, AP21967 and anti-CCL2 antibody were treated i.p from week 4 to week 13, twice a week, alone or in combination* ***B.*** *Tumor growth was measure twice a week and mean tumor volumes are represented along with their corresponding standard deviations.* ***C.*** *IF staining of CD68 (red) and CCL2 (green) in 13-weeks mammary gland samples of mice treated with vehicle (-,-), AP21967 (+,-), anti-CCL2 (-,+) or the combination of AP21967 and anti-CCL2 (+,+)* ***D.*** *IHC staining for CD3 (top) and CD8 (bottom) in 13-week-old samples treated with anti-CCL2 antibody alone (+,-) or in combination with AP21967 (+,+). Quantification is represented as the mean percentage of positive cells for CD3 (top) and CD8 (bottom) with their standard deviations. Statistical comparisons were performed using two-way ANOVA for* ***B*** *and Student's t-test for* ***C*** *and* ***D****. A p-value <0.05 was considered statistically significant.*

Finally, when analyzing metastasis, results showed that blocking CCL2 not only prevents the effect of AP21967 treatment in the tumor growth but also reduced the number of metastases **(Figure 38**, **A)**. Interestingly, blockade of CCL2 alone had no effect on metastasis, as the average of metastasis in these samples was comparable to that observed in the vehicle-treated samples **(Figure 38**, **B).** This result reinforeces the role of CCL2 in the pro-tumorigenic phenotype derived from early senolysis, providing a potential therapeutic target.

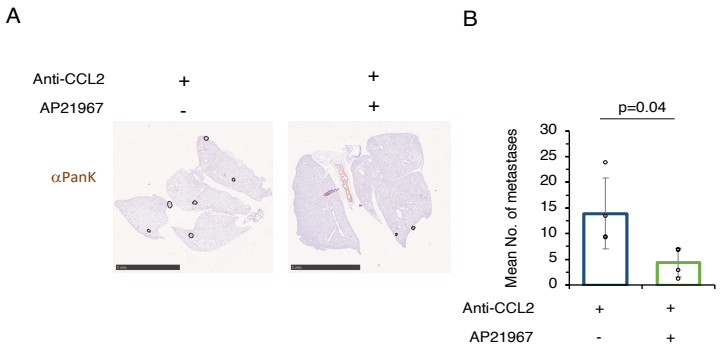


Figure 38. Blocking CCL2 in combination with early senolysis reduces the number of lung metastasis.

A. *IHC of pan-K in lungs from 13-week mice treated with anti-CCL2 alone (-) or in combination with AP21967 (+).* ***B.*** *Quantification of number of metastasis is represented as means for four mice with their standard deviations. Statistical comparisons were performed using Student's t-test. A p-value <0.05 was considered statistically significant.*

In summary, we have proven with our PyMT/SuSe model that the high senescence activity seen in the early stages of tumor development maintain an immune microenvironment necessary for tumor surveillance. When senolysis is applied in this stage, changes in the cytokine release pattern promote the expansion of pro-tumorigenic macrophages that will maintain an immunosuppressive environment that will favor tumor growth and metastasis. Elimination of these macrophages, either through clodronate or anti-CCL2 treatment, can reverse the pro-tumorigenic effect and restore a beneficial effect of senolysis in cancer treatment **(Figure 39)**.

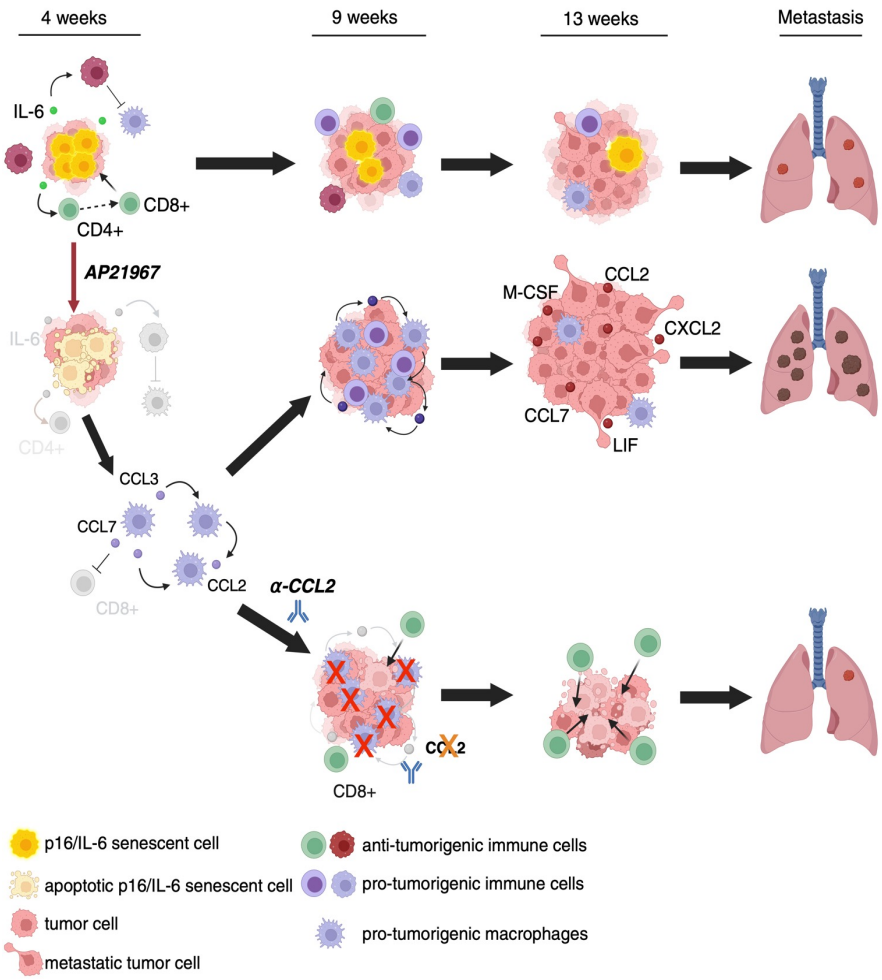


Figure 39. Early senolysis has a pro-tumorigenic effect driven by macrophages.

Working model showing that at 4 weeks, p16/IL-6+ senescent cells (yellow) are surrounded by anti-tumorigenic immune cells, like CD4+ and CD8+ T cells. Treatment with AP21967 induces apoptosis of these senescent cells, leading to a reduction in anti-tumorigenic immune cell infiltration. By 9 weeks, this shift in the TME results in an increase in pro-tumorigenic macrophages, releasing cytokines such as CCL2, CCL7, and CCL3, promoting tumor growth. At 13 weeks, continued tumor progression, accompanied by the release of additional cytokines like CXCL2 and LIF, leads to increased metastasis. Blocking CCL2 with α-CCL2 restores immune control and reduces tumor growth and metastasis formation.

5. Understanding the role of TIS in cancer treatment efficacy

The final objective of this thesis was to explore the role of senescent cells in the context of TIS. It is important to highlight that while many chemotherapy treatments initially result in complete responses, patients frequently experience relapse. This recurrence may be attributed to the presence of residual cells, which could be senescent. We aimed to elucidate if eliminating senescent cells could potentially prevent such relapses.

5.1 Utilizing the SuSe model to study TIS in syngeneic tumor systems

To investigate the independent impacts of chemotherapy on tumor cells and the surrounding non-tumor cells, we establish two different syngeneic models based on our SuSe system. First, we implanted PyMT/SuSe-derived cells into wild-type (WT) mice to study the effects of eliminating senescent tumor cells **(Figure 40, A)**. Second, we implanted PyMT/+ cells into SuSe mice to assess the impact of eliminating senescent cells from the TME

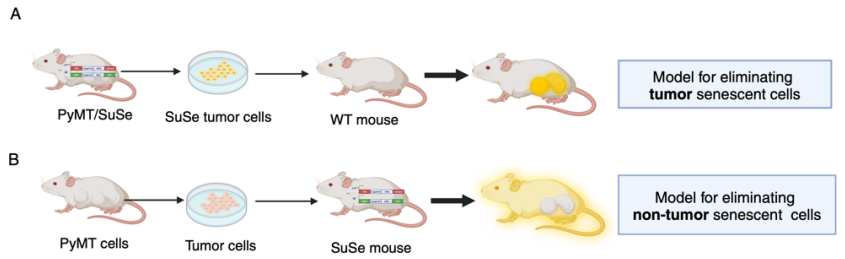


Figure 40. Scheme design of two syngeneic mouse model used for studying TIS.
A. *PyMT/SuSe tumor cells were explanted, cultured, and implanted into WT mice.*
B. *PyMT tumor cells were explanted, cultured, and implanted in SuSe mice.*

We successfully established and cultured tumors from both PyMT/SuSe and PyMT/+ mice. We then validated the induction of senescence in these cells following chemotherapy treatment in vitro. Doxorubicin was chosen as the senescence inducer, and a dose-response experiment was conducted to identify the optimal dose that would prevent cell proliferation without inducing cell death. After five days of treatment, a dose of 92 nM was selected as optimal, based on cell count and morphology. We confirmed that this doxorubicin dose induced senescence in PyMT/SuSe tumor cells, as evidenced by positive SA-ß-gal staining and mCherry and GFP expression **(Figure 41, A)**. Quantification revealed that 80% of the cells expressed both reporters following doxorubicin treatment **(Figure 41, B)**. Interestingly, chemotherapy induced a similar percentage of cells expressing either mCherry or GFP alone as those expressing both simultaneously, indicating that in this context, there is no significant difference between cells expressing p16 alone and those expressing both p16 and IL-6.

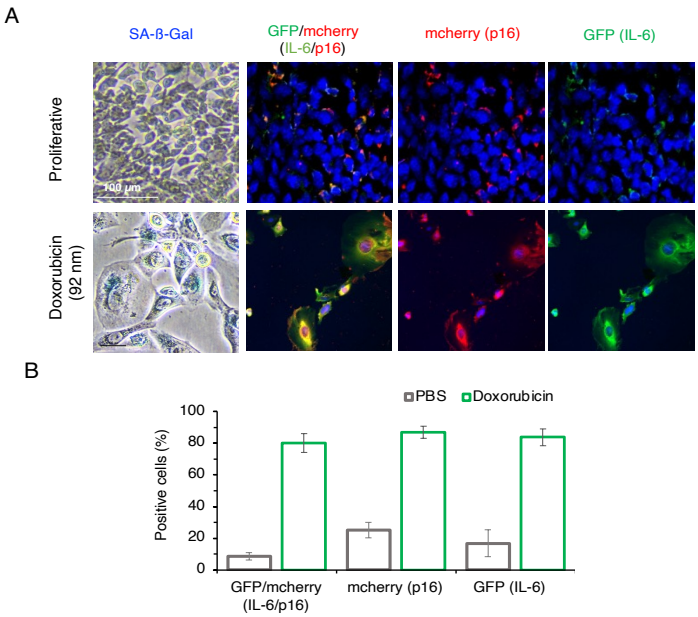


Figure 41. Doxorubicin treatment induces senescence in PyMT/SuSe cells in vitro.
A. *SA-ß-gal staining and IF of GFP and mCherry in PyMT/SuSe cells treated with PBS (top) or doxorubicin at a concentration of 92nM (bottom) for 5 days.* ***B.*** *Quantification of the percentage of cells expressing mCherry and GFP, alone and in combination, after treatment with PBS (grey) or doxorubicin (green). Results are represented as mean of two biological replicates with their standard deviations.*

After confirming that we could induce the expression of the SuSe construct after TIS, we moved forward to examinate the impact of senolysis in combination with TIS *in vivo*.

5.2 Targeting therapy-induced tumor senescent cells with the SuSe system demonstrates anti-tumor efficacy

We established the first syngeneic grafting model, implanting PyMT/SuSe cells in FVB WT mice and we treated the mice with either vehicle, AP21967, doxorubicin or doxorubicin in combination with AP21967 **(Figure 42**, **A)**. The results indicated that senolysis alone had no effect on tumor growth, likely due to the enhanced proliferative capacity of the cultured tumor cells, which bypassed OIS. In contrast, doxorubicin, effectively halted tumor growth

compared to the vehicle, and importantly, senolysis combined with doxorubicin treatment exhibited an enhanced anti-tumor effect **(Figure 42**, **A)**. To confirm that these effects were due to senescence induction and subsequent senolysis, we performed immunofluorescence staining for mCherry and GFP in endpoint samples **(Figure 42**, **B)**. Importantly, doxorubicin treatment induced 60% of the tumor cells to express both reporters, while the combination with AP21967 reduced the number of positive cells near zero **(Figure 42**, **B)**. These results confirmed both the induction of senescence in the tumor cell population and successful senolysis.

To further understand the impact of senolysis in tumor growth we performed IHC staining for CD8 in the same samples and observed that tumors treated with the combination of doxorubicin and AP21967 exhibited higher CD8+ T cell infiltration compared to those treated with any of the individual treatments **(Figure 42**, **A)**. This suggests that eliminating therapy-induced senescent cells enhances tumor immunosurveillance of the tumor driven by CD8 T cells.

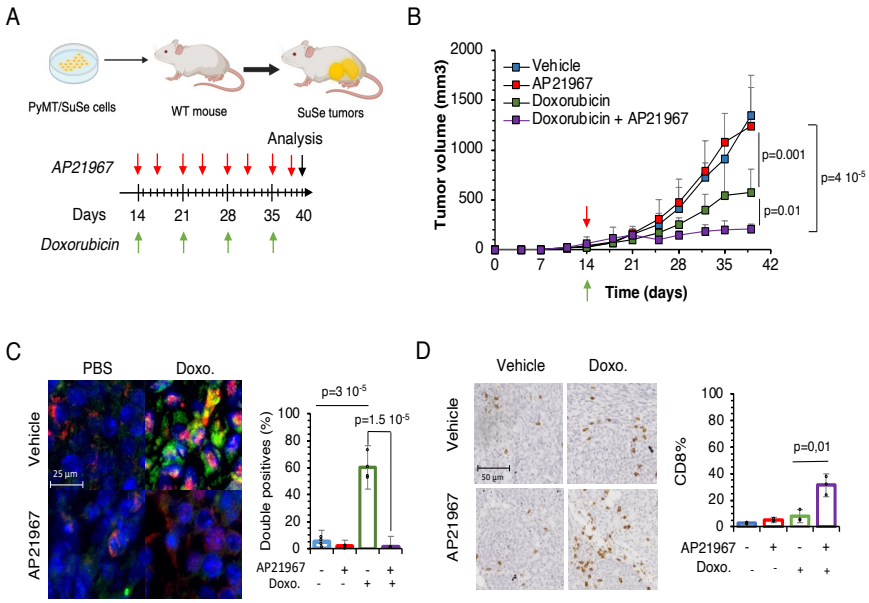


Figure 42. Killing therapy-induced senescent tumor cells has an antitumorigenic effect.

A. *Scheme of the treatment schedule for WT mice implanted with PyMT/SuSe cells. Doxorubicin was administered via i.p once a week, starting 14 days after cells implantation. AP21967 or vehicle were treated twice a week, also starting at day 14.* ***B.*** *Tumor growth was monitored from the day of implantation (0) for 40 days. Measures are represented as the mean of 6 tumor volumes, with their standard deviation.* ***C.*** *IF staining of mCherry (red) and GFP (green) in tumor samples of the mice treated. Quantification of the percentage of cells expressing mCherry and GFP is represented as mean of 6 tumors with their standard deviations.* ***D.*** *IHC staining of CD8. Quantification of the percentage of CD8 positive cells is represented as mean of 6 tumors with their standard deviations Statistical comparisons were performed using two-way ANOVA for* ***B*** *(p-values of last points of the curves are represented in the graph) and Student's t-test for* ***C*** *and* ***D****. A p-value <0.05 was considered statistically significant.*

To further confirmed that the anti-tumor effect of senolysis is mediated by CD8+ T cells, we added an anti-CD8 blocking antibody to the combination of doxorubicin and AP21967, following the same treatment strategy as before **(Figure 43**, **A)**. The results showed that the anti-tumor effect of senolysis combined with chemotherapy was reversed when CD8+ T cells were blocked **(Figure 43**, **B)**, confirming the necessity of CD8+ T cells for the reduction in tumor burden observed after eliminating senescent tumor cells.

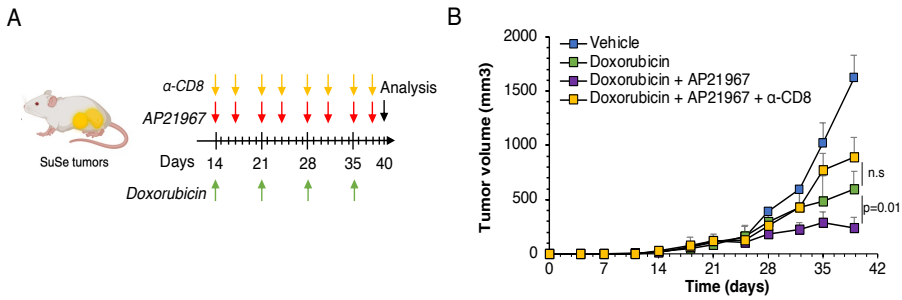


Figure 43. Blocking CD8 T cells prevents the anti-tumor effect of senolysis.
A. *Scheme of treatment schedule. Doxorubicin was administered via i.p once a week, AP21967 and α-CD8 antibody were treated twice a week, starting at day 14 after implantation.* ***B.*** *Tumor growth of mice implanted with PyMT/SuSe cells was monitored from the day of implantation (0) for 40 days. Measures are represented as the mean of 6 tumor volumes, with their standard deviation. Statistical comparisons were performed using two-way ANOVA. A p-value <0.05 was considered statistically significant.*

Next, we used the second syngeneic model to assess the effects of inducing senescence and promoting senolysis in the tumor microenvironment, while avoiding direct targeting of the tumor cells. In this model, PyMT cells were implanted into SuSe mice, and the mice were treated with vehicle, AP21967, doxorubicin, or their combination, following the same treatment schedule as before **(Figure 44, A)**. In this case, senolysis of non-tumor cells had no effect in tumor growth, as tumors treated with doxorubicin grew similar to those treated with the combination of doxorubicin and AP21967 **(Figure 44, B)**. These findings suggest that while senolysis of therapy-induced senescent tumor cells enhances immunosurveillance and reduces tumor burden, senolysis in the TME has a lesser impact on tumor growth.

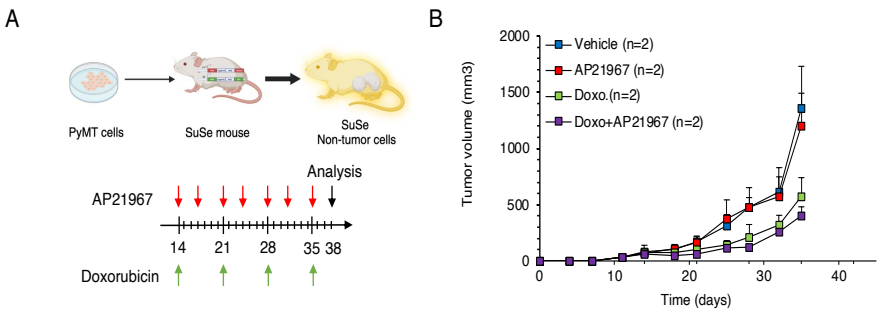


Figure 44. Eliminating senescent cells from the environment doesn't have an effect on tumor growth.

A. *Scheme of the treatment schedule of SuSe mice implanted with PyMT cells. Doxorubicin was administered via i.p once a week and AP21967 was i.p administered twice a week. Treatments started in day 14 after implantation.* ***B.*** *Tumor growth was monitored from the day of implantation (0) for 40 days. Measures are represented as the mean of 4 tumor volumes, with their standard deviation.*

Up to this point, we have explored the role of senescent cells identifying the optimal timings for their elimination in both OIS and TIS. Throughout this thesis, the SuSe cassette has been employed as a tool to selectively eliminate senescent cells. However, advancing these findings toward clinical application requires investigation of more translational approaches.

5.3 PD-L2 blockade enhances anti-tumor efficacy by enabling CD8 T cell elimination of therapy-induced senescent cells

We further characterized the impact of eliminating TIS cells through collaborative research with Manuel Serrano's laboratory at the IRB, published in Nature Cancer in 2024 (81). This study demonstrated that therapy-induced senescence in tumor cells leads to upregulation of PD-L2, which helps senescent cells evade immune clearance by CD8+ T cells. The accumulation of senescent cells in the tumor recruits myeloid-derived suppressor cells through the SASP, aiding tumor immune evasion. My contribution to this research was using our PyMT model to demonstrate the efficacy of blocking PD-L2 with a commercially available anti-PD-L2 antibody (αPD-L2, TY25) in a therapy-induced senescence context.

We initiated treatment in 9-week-old PyMT mice with PBS, anti-PD-L2, or a combination of doxorubicin and PD-L2 or an anti-IgG antibody. Doxorubicin was administered once a week, and antibodies every three days, both intraperitoneally **(Figure 45**, **A)**. We first observed abundant senescent cells in tumors, identified as SA-ß-Gal positive, after therapy at 13 weeks of age. Notably, these cells were also PD-L2+ using IHC, further confirming that PD-L2 is a marker of TIS **(Figure 45**, **B)**. Regarding tumor growth, we showed how only the combination of both treatments, anti-PD-L2 antibody and doxorubicin, resulted in complete tumor regression **(Figure 45**, **C)**. To characterize the antitumor effect of combined chemotherapy and PD-L2 antibody, we analyzed lymphocytic infiltration using IHC in residual tumors at 13 weeks of age and observed a highly significant increase of CD8+ T cells, but not CD4+ T cells **(Figure 45**, **D)**. These results matched the ones obtained with our SuSe system, implying the need for CD8+ T cells infiltration for tumor regression.

To confirm the role of CD8+ T cells in the remission elicited by anti-PD-L2 treatment in combination with doxorubicin, we again performed an experiment including anti-CD8-depleting antibody and, in this case, we also tested anti-CD4-depleting antibodies. Accordingly, while targeting CD4+ cells had little effect, absence of CD8+ cells led to tumor regrowth, confirming the role of this population in tumor regression **(Figure 45**, **E)**.

These findings, combined with those obtained with our PyMT/SuSe syngeneic model, demonstrate that the elimination of therapy-induced senescent tumor cells can be an effective therapy.

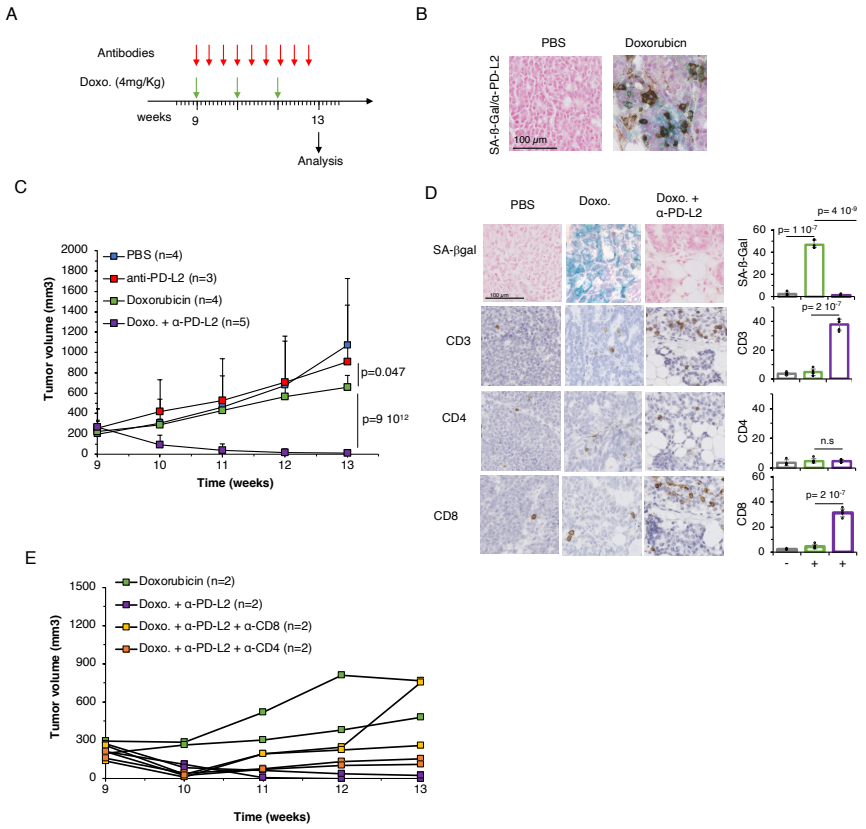


Figure 45. Combining TIS and PD-L2 blockade has an anti-tumoral effect.

A. *Scheme of treatment schedule of PyMT mice. Doxorubicin (4mg/Kg) was administered via i.p once a week (from week 9 until week 12) in combination with α-PD-L2 antibody (10 mg/Kg) or with an IgG control at the same concentration. Antibodies were administered via i.p every 3 days, in combination or alone.* ***B.*** *Tumor growth was monitored once a week from week 9 until week 13. Measures are represented as the mean of 20 tumor volumes, with their standard deviation.* ***C.*** *SA-ß-Gal staining and IHC staining for CD3, CD4 and CD8 were performed in 13-weeks mammary samples. Quantification of positive cells is represented as means of samples analyzed along with their standard deviations.* ***D.*** *Tumor growth of 2 mice treated with doxorubicin, alone or in combination with α-PD-L2. Doxorubicin and α-PD-L2 were also combined with α-CD8 or α-CD4. Statistical comparisons were performed using two-way ANOVA in* ***C*** *and Student's t-test for* ***D.*** *A p-value <0.05 was considered statistically significant.*

In summary, this thesis presents a novel model for monitoring senescent cells *in vivo*, utilizing both p16 and IL-6 markers. This dual-marker approach overcomes the limitations of identifying senescent cells with a single marker, providing a more accurate representation. Using this tool, we have established the significant role of senescent cells in tumor progression, both in the context of OIS and TIS. In both scenarios, we demonstrated that optimizing the timing of senolysis or employing an induction-plus-killing strategy holds therapeutic potential. More importantly, we have identified that the influence of senescent cells on tumor growth is mediated by the immune system, unveiling potential therapeutic targets such as CCL2 or PD-L2.

DISCUSSION

Cellular senescence is a complex and multifaceted process defined by a stable cell cycle arrest and the secretion of a variety of pro-inflammatory factors collectively known as the SASP (21). In recent years it has gained significant interest within the scientific community as a potential contributor to cancer development and is now recognized as one of the emerging hallmarks of cancer (10).

Previous studies have demonstrated the dual role of senescent cells in cancer: they can act as a crucial tumor-suppressive mechanism by preventing the proliferation of damaged cells, but their accumulation can also promote tumor progression through the SASP (9,18). Despite extensive research, the mechanisms underlying this duality remain incompletely understood. Therefore, gaining new insights into the role of senescent cells at different stages of tumor development is crucial for advancing anti-cancer and senolytic therapies.

In vivo models are invaluable for studying the dynamic processes and systemic effects of senescent cells. However, current models that detect and eliminate senescent cells typically rely on a single marker, such as p16 (55,88,90). This approach is limited by the inherent heterogeneity of senescent cells, making it challenging to accurately identify them using only one marker, which complicates their therapeutic targeting in clinical settings

In this thesis, I describe a novel transgenic mouse model capable of tracking and eliminating cells expressing the senescence markers p16 and IL-6. By combining these two markers, we aimed to selectively target senescent cells *in vivo*, providing deeper insights into their contributions to breast cancer biology. Furthermore, this model has enabled us to unravel potential molecular pathways influenced by senescent cells, thereby opening new avenues for the use of senolysis as an anti-cancer strategy.

Senescent cell identification: the challenge of lacking a universal marker

The term "senescence" comes from the Latin word "senex" that translates to "old." The concept was originally employed to describe the phenomenon of cellular aging, whereby cells undergo a gradual deterioration of the machinery that regulates their division over time (11). However, evidence from studies of OIS and TIS demonstrates that senescence is a process that can be triggered by a variety of factors beyond aging (9,27).

Similar to cancer, which exhibits a spectrum of mutations and behaviors depending on tissue origin and environmental influences that makes it challenging to apply a singular approach for diagnosis and treatment (6), senescent cells also display a wide range of characteristics. Cells may enter into senescence through different mechanisms, manifesting diverse phenotypes influenced by cell type, prior stress, tissue environment, and the specific inducing factors that complicate their identification as senescent cells (40).

In retrospect, the idea of the existence of a universal marker of senescence seems overly simplistic. After all, senescence involves complex networks of genetic and epigenetic changes, such as the upregulation of the proteins controlling the cell cycle, chromatin remodeling, and alterations in the secretome, referred to as the SASP (21). Thus, considering the diverse and dynamic nature of this cellular state, defining senescence requires a multifaceted approach.

In vivo models are critical tools for studying the complexity of senescence. However, most current *in vivo* models for studying the role of senescence in aging-related pathologies typically rely on a single marker to identify senescent cells (42,85–87). For example, models developed by researchers such as Prof. Jan van Deursen

and Prof. Campisi use p16 as the sole marker to track and eliminate these cells (88,92). While their studies have independently demonstrated the benefits of senescent cell elimination and provided valuable insights into the potential use of senolytics, using p16 a singular marker for senescence evidence some limitations. For instance, p16 is frequently overexpressed in highly proliferative tumors, including breast cancer, making these models hardly useful to study the role of senescence in this context (24).

Our SuSe model overcomes the limitation of using p16 as a single marker, adding the condition of expressing IL-6, one of the main effectors of the SASP, allowing us to track and eliminate senescent cells more accurately. We claim that using pro-inflammatory markers, as IL-6, is crucial for predicting the pathological function of senescent cells *in vivo*. Our strategy involved using the promoters of *Cdkn2a* and *il6* to control the expression of a suicide system, ensuring we did no interfere with the biological function of p16 and IL-6. This system acts both as a surrogate of p16 and IL-6 expression and a means to induce apoptosis in cells expressing both genes.

Results from our model reveal differences between the number of cells reporting for p16 and those reporting for p16 and IL-6, being the ones that express p16 alone more abundant than those co-expressing both surrogate markers **(Figure 20, B)**. Notably, only the percentage of cells reporting for both markers aligns with the percentage of SA-ß-Gal-positive cells **(Figure 20, B)** confirming the accurate identification of these cells as senescent. These findings highlight a critical consideration for previous models that rely solely on p16-driven reports, as they may inadvertently target non-senescent cells or senescent cells lacking a SASP.

Given the lack of specificity and universality of senescence-associated features, using multiple markers remains the best

approach for accurately validating senescence in cultured cells and *in vivo*. Beyond the traditional markers, there is a pressing need to identify new ones that can not only detect senescent cells but also serve as targets for therapeutic intervention. In this line, our findings, which validate previous work by Serrano's Lab in identifying PD-L2 as a TIS marker, suggest new strategies for targeting senescent cells. However, it is important to note that PD-L2 upregulation has been observed primarily in TIS, and not in OIS.

This discrepancy underscores the need to further explore the heterogeneity of senescent cells. In this regard, technological advances such as scRNA-seq may provide valuable insights. For example, *Kim et al.* conducted scRNA-seq analysis on human senescent fibroblasts induced by various stressors and identified distinct subpopulations of senescent cells. They defined two divergent senescence programs, one expressing the traditional marker p16 and the other characterized by long non-coding RNA expression and dysregulated splicing (105). These results evidenced one more time the challenges of accurately identifying senescent cell populations even coming from the same tissue. Moreover, the inherent complexity of analyzing scRNA-seq data presents another layer of difficulty. The high-dimensional nature of the data and the variability introduced during sample processing requires robust selection of reference datasets and algorithms used to define cell populations by the use of this technique.

In our scRNA-seq analysis, we were unable to detect senescent cells. Initially, we hypothesized that this absence might be due to misclassification or omission caused by suboptimal reference data or analytical pipelines. However, when attempting to identify this population using *Cdk2na* and *il6*, based on the results obtained from characterizing our PyMT/SuSe model, we found that *cdkn2a* was not

represented in the analysis, and the expression of *il6* was too broad to serve as a specific identificatory marker. Additionally, we used other canonical markers of senescence, such as *cdkn1a* (encoding for p21), as well as established SASP factors like *il8* and *il1*, to identify this population. Despite these efforts, *cdkn1a* was not represented in the tumor population, and the expression of canonical SASP factors was not specific enough to clearly identify a distinct population. The inability to identify senescent cells using well-stablished features suggests that technical issues during sample processing may be a more likely explanation. In fact, SA-ß-Gal staining and IF for mCherry and GFP in tumor sections of the same samples employed in the scRNA-seq analysis confirmed the senescent cells presence.

It is well-documented that traditional methods of tissue disaggregation can introduce stress and affect the viability of cells, especially large or fragile cells like senescent ones. The fragility of these cells and their tendency to undergo apoptosis during the preparation process can make their detection particularly challenging in scRNA-seq studies (106,107). Our findings lead us to conclude that current disaggregation protocols may not be optimized for preserving the integrity of senescent cells, thereby leading to their absence in our scRNA-seq dataset.

Given the challenges encountered with scRNA-seq in identifying senescent cells, another promising approach to find novel markers of senescence would be the use of spatial imaging techniques, particularly spatial transcriptomics and proteomics. Spatial transcriptomics enables the measurement of gene expression across a tissue section while preserving the spatial context of the cells. Similarly, spatial proteomics allows for the localization and quantification of proteins within the tissue architecture (108). These methods offer a significant advantage over scRNA-seq by providing not only the molecular information but also a spatial map that shows

where each cell type is located within the tissue (109). Moreover, paraffin-embedded tissues are more stable and easier to handle than fragile scRNA-seq or bulk RNAseq samples, preserving tissue architecture, including senescent cells, as demonstrated in our IF **(Figure 20).**

A recent review in Nature Aging discusses the potential of spatial transcriptomics to more accurately identify senescent cells within tissues (110). It focuses on potentially mapping the expression of SASP-related protein, which could provide deeper insights into how senescent cells contribute to the microenvironment (110). Understanding the spatial context might be crucial for deciphering interactions between senescent cells, neighboring cancer cells and the surrounding stroma.

In our study, the application of spatial imaging could be particularly effective when combined with our reporter model (p16-mCherry and IL6-GFP) **(Figure 15)**. Our SuSe model has proven to fluorescently label senescent cells **(Figure 20)** making them easily identifiable within tissue sections. Spatial imaging would enable us to identify senescent cells with high specificity and use a broad array of antibodies to detect various characteristics, focusing on cytokines to achieve a comprehensive SAPS characterization. Multiplex cytokine assay results already showed differences in the cytokine pattern depending on the presence of senescent cells in the TME (**Figure 31).** This approach would allow us to confirm their direct contribution to the changes in the TME by analyzing their secretome in situ.

In summary, identifying senescent cells remains challenging due to their inherent heterogeneity. To address this, we adopted a double-marker strategy utilizing both p16 and IL-6, which has proven to be more effective than relying solely on p16, as previous models have done. However, our efforts to identify novel senescent markers

through scRNAseq were technically inviable. As an alternative, techniques such spatial proteomics may present a more viable solution, offering a more detailed and context-specific understanding of senescent cell populations.

Importantly, even if a universal and targetable marker for senescent cells were identified, the dual role of these cells during tumor progression necessitates careful consideration to optimize senolysis as a cancer treatment.

To kill or not to kill senescent cells? In cancer, timing holds the answer

Senescent cells, while playing a protective role in the short term by halting the proliferation of damaged cells, contribute to aging and age-related diseases when they accumulate over time (32). Therefore, numerous studies on the aging field have highlighted the significant benefits of eliminating senescent cells. For instance, *Baker et al.* demonstrated that the clearance of senescent cells using INK-ATTAC Van Deursen's transgenic mouse model delayed the onset of age-related pathologies, such as cataracts and sarcopenia, extending the healthspan of these animals (88). This groundbreaking study laid the foundation for the development of senolytic drugs—compounds that selectively induce apoptosis in senescent cells.

However, despite the growing approval of the use of senolytics in broader contexts, their use in cancer treatment remains a subject of ongoing debate. Senescent cells have been recognized for their dual roles in cancer, acting both as tumor suppressors and promoters, so eliminating them not always may be beneficial. To provide new insights on the importance of choosing the right time for applying senolysis as a cancer treatment, we used the well-characterized PyMT model to determine how the role of senescent cells changes throughout tumor progression.

Our findings using our PyMT/SuSe model indicate that the number of senescent cells is higher in the early stages of tumor development **(Figure 19**, **Figure 20)** and that eliminating them at this point promotes tumor growth and metastasis **(Figure 22**, **Figure 23).** This observation aligns with studies that emphasize the protective effects of OIS at the onset of tumorigenesis. Early research in this area, such as studies by *Braig et al*, *Collado et al*. and *Chen et al*., highlighted OIS as a crucial mechanism that prevents the progression of oncogene-activated cells into malignant tumors by inducing a state of permanent cell cycle arrest (43,48,64). Later studies linked this tumor-suppressive role to the secretion of factors that not only reinforce cell cycle arrest but also stimulate the immune clearance of potential cancer cells. A study by *Kang et al.* discusses how senescent pre-malignant hepatocytes driven by Nras expression can trigger an immune response, particularly by attracting CD4+T cells (71). They showed that senescent cells directly secrete cytokines such as IL-1 and CCL2, while others, like IFNγ, are secreted by infiltrating immune cells. The presence of infiltrating immune cells, mainly NK cells and macrophages, was associated with cytokine secretion by senescent cells.

Conversely, this perspective of OIS as a protection mechanism against tumorigenesis contrast with findings from other studies, such as those by *Baker et al..* They suggest that eliminating senescent cells using the INK-ATTAC model can prevent the incidence of lung tumors, thereby supporting the use of senolytics as a preventive cancer treatment (88). While this conclusion might seem to conflict with our results using the SuSe model, it is important to note that our model is more specific in targeting senescent cells within a tumorigenic context. However, the difference in outcomes cannot be attributed solely to the specificity of the model; instead, our findings underscore that the timing of senolysis is a critical factor. In our

study, we targeted senescent cells in tumors that had already initiated, focusing on cells that arose under oncogenic pressure. In contrast, the INK-ATTAC model used by *Baker et al.* primarily targets normal, aged cells before malignant transformation.

This difference in timing, meaning eliminating senescent cells before versus after tumor initiation, may explain the divergent outcomes observed between our studies. Thus, while *Baker et al.*'s findings support the potential of senolytics in cancer prevention, our results emphasize the need for a more accurate approach in already initiated tumors, where the protective role of senescent cells in early stages may outweigh the benefits of their elimination.

Moreover, we have demonstrated that eliminating senescent cells that accumulate at advance stages **(Figure 24)** or in response to chemotherapy **(Figure 42)** can reduce tumor burden, showing significant differences in outcomes depending on both the timing of senolysis during tumor progression and the method of senescence induction. This is in line with other studies that have already demonstrated that senescent cells accumulation can create a pro-tumorigenic microenvironment through the SASP, contributing to cancer progression (60). These differences suggest that the role of senescent cells shifts from anti-tumorigenic in the early stages to pro-tumorigenic in later stages, particularly when induced by chemotherapy.

In summary, these results demonstrate that while senolysis might be beneficial in late-stage tumors or when combined with therapies that induce senescence, its application at early stages of cancer could have adverse consequences. This understanding of the critical role of timing in senolysis underscores the necessity of further exploring the molecular pathways and interactions between senescent cells and the TME to fully explain why senescent cells shift their role during tumor progression.

The immune system dictates the timing

Mechanistically, our data suggest that the role of senescent cells in cancer progression is mediated through cytokine signaling and modulation of the immune microenvironment. In our sc-RNAseq analysis we observed the disappearance of the T cell population following early senolysis **(Figure 26)**, which correlates with the aforementioned studies demonstrating the ability of senescent cells to attract these cells (71). Additionally, we noted an increase in the macrophage population **(Figure 26)** which not just increase in number but, according to our RNAseq data on the CD45+ population, also became polarized to a more pro-tumorigenic phenotype **(Figure 28)**. This finding is consistent with other studies, such as that of Lujambio et al., who reported that p53-dependent senescent cells can polarize macrophages toward a tumor-inhibiting state (111). They attributed this effect to SASP factors, though specific factors were not detailed beyond IL-6 and IFNγ secretion by senescent cells. Accordingly, the downregulation of IL-6 expression in samples treated with AP21967 **(Figure 26)** in addition to indicating the elimination of the p16/IL-6 population, can also be related with the shift in macrophage polarization toward a more pro-tumorigenic phenotype **(Figure 35)**.

Therefore, both the disappearance of T cells and the increase presence of pro-tumorigenic macrophages highlight the importance of senescent cells in maintaining the immunosurveillance at the beginning of tumorigenesis **(Figure 35)**. The implication of senescent cells in modulating the TME is also evident in our findings within a TIS context. Using our PyMT/SuSe syngeneic model, which allows for the specific study of eliminating therapy-induced senescent cancer cells, we observed an antitumor effect driven by increased CD8+ T cell infiltration following the removal of these cells

(Figure 42). These results coupled with the findings regarding PD-L2 expression obtained in collaboration with Serrano's group in which we demonstrated that the protection of senescent cells from T cell-mediated killing, due to the upregulation of PD-L2, not only allows these cells to evade immune surveillance but also contributes to shaping a pro-tumoral microenvironment **(Figure 45)**. This immune evasion is facilitated by the recruitment of MDSCs, which are attracted by SASP factors secreted by senescent cells (81). All these findings together have further clarified the role of therapy-induced senescent cells within the TME.

The potential role of senescence in promoting tumorigenesis could be further clarified by examining non-cancerous cells that also undergo senescence as a result of chemotherapy. Demaria et al. explored this in their study using the 3MR mouse model, where they implanted PyMT cells similarly to our approach with the SuSe model. Their research targeted and eliminated normal host cells induced to senescence by chemotherapy (55). Although they did not observe a reduction in the growth of primary tumors—consistent with our findings **(Figure 44)**— they demonstrated that eliminating therapy-induced normal senescent cells delayed relapse and metastasis and reduced chemotherapy side effects. This raises the possibility of using our SuSe syngeneic mode to explore whether these benefits stem from correcting the alterations in the TME caused by senescence induction.

In summary, these findings highlight the potential of integrating immune modulators, such as drugs targeting macrophages in the early stages of tumorigenesis or combining immune checkpoint inhibitors like anti-PD-L2 with senolytic agents, to counteract the limitations posed by therapy-induced tumor cells. This approach of selective elimination of pro-tumorigenic senescent cells or the modulation of their mediators holds significant promise for advancing cancer treatment.

Future perspectives of senolysis as cancer treatment

Further research has shown that senolytics can improve the function of multiple tissues and organs. For example, Xu et al. reported that a combination of dasatinib and quercetin effectively reduced senescent cell burden in aged mice, leading to improved cardiovascular function, enhanced exercise endurance, and increased lifespan (112). These findings have increased the interest in translating senolytic therapies to human clinical trials, with the goal of alleviating age-related diseases and improving the quality of life in older adults. In fact, the enthusiasm for senolytics extends beyond aging research, as studies have also explored their potential in treating cancer. One notable example is the study published by Collado's group, which investigated the use of cardiac drugs such as digoxin as senolytic compounds in cancer therapy (83). Collaborative experiments conducted by our group demonstrated that combining chemotherapy with digoxin reduced tumor burden by eliminating senescent cells, demonstrating the potential use of already approved drugs as senolytics.

As companies in the biotech industry are now heavily invested in the development and testing of senolytic drugs that target the root causes of aging (113), the notion that timing is crucial when considering senolysis in cancer treatment extends beyond an academic observation, carrying significant implications for clinical practice. The results presented in this thesis underscore the importance of understanding when senolysis can be beneficial and when it might inadvertently exacerbate cancer progression. Translating these findings into clinical practice will require carefully designed clinical trials that consider the timing and context of senolytic therapy. These trials should aim to identify not only the efficacy of senolytic drugs but also the potential risks associated with

their use, particularly in the context of early-stage cancers. This concept aligns with the growing interest in personalized medicine, where treatments are tailored to the specific biological context of the patient. In this regard, the use of biomarkers to identify the stage of tumor progression and the specific senescent cell populations present could guide the decision on whether to implement senolytic therapy. For instance, in patients with early-stage tumors, preserving senescent cells might be advantageous due to their tumor-suppressive effects. Conversely, in more advanced stages, where the tumor microenvironment has been remodeled by senescent cells to support malignancy, senolysis could prove beneficial. In this thesis we propose that senescent biomarkers, such as p16 or IL-6, could thus be employed to monitor both the presence of senescent cells and the effectiveness of senolytic treatments.

Furthermore, the findings presented in this thesis underscore the critical importance of identifying additional factors that influence the dual role of senescent cells in cancer. In this regard, our PyMT/SuSe model has proven to be an invaluable tool for gaining deeper insights into the characteristics of senescent cells at various stages of tumor progression and following senescence induction. Although we were not able to definitively determine whether the change in their role is intrinsic to the cells as they alter their SASP throughout tumor progression, or if it is driven by environmental pressures within the tumor, we have confirmed that eliminating senescent cells significantly modulates the immune response during tumor progression **(Figure 39)**. Therefore, this model provides a robust platform to test the effects of senolytic therapy across different cancer types and stages, potentially aiding in the refinement of treatment protocols. In line with this, our findings showing a dependency of tumor growth on macrophage presence post-senolysis offer new insights into the potential molecular pathways influenced by senescent cells and their impact on the tumor

microenvironment **(Figure 35)**. More importantly, these findings open the door to new strategies that could make the targeted elimination of senescent cells a viable and efficacious approach in cancer therapy.

In our study, the use of clodronate to eliminate macrophages after early senolysis has proven effective in mitigating the adverse impact of early senolysis on both tumor growth and metastasis. However, while this treatment strategy did reduce the number of metastases to levels seen in vehicle-treated animals, the size of these metastases remained unchanged compared to those that developed after senolysis **(Figure 30)**. The persistence of large metastases even after macrophage depletion suggests that the pre-metastatic niche may have been disrupted by early senolysis, prior to macrophage elimination. This implies that targeting macrophages earlier, perhaps in conjunction with senolysis, could be necessary to fully mitigate the pro-metastatic environment created post-senolysis. However, from a clinical perspective, early and sustained macrophage depletion is challenging and may not be feasible due to the essential role macrophages play in normal immune function and tissue homeostasis.

These results highlight the need for strategies that can specifically target pro-tumorigenic macrophages without compromising overall immune function. Notably, our scRNA-seq results show that macrophages act as both sources and responders to CCL2 and CCL3, thereby creating a pro-tumoral microenvironment that supports the survival and outgrowth of tumor cells **(Figure 33**, **Figure 34)**. This idea is further supported by a study conducted by *Yoshimura et al.*, which demonstrated that CCL2 not only increases the expression of the CCR1 ligand CCL3 in macrophages via CCR2, but also that the signaling generated by the CCL3/CCR1 interaction

enhances and stabilizes the presence of these macrophages in the tumor microenvironment (104). Furthermore, we demonstrated how the selective pressure of the tumor environment seems to favor the emergence of more aggressive, metastasis-prone tumor cells, which continue to express these cytokines as the tumor progresses to its full carcinoma stage. Together, these findings, which highlight the major role of CCL2 and CCL3 in the recruitment of the macrophage population post-senolysis, suggest that these cytokines could be effective targets for more precise modulation of macrophage activity and, consequently, the effects of senolysis **(Figure 39)**.

Building on this understanding, we explored the potential of targeting CCL2 as a therapeutic strategy to complement senolysis. Previous studies, such as those by *Fujimoto et al*., have demonstrated that blocking CCL2 with antibodies can effectively reduce macrophage infiltration, tumor growth, and angiogenesis in breast cancer models (114). In our study, we extended this approach by combining CCL2 blockade with senolysis. Our results revealed that the combination of anti-CCL2 treatment with senolysis not only further reduced tumor burden **(Figure 37)** but also led to a significant decrease in metastasis compared to senolysis and anti-CCL2 alone **(Figure 38)**. This suggests that targeting CCL2 may enhance the efficacy of senolysis by disrupting the recruitment and stabilization of pro-tumorigenic macrophages in the tumor microenvironment. These findings underscore the potential of CCL2 as a valuable target, particularly when used in combination with senolytic strategies **(Figure 39)**.

Therefore, the application of immunotherapies in combination with senolytic strategies holds significant promise. An especially interesting approach is the use of CAR-T cell therapy specifically designed to target senescent cells. However, the success of this approach hinges on the identification of precise biomarkers that can guide the targeted elimination of these cells. As discussed, the lack

of a universal marker for senescence presents a significant challenge, necessitating the development of customized CAR-T therapies tailored to the specific senescent phenotypes, making impossible the use of a universal senolytic CAR-T.

While further research is required to fully realize this potential, there have been promising advancements. For example, Corina Amor's study demonstrated the successful use of CAR-T cells to eliminate senescent cells expressing uPAR, highlighting the feasibility of this strategy (84). In this context, targeting molecules like PD-L2 could also prove effective in developing CAR-T cells aimed at senescent cells. Additionally, considering the role of CCL2 in regulating the senescence-associated microenvironment, combining CAR-T therapy with blocking antibodies against CCL2 could further enhance the efficacy of these treatments by preventing the recruitment and activation of pro-tumorigenic immune cells.

In conclusion, this thesis underscores the importance of timing in the decision to target senescent cells during cancer therapy and highlight the need for precise therapeutic strategies consider the temporal dynamics of senescent cells in cancer progression.

CONCLUSIONS

1. We successfully developed a transgenic model that enables the tracking of p16/IL-6 positive cells. This model, called SuSe, is instrumental in studying the dynamics of senescent cell populations *in vivo*.
2. Using the SuSe model, we demonstrated the capability to selectively eliminate p16/IL-6 positive cells upon AP21967 treatment, providing a valuable tool for testing senolytic therapies *in vivo*.
3. The PyMT/Suse model, derived from the cross between the oncogenic model PyMT and our Suse model, confirm that p16/IL-6 positive cells in a breast cancer model coincide with SA-ß-Gal positive cells, a classical marker of senescence. This correlation supports the identification of these cells as senescent.
4. We observed that eliminating p16/IL-6 positive senescent cells at early stages of tumorigenesis promotes tumor growth and metastasis. Conversely, senolysis in late-stage tumors has an inhibitory effect on tumor progression, highlighting the critical importance of timing in senolytic therapies.
5. scRNA-seq results show that early senolysis is associated with significant changes in the immune microenvironment, characterized by the disappearance of T cells and an increase in the macrophage population. This shift contributes to a more pro-tumorigenic environment.
6. The macrophage population observed post-senolysis exhibited a more pro-tumorigenic phenotype, as indicated by the expression of MRC1.
7. Depleting the macrophage population with clodronate treatment effectively reverted the pro-tumorigenic phenotype, underscoring the pivotal role of macrophages in mediating the effects of early senolysis.

8. The observed changes in the immune cell population were driven by alterations in the cytokine release pattern, specifically an increase in CCL2, CCL3, and CCL7, and a decrease in IL-6, IL-17, and IL-31. These cytokine shifts likely contribute to the recruitment and polarization of pro-tumorigenic immune cells.
9. The upregulation of CCL2, CCL3, and CCL7 was predominantly observed in macrophages, as their receptors CCR1, CCR2 and CCR5, suggesting these cytokines play a central role in fostering a pro-tumorigenic microenvironment.
10. We found that blocking CCL2 effectively inhibited the recruitment of pro-tumorigenic macrophages and mitigated the adverse effects of early senolysis, presenting CCL2 as a promising therapeutic target.
11. Our results demonstrate that TIS contributes to a pro-tumorigenic environment. However, eliminating senescent tumor cells led to an anti-tumor effect, largely due to an increase in CD8+ T cell infiltration.
12. PD-L2 was identified as a marker associated with senescence, particularly in the context of TIS. This finding opens new avenues for targeting senescent cells in cancer therapy.

BIBLIOGRAPHY

1. International Agency of Research of Cancer. https://gco.iarc.fr/today/en/dataviz/pie?mode=population. 2024. Global Cancer Observatory - Cancer Today.

2. International Agency of Research in Cancer. https://gco.iarc.fr/today/en/dataviz/population_pyramid?mode=population&group_populations=0&types=1&reset=1. 2024. Global Cancer Observatory-Types of Cancer by Gender.

3. International Agency of Research of Cancer (IARC). https://gco.iarc.fr/tomorrow/en/dataviz/isotype?bar_mode=stacked&types=0. 2024. Global Cancer Observatory - Cancer Tomorrow.

4. Hanahan D, Weinberg RA. The Hallmarks of Cancer Review evolve progressively from normalcy via a series of pre. Vol. 100, Cell. 2000.

5. Yang L, Pang Y, Moses HL. TGF-β and immune cells: an important regulatory axis in the tumor microenvironment and progression. Trends Immunol [Internet]. 2010 Jun 1 [cited 2024 Jun 24];31(6):220–7. Available from: http://www.cell.com/article/S1471490610000530/fulltext

6. Hanahan D, Weinberg RA. Hallmarks of cancer: The next generation. Vol. 144, Cell. 2011. p. 646–74.

7. Yuan S, Norgard RJ, Stanger BZ. Cellular plasticity in cancer. Cancer Discov [Internet]. 2019 Jul 1 [cited 2024 Jun 24];9(7):837–51. Available from: /cancerdiscovery/article/9/7/837/41866/Cellular-Plasticity-in-CancerCancer-Cells-Change

8. Negrini S, Gorgoulis VG, Halazonetis TD. Genomic instability — an evolving hallmark of cancer. Nature Reviews Molecular Cell Biology 2010 11:3 [Internet]. 2010 Mar [cited 2024 Jun 24];11(3):220–8. Available from: https://www.nature.com/articles/nrm2858

9. Collado M, Serrano M. Senescence in tumours: evidence from mice and humans. Nature Reviews Cancer 2010 10:1 [Internet]. 2010 Jan [cited 2024 May 15];10(1):51–7. Available from: https://www.nature.com/articles/nrc2772

10. Hanahan D. Hallmarks of Cancer: New Dimensions. Vol. 12, Cancer Discovery. American Association for Cancer Research Inc.; 2022. p. 31–46.

11. Hayflick L, Moorhead PS. The serial cultivation of human diploid cell strains. Exp Cell Res. 1961 Dec 1;25(3):585–621.

12. Hayflick L. The limited in vitro lifetime of human diploid cell strains. Exp Cell Res. 1965 Mar 1;37(3):614–36.

13. Bodnar AG, Ouellette M, Frolkis M, Holt SE, Chiu CP, Morin GB, et al. Extension of life-span by introduction of telomerase into normal human cells. Science [Internet]. 1998 Jan 16 [cited 2024 Apr 8];279(5349):349–52. Available from: https://pubmed-ncbi-nlm-nih-gov.are.uab.cat/9454332/

14. Blasco MA. Telomeres and human disease: ageing, cancer and beyond. Nature Reviews Genetics 2005 6:8 [Internet]. 2005 Aug [cited 2024 Apr 9];6(8):611–22. Available from: https://www.nature.com/articles/nrg1656

15. Collins K, Mitchell JR. Telomerase in the human organism. Oncogene 2002 21:4 [Internet]. 2002 Feb 11 [cited 2024 Jun 24];21(4):564–79. Available from: https://www.nature.com/articles/1205083

16. Van Deursen JM. The role of senescent cells in ageing. Nature 2014 509:7501 [Internet]. 2014 May 21 [cited 2024 Apr 8];509(7501):439–46. Available from: https://www.nature.com/articles/nature13193

17. Collado M, Blasco MA, Serrano M. Cellular senescence in cancer and aging. Cell [Internet]. 2007 Jul 27 [cited 2024 Apr 9];130(2):223–33. Available from: https://pubmed-ncbi-nlm-nih-gov.are.uab.cat/17662938/

18. Muñoz-Espín D, Serrano M. Cellular senescence: from physiology to pathology. Nature Reviews Molecular Cell

Biology 2014 15:7 [Internet]. 2014 Jun 23 [cited 2024 Apr 8];15(7):482–96. Available from: https://www.nature.com/articles/nrm3823

19. Lozano-Torres B, Estepa-Fernández A, Rovira M, Orzáez M, Serrano M, Martínez-Máñez R, et al. The chemistry of senescence. Vol. 3, Nature Reviews Chemistry. Nature Publishing Group; 2019. p. 426–41.

20. Herranz N, Gil J. Mechanisms and functions of cellular senescence. Journal of Clinical Investigation. 2018 Apr 2;128(4):1238–46.

21. Hernandez-Segura A, Nehme J, Demaria M. Hallmarks of Cellular Senescence. Trends Cell Biol [Internet]. 2018 Jun 1 [cited 2024 Apr 8];28(6):436–53. Available from: http://www.cell.com/article/S0962892418300205/fulltext

22. Collado M, Serrano M. The power and the promise of oncogene-induced senescence markers. Nature Reviews Cancer 2006 6:6 [Internet]. 2006 Jun [cited 2024 Apr 12];6(6):472–6. Available from: https://www.nature.com/articles/nrc1884

23. Serrano M, Hannon GJ, Beach D. A new regulatory motif in cell-cycle control causing specific inhibition of cyclin D/CDK4. Nature [Internet]. 1993 [cited 2024 Apr 11];366(6456):704–7. Available from: https://pubmed.ncbi.nlm.nih.gov/8259215/

24. Safwan-Zaiter H, Wagner N, Wagner KD. P16INK4A—More Than a Senescence Marker. Vol. 12, Life. MDPI; 2022.

25. Li J, Poi MJ, Tsai MD. Regulatory mechanisms of tumor suppressor P16INK4A and their relevance to cancer. Biochemistry [Internet]. 2011 Jun 28 [cited 2024 Apr 15];50(25):5566–82. Available from: https://pubs-acs-org.are.uab.cat/doi/abs/10.1021/bi200642e

26. Serrano M, Lee HW, Chin L, Cordon-Cardo C, Beach D, DePinho RA. Role of the INK4a locus in tumor suppression and cell mortality. Cell [Internet]. 1996 Apr 5 [cited 2024 Apr 11];85(1):27–37. Available from: https://pubmed.ncbi.nlm.nih.gov/8620534/

27. Collado M, Blasco MA, Serrano M. Cellular Senescence in Cancer and Aging. Cell. 2007 Jul 27;130(2):223–33.

28. Levine AJ. p53, the cellular gatekeeper for growth and division. Cell. 1997 Feb 7;88(3):323–31.

29. Sherr CJ, Weber JD. The ARF/p53 pathway. Curr Opin Genet Dev. 2000 Feb 1;10(1):94–9.

30. Pomerantz J, Schreiber-Agus N, Liégeois NJ, Silverman A, Alland L, Chin L, et al. The Ink4a tumor suppressor gene product, p19(Arf), interacts with MDM2 and neutralizes MDM2's inhibition of p53. Cell. 1998 Mar 20;92(6):713–23.

31. Engeland K. Cell cycle regulation: p53-p21-RB signaling. Cell Death & Differentiation 2022 29:5 [Internet]. 2022 Mar 31 [cited 2024 Apr 16];29(5):946–60. Available from: https://www.nature.com/articles/s41418-022-00988-z

32. Campisi J. Aging, cellular senescence, and cancer. Vol. 75, Annual Review of Physiology. 2013. p. 685–705.

33. Debacq-Chainiaux F, Erusalimsky JD, Campisi J, Toussaint O. Protocols to detect senescence-associated beta-galactosidase (SA-βgal) activity, a biomarker of senescent cells in culture and in vivo. Nature Protocols 2009 4:12 [Internet]. 2009 Nov 19 [cited 2024 Apr 19];4(12):1798–806. Available from: https://www.nature.com/articles/nprot.2009.191

34. Dimri GP, Lee X, Basile G, Acosta M, Scott G, Roskelley C, et al. A biomarker that identifies senescent human cells in culture and in aging skin in vivo. Proceedings of the National Academy of Sciences [Internet]. 1995 Sep 26 [cited 2024 Apr 19];92(20):9363–7. Available from: https://www.pnas.org/doi/abs/10.1073/pnas.92.20.9363

35. Kurz DJ, Decary S, Hong Y, Erusalimsky JD. Senescence-associated (beta)-galactosidase reflects an increase in lysosomal mass during replicative ageing of human endothelial cells. J Cell Sci [Internet]. 2000 [cited 2024 Apr

19];113 (Pt 20)(20):3613–22. Available from: https://pubmed.ncbi.nlm.nih.gov/11017877/

36. Cristofalo VJ, Lorenzini A, Allen RG, Torres C, Tresini M. Replicative senescence: a critical review. Mech Ageing Dev [Internet]. 2004 [cited 2024 Apr 19];125(10–11):827–48. Available from: https://pubmed.ncbi.nlm.nih.gov/15541776/

37. Faget D V., Ren Q, Stewart SA. Unmasking senescence: context-dependent effects of SASP in cancer. Nature Reviews Cancer 2019 19:8 [Internet]. 2019 Jun 24 [cited 2024 May 2];19(8):439–53. Available from: https://www.nature.com/articles/s41568-019-0156-2

38. Freund A, Patil CK, Campisi J. p38MAPK is a novel DNA damage response-independent regulator of the senescence-associated secretory phenotype. EMBO J [Internet]. 2011 Apr 4 [cited 2024 May 3];30(8):1536. Available from: /pmc/articles/PMC3102277/

39. Özcan S, Alessio N, Acar MB, Mert E, Omerli F, Peluso G, et al. Unbiased analysis of senescence associated secretory phenotype (SASP) to identify common components following different genotoxic stresses. Aging [Internet]. 2016 Jul 1 [cited 2024 May 3];8(7):1316–29. Available from: https://pubmed.ncbi.nlm.nih.gov/27288264/

40. Gorgoulis V, Adams PD, Alimonti A, Bennett DC, Bischof O, Bishop C, et al. Cellular Senescence: Defining a Path Forward. Cell [Internet]. 2019 Oct 31 [cited 2024 Apr 4];179(4):813–27. Available from: http://www.cell.com/article/S0092867419311213/fulltext

41. Shay JW, Roninson IB. Hallmarks of senescence in carcinogenesis and cancer therapy. Vol. 23, Oncogene. 2004. p. 2919–33.

42. Serrano M, Lin AW, McCurrach ME, Beach D, Lowe SW. Oncogenic ras provokes premature cell senescence associated with accumulation of p53 and p16(INK4a). Cell [Internet]. 1997 Mar 7 [cited 2024 May 13];88(5):593–602. Available from: http://www.cell.com/article/S0092867400819029/fulltext

43. Collado M, Gil J, Efeyan A, Guerra C, Schuhmacher AJ, Barradas M, et al. Senescence in premalignant tumours. Nature 2005 436:7051 [Internet]. 2005 Aug 4 [cited 2024 May 13];436(7051):642–642. Available from: https://www.nature.com/articles/436642a

44. Schmitt CA. Cellular senescence and cancer treatment. Biochimica et Biophysica Acta (BBA) - Reviews on Cancer. 2007 Jan 1;1775(1):5–20.

45. Guerra C, Mijimolle N, Dhawahir A, Dubus P, Barradas M, Serrano M, et al. Tumor induction by an endogenous K-ras oncogene is highly dependent on cellular context. Cancer Cell [Internet]. 2003 Aug 1 [cited 2024 Apr 16];4(2):111–20. Available from: https://pubmed.ncbi.nlm.nih.gov/12957286/

46. Michaloglou C, Vredeveld LCW, Soengas MS, Denoyelle C, Kuilman T, Van Der Horst CMAM, et al. BRAFE600-associated senescence-like cell cycle arrest of human naevi. Nature 2005 436:7051 [Internet]. 2005 Aug 4 [cited 2024 May 13];436(7051):720–4. Available from: https://www.nature.com/articles/nature03890

47. Astle M V., Hannan KM, Ng PY, Lee RS, George AJ, Hsu AK, et al. AKT induces senescence in human cells via mTORC1 and p53 in the absence of DNA damage: implications for targeting mTOR during malignancy. Oncogene 2012 31:15 [Internet]. 2011 Sep 12 [cited 2024 May 13];31(15):1949–62. Available from: https://www.nature.com/articles/onc2011394

48. Chen HA, Ho YJ, Mezzadra R, Adrover JM, Smolkin R, Zhu C, et al. Senescence Rewires Microenvironment Sensing to Facilitate Antitumor Immunity. Cancer Discov. 2023 Feb 1;13(2):433–53.

49. Igor B Roninson. Tumor cell senescence in cancer treatment. Cancer Res. 2003 Jun;63(11):2705–15.

50. Ewald JA, Desotelle JA, Wilding G, Jarrard DF. Therapy-induced senescence in cancer. J Natl Cancer Inst. 2010 Oct 20;102(20):1536–46.

51. Bousset L, Gil J. Targeting senescence as an anticancer therapy. Vol. 16, Molecular Oncology. John Wiley and Sons Ltd; 2022. p. 3855–80.

52. Yang J, Liu M, Hong D, Zeng M, Zhang X. The Paradoxical Role of Cellular Senescence in Cancer. Front Cell Dev Biol. 2021 Aug 12;9:722205.

53. Wang B, Kohli J, Demaria M. Senescent Cells in Cancer Therapy: Friends or Foes? Trends Cancer [Internet]. 2020 Oct 1 [cited 2024 Apr 4];6(10):838–57. Available from: http://www.cell.com/article/S240580332030159X/fulltext

54. Paclitaxel - NCI [Internet]. [cited 2024 Jun 25]. Available from: https://www.cancer.gov/about-cancer/treatment/drugs/paclitaxel

55. Demaria M, O'Leary MN, Chang J, Shao L, Liu S, Alimirah F, et al. Cellular senescence promotes adverse effects of chemotherapy and cancer relapse. Cancer Discov. 2017 Feb 1;7(2):165–76.

56. Braal CL, Jongbloed EM, Wilting SM, Mathijssen RHJ, Koolen SLW, Jager A. Inhibiting CDK4/6 in Breast Cancer with Palbociclib, Ribociclib, and Abemaciclib: Similarities and Differences. Drugs [Internet]. 2021 Feb 1 [cited 2024 Jun 25];81(3):317–31. Available from: https://link.springer.com/article/10.1007/s40265-020-01461-2

57. Hu W, Sung T, Jessen BA, Thibault S, Finkelstein MB, Khan NK, et al. Mechanistic investigation of bone marrow suppression associated with palbociclib and its differentiation from cytotoxic chemotherapies. Clinical Cancer Research [Internet]. 2016 Apr 15 [cited 2024 Jun 25];22(8):2000–8. Available from: /clincancerres/article/22/8/2000/265979/Mechanistic-Investigation-of-Bone-Marrow

58. Yoshida A, Lee EK, Diehl JA. Induction of therapeutic senescence in vemurafenib-resistant melanoma by extended inhibition of CDK4/6. Cancer Res [Internet]. 2016 May 15 [cited 2024 Jun 25];76(10):2990–3002. Available from: /cancerres/article/76/10/2990/609367/Induction-of-Therapeutic-Senescence-in-Vemurafenib

59. O'Leary B, Finn RS, Turner NC. Treating cancer with selective CDK4/6 inhibitors. Nature Reviews Clinical Oncology 2016 13:7 [Internet]. 2016 Mar 31 [cited 2024 May 14];13(7):417–30. Available from: https://www.nature.com/articles/nrclinonc.2016.26

60. Schmitt CA, Wang B, Demaria M. Senescence and cancer — role and therapeutic opportunities. Nature Reviews Clinical Oncology 2022 19:10 [Internet]. 2022 Aug 31 [cited 2024 May 14];19(10):619–36. Available from: https://www.nature.com/articles/s41571-022-00668-4

61. Baskar R, Lee KA, Yeo R, Yeoh KW. Cancer and Radiation Therapy: Current Advances and Future Directions. Int J Med Sci [Internet]. 2012 Feb 27 [cited 2024 Jun 25];9(3):193. Available from: /pmc/articles/PMC3298009/

62. A Senescence-like Phenotype Distinguishes Tumor Cells That Undergo Terminal Proliferation Arrest after Exposure to Anticancer Agents1 | Cancer Research | American Association for Cancer Research [Internet]. [cited 2024 Jun 25]. Available from: https://aacrjournals.org/cancerres/article/59/15/3761/505357/A-Senescence-like-Phenotype-Distinguishes-Tumor

63. Jones KR, Elmore LW, Jackson-Cook C, Demasters G, Povirk LF, Holt SE, et al. p53-Dependent accelerated senescence induced by ionizing radiation in breast tumour cells. Int J Radiat Biol [Internet]. 2005 Jun [cited 2024 Jun 25];81(6):445–58. Available from: https://www.tandfonline.com/doi/abs/10.1080/09553000500168549

64. Braig M, Schmitt CA. Oncogene-Induced Senescence: Putting the Brakes on Tumor Development. Cancer Res [Internet]. 2006 Mar 15 [cited 2024 Apr 16];66(6):2881–4. Available from: /cancerres/article/66/6/2881/526719/Oncogene-Induced-Senescence-Putting-the-Brakes-on

65. Campisi J. Cellular senescence as a tumor-suppressor mechanism. Trends Cell Biol [Internet]. 2001 Nov 1 [cited

2024 May 10];11(11):S27–31. Available from: http://www.cell.com/article/S0962892401021511/fulltext

66. Amati B, Alevizopoulos K, Vlach J. Myc and the cell cycle. Front Biosci [Internet]. 1998 [cited 2024 Apr 17];3. Available from: https://pubmed.ncbi.nlm.nih.gov/9468463/

67. Haraoka Y, Akieda Y, Nagai Y, Mogi C, Ishitani T. Zebrafish imaging reveals TP53 mutation switching oncogene-induced senescence from suppressor to driver in primary tumorigenesis. Nature Communications 2022 13:1 [Internet]. 2022 Mar 18 [cited 2024 Apr 17];13(1):1–15. Available from: https://www.nature.com/articles/s41467-022-29061-6

68. Ghebranious N, Donehower LA. Mouse models in tumor suppression. Oncogene 1998 17:25 [Internet]. 1999 Jan 12 [cited 2024 May 10];17(25):3385–400. Available from: https://www.nature.com/articles/1202573

69. Sherr CJ, Mccormick F. R E V I E W The RB and p53 pathways in cancer The life history of cancer cells encompasses a series of genetic missteps in which normal cells are progressively transformed into tumor cells that invade surrounding tissues and become malignant. 2002.

70. Olivier M, Hussain SP, Caron de Fromentel C, Hainaut P, Harris CC. TP53 mutation spectra and load: a tool for generating hypotheses on the etiology of cancer. IARC Sci Publ [Internet]. 2004 Jan 1 [cited 2024 Apr 17];(157):247–70. Available from: https://europepmc.org/article/med/15055300

71. Kang TW, Yevsa T, Woller N, Hoenicke L, Wuestefeld T, Dauch D, et al. Senescence surveillance of pre-malignant hepatocytes limits liver cancer development. Nature 2011 479:7374 [Internet]. 2011 Nov 9 [cited 2024 Jun 25];479(7374):547–51. Available from: https://www.nature.com/articles/nature10599

72. Iannello A, Thompson TW, Ardolino M, Lowe SW, Raulet DH. p53-dependent chemokine production by senescent tumor cells supports NKG2D-dependent tumor elimination by natural killer cells. Journal of Experimental Medicine [Internet]. 2013 Sep 23 [cited 2024 May 13];210(10):2057–69. Available from: www.jem.org/cgi/doi/10.1084/jem.20130783

73. Marin I, Boix O, Garcia-Garijo A, Sirois I, Caballe A, Zarzuela E, et al. Cellular Senescence Is Immunogenic and Promotes Antitumor Immunity. Cancer Discov [Internet]. 2023 Feb 1 [cited 2024 May 13];13(2):410–31. Available from: /cancerdiscovery/article/13/2/410/716304/Cellular-Senescence-Is-Immunogenic-and-Promotes

74. Iannello A, Raulet DH. Immunosurveillance of senescent cancer cells by natural killer cells. Oncoimmunology [Internet]. 2014 [cited 2024 Jul 19];3(1). Available from: /pmc/articles/PMC4006855/

75. Takasugi M, Yoshida Y, Ohtani N. Cellular senescence and the tumour microenvironment. Mol Oncol [Internet]. 2022 Sep 1 [cited 2024 May 13];16(18):3333. Available from: /pmc/articles/PMC9490140/

76. Lowe SW, Cepero E, Evan G. Intrinsic tumour suppression. Nature 2004 432:7015 [Internet]. 2004 Nov 17 [cited 2024 May 10];432(7015):307–15. Available from: https://www.nature.com/articles/nature03098

77. Takasugi M, Yoshida Y, Ohtani N. Cellular senescence and the tumour microenvironment. Mol Oncol [Internet]. 2022 Sep 1 [cited 2024 May 14];16(18):3333. Available from: /pmc/articles/PMC9490140/

78. Park SS, Choi YW, Kim JH, Kim HS, Park TJ. Senescent tumor cells: an overlooked adversary in the battle against cancer. Experimental & Molecular Medicine 2021 53:12 [Internet]. 2021 Dec 16 [cited 2024 May 14];53(12):1834–41. Available from: https://www.nature.com/articles/s12276-021-00717-5

79. Pereira BI, Devine OP, Vukmanovic-Stejic M, Chambers ES, Subramanian P, Patel N, et al. Senescent cells evade immune clearance via HLA-E-mediated NK and CD8+ T cell inhibition. Nature Communications 2019 10:1 [Internet]. 2019 Jun 3 [cited 2024 May 15];10(1):1–13. Available from: https://www.nature.com/articles/s41467-019-10335-5

80. Marin I, Serrano M, Pietrocola F. Recent insights into the crosstalk between senescent cells and CD8 T lymphocytes. npj Aging 2023 9:1 [Internet]. 2023 Apr 4 [cited 2024 May 15];9(1):1–4. Available from: https://www.nature.com/articles/s41514-023-00105-5

81. Chaib S, López-Domínguez JA, Lalinde-Gutiérrez M, Prats N, Marin I, Boix O, et al. The efficacy of chemotherapy is limited by intratumoral senescent cells expressing PD-L2. Nature Cancer 2024 5:3 [Internet]. 2024 Jan 24 [cited 2024 May 15];5(3):448–62. Available from: https://www.nature.com/articles/s43018-023-00712-x

82. Wang L, Lankhorst L, Bernards R. Exploiting senescence for the treatment of cancer. Nature Reviews Cancer 2022 22:6 [Internet]. 2022 Mar 3 [cited 2024 May 7];22(6):340–55. Available from: https://www.nature.com/articles/s41568-022-00450-9

83. Triana-Martínez F, Picallos-Rabina P, Da Silva-Álvarez S, Pietrocola F, Llanos S, Rodilla V, et al. Identification and characterization of Cardiac Glycosides as senolytic compounds. Nat Commun. 2019 Dec 1;10(1).

84. Amor C, Feucht J, Leibold J, Ho YJ, Zhu C, Alonso-Curbelo D, et al. Senolytic CAR T cells reverse senescence-associated pathologies. Nature 2020 583:7814 [Internet]. 2020 Jun 17 [cited 2024 May 21];583(7814):127–32. Available from: https://www.nature.com/articles/s41586-020-2403-9

85. Wang B, Wang L, Gasek NS, Zhou Y, Kim T, Guo C, et al. An inducible p21-Cre mouse model to monitor and manipulate p21-highly-expressing senescent cells in vivo. Nature Aging 2021 1:10 [Internet]. 2021 Oct 7 [cited 2024 Jul 19];1(10):962–73. Available from: https://www.nature.com/articles/s43587-021-00107-6

86. Burd CE, Sorrentino JA, Clark KS, Darr DB, Krishnamurthy J, Deal AM, et al. Monitoring tumorigenesis and senescence in vivo with a p16 INK4a-luciferase model. Cell [Internet]. 2013 Jan 7 [cited 2024 May 15];152(1–2):340–51. Available from: http://www.cell.com/article/S0092867412014973/fulltext

87. Baker DJ, Childs BG, Durik M, Wijers ME, Sieben CJ, Zhong J, et al. Naturally occurring p16 Ink4a-positive cells shorten healthy lifespan. Nature. 2016 Feb 11;530(7589):184–9.

88. Baker DJ, Wijshake T, Tchkonia T, Lebrasseur NK, Childs BG, Van De Sluis B, et al. Clearance of p16 Ink4a-positive senescent cells delays ageing-associated disorders. Nature. 2011 Nov 10;479(7372):232–6.

89. Demaria M, Ohtani N, Youssef SA, Rodier F, Toussaint W, Mitchell JR, et al. An essential role for senescent cells in optimal wound healing through secretion of PDGF-AA. Dev Cell [Internet]. 2014 Dec 22 [cited 2024 Aug 17];31(6):722–33. Available from: https://pubmed.ncbi.nlm.nih.gov/25499914/

90. Chang J, Wang Y, Shao L, Laberge RM, Demaria M, Campisi J, et al. Clearance of senescent cells by ABT263 rejuvenates aged hematopoietic stem cells in mice. Nature Medicine 2015 22:1 [Internet]. 2015 Dec 14 [cited 2024 Aug 17];22(1):78–83. Available from: https://www.nature.com/articles/nm.4010

91. Demaria M, Ohtani N, Youssef SA, Rodier F, Toussaint W, Mitchell JR, et al. An essential role for senescent cells in optimal wound healing through secretion of PDGF-AA. Dev Cell [Internet]. 2014 Dec 22 [cited 2024 May 15];31(6):722–33. Available from: http://www.cell.com/article/S1534580714007291/fulltext

92. Patil P, Dong Q, Wang D, Chang J, Wiley C, Demaria M, et al. Systemic clearance of p16INK4a-positive senescent cells mitigates age-associated intervertebral disc degeneration. Aging Cell. 2019 Jun 1;18(3).

93. Milde-Langosch K, Bamberger AM, Rieck G, Kelp B, Löning T. Overexpression of the p16 cell cycle inhibitor in breast cancer is associated with a more malignant phenotype. Breast Cancer Res Treat [Internet]. 2001 [cited 2024 Jun 3];67(1):61–70. Available from: https://link.springer.com/article/10.1023/A:1010623308275

94. Fluck MM, Schaffhausen BS. Lessons in Signaling and Tumorigenesis from Polyomavirus Middle T Antigen. Microbiology and Molecular Biology Reviews. 2009 Sep;73(3):542–63.

95. Van Rooijen N, Van Kesteren-Hendrikx E. CLODRONATE LIPOSOMES: PERSPECTIVES IN RESEARCH AND THERAPEUTICS. J Liposome Res [Internet]. 2002 [cited 2024 Sep 3];12(1–2):81–94. Available from: https://www.tandfonline.com/doi/abs/10.1081/LPR-120004780

96. Mempel TR, Lill JK, Altenburger LM. How chemokines organize the tumour microenvironment. Vol. 24, Nature Reviews Cancer. Nature Research; 2024. p. 28–50.

97. Linde N, Casanova-Acebes M, Sosa MS, Mortha A, Rahman A, Farias E, et al. Macrophages orchestrate breast cancer early dissemination and metastasis. Nature Communications 2017 9:1 [Internet]. 2018 Jan 2 [cited 2024 Jul 24];9(1):1–14. Available from: https://www.nature.com/articles/s41467-017-02481-5

98. Crusio WE, Lambris JD, Radeke HH. Advances in Experimental Medicine and Biology Volume 1240 Series Editors [Internet]. Available from: http://www.springer.com/series/5584

99. Kan T, Feldman E, Timaner M, Raviv Z, Shen-Orr S, Aronheim A, et al. IL-31 induces antitumor immunity in breast carcinoma. J Immunother Cancer. 2020 Aug 24;8(2).

100. Mempel TR, Lill JK, Altenburger LM. How chemokines organize the tumour microenvironment. Vol. 24, Nature Reviews Cancer. Nature Research; 2024. p. 28–50.

101. Rogic A, Pant I, Grumolato L, Fernandez-Rodriguez R, Edwards A, Das S, et al. High endogenous CCL2 expression promotes the aggressive phenotype of human inflammatory breast cancer. Nat Commun. 2021 Dec 1;12(1).

102. Bied M, Ho WW, Ginhoux F, Blériot C. Roles of macrophages in tumor development: a spatiotemporal perspective. Cellular & Molecular Immunology 2023 20:9 [Internet]. 2023 Jul 10

[cited 2024 Jul 24];20(9):983–92. Available from: https://www.nature.com/articles/s41423-023-01061-6

103. Werbeck JL, Thudi NK, Martin CK, Premanandan C, Yu L, Ostrowksi MC, et al. Tumor Microenvironment Regulates Metastasis and Metastasis Genes of Mouse MMTV-PymT Mammary Cancer Cells In Vivo. Vet Pathol. 2014 Jul 1;51(4):868–81.

104. Yoshimura T, Li C, Wang Y, Matsukawa A. The chemokine monocyte chemoattractant protein-1/CCL2 is a promoter of breast cancer metastasis. Cellular & Molecular Immunology 2023 20:7 [Internet]. 2023 May 19 [cited 2024 Aug 22];20(7):714–38. Available from: https://www.nature.com/articles/s41423-023-01013-0

105. Kim S, Kim C. Transcriptomic Analysis of Cellular Senescence: One Step Closer to Senescence Atlas. Mol Cells [Internet]. 2021 Mar 3 [cited 2024 Aug 19];44(3):136. Available from: /pmc/articles/PMC8019598/

106. Tao W, Yu Z, Han JDJ. Single-cell senescence identification reveals senescence heterogeneity, trajectory, and modulators. Cell Metab [Internet]. 2024 Apr [cited 2024 Apr 19];0(0). Available from: http://www.cell.com/article/S1550413124000883/fulltext

107. Van Den Brink SC, Sage F, Vértesy Á, Spanjaard B, Peterson-Maduro J, Baron CS, et al. Single-cell sequencing reveals dissociation-induced gene expression in tissue subpopulations. Nature Methods 2017 14:10 [Internet]. 2017 Sep 29 [cited 2024 Aug 19];14(10):935–6. Available from: https://www.nature.com/articles/nmeth.4437

108. Marx V. Method of the Year: spatially resolved transcriptomics. Nature Methods 2021 18:1 [Internet]. 2021 Jan 6 [cited 2024 Aug 19];18(1):9–14. Available from: https://www.nature.com/articles/s41592-020-01033-y

109. Moncada R, Barkley D, Wagner F, Chiodin M, Devlin JC, Baron M, et al. Integrating microarray-based spatial transcriptomics and single-cell RNA-seq reveals tissue

architecture in pancreatic ductal adenocarcinomas. Nature Biotechnology 2020 38:3 [Internet]. 2020 Jan 13 [cited 2024 Aug 19];38(3):333–42. Available from: https://www.nature.com/articles/s41587-019-0392-8

110. Gurkar AU, Gerencser AA, Mora AL, Nelson AC, Zhang AR, Lagnado AB, et al. Spatial mapping of cellular senescence: emerging challenges and opportunities. Nature Aging 2023 3:7 [Internet]. 2023 Jul 3 [cited 2024 Aug 19];3(7):776–90. Available from: https://www.nature.com/articles/s43587-023-00446-6

111. Lujambio A, Akkari L, Simon J, Grace D, Tschaharganeh DF, Bolden JE, et al. Non-cell-autonomous tumor suppression by p53. Cell [Internet]. 2013 Apr 11 [cited 2024 May 17];153(2):449–60. Available from: http://www.cell.com/article/S0092867413003425/fulltext

112. Xu M, Pirtskhalava T, Farr JN, Weigand BM, Palmer AK, Weivoda MM, et al. Senolytics improve physical function and increase lifespan in old age. Nature Medicine 2018 24:8 [Internet]. 2018 Jul 9 [cited 2024 Aug 20];24(8):1246–56. Available from: https://www.nature.com/articles/s41591-018-0092-9

113. Chaib S, Tchkonia T, Kirkland JL. Cellular senescence and senolytics: the path to the clinic. Vol. 28, Nature Medicine. Nature Research; 2022. p. 1556–68.

114. Fujimoto H, Sangai T, Ishii G, Ikehara A, Nagashima T, Miyazaki M, et al. Stromal MCP-1 in mammary tumors induces tumor-associated macrophage infiltration and contributes to tumor progression. Int J Cancer. 2009 Sep 15;125(6):1276–84.